

Characterization of Nup155 and Mel28 in
nuclear envelope assembly *in vitro*

Dissertation

to obtain the academic title

doctor rerum naturalium (Dr. rer. nat.)

submitted to the

Faculty of Mathematics, Natural Sciences and Engineering

at the Martin-Luther Universität Halle-Wittenberg

by

CERSTIN FRANZ

born October 7, 1976 in Gießen

Referees:

1. Prof. Dr. Elmar Wahle
2. PD Dr. Gero Steinberg

Oral Examination: 20.02.2006

Halle (Saale)

urn:nbn:de:gbv:3-000010552

[<http://nbn-resolving.de/urn/resolver.pl?urn=nbn%3Ade%3Agbv%3A3-000010552>]

Charakterisierung von Nup155 und Mel28 bei
der Bildung der Kernhülle *in vitro*

Dissertation

zur Erlangung des akademischen Grades

doctor rerum naturalium (Dr. rer. nat.)

vorgelegt der

Mathematisch-Naturwissenschaftlich-Technischen Fakultät
(mathematisch-naturwissenschaftlicher Bereich)
der Martin-Luther Universität Halle-Wittenberg

von Frau

CERSTIN FRANZ

geboren am 7. Oktober 1976 in Gießen

Gutachter:

1. Prof. Dr. Elmar Wahle
2. PD Dr. Gero Steinberg

Tag der mündlichen Prüfung: 20.02.2006

Halle (Saale)

urn:nbn:de:gbv:3-000010552

[<http://nbn-resolving.de/urn/resolver.pl?urn=nbn%3Ade%3Agbv%3A3-000010552>]

Das Geheimnis des Erfolgs ist die Beständigkeit des Ziels.

Benjamin Disraeli

Summary

Cell division is a fundamental feature of life. In metazoa the nuclear envelope (NE) disassembles at the onset of cell division and reforms around decondensing chromatin. This thesis aims to functionally characterize new proteins involved in the process of NE reassembly.

Genetic depletion of Nup155 and Mel28 by RNAi in *Caenorhabditis elegans* (*C. elegans*) led to dramatic defects in nuclear formation and morphology. This suggested that these proteins might also be essential for NE reconstitution in vertebrates. Nup155 is a nucleoporin, a component of the nuclear pore complex (NPC). Mel28 is a largely uncharacterized protein.

Using the *Xenopus laevis* (*X. laevis*) egg extract system, nuclei can be assembled *in vitro*. This system is amenable to address the role of individual proteins in NE reformation. It permits biochemical manipulation and thereby permits the investigation of complex processes at molecular levels.

Characterization of proteins in *X. laevis* egg extracts revealed distinct functional steps in NE formation. First, some nucleoporins like Nup107 and Pom121 are recruited to chromatin and build a template for further nuclear pore complex assembly. Simultaneously, nuclear membrane vesicles associate with chromatin. Second, further nucleoporins bind to those already recruited in the previous step and membrane vesicles fuse to form a network. In the final step, a functional nucleus is built after all nucleoporins are incorporated into NPCs and the nuclear membrane is sealed. *In vitro* reconstituted nuclei are transport- and replication-competent.

In this study, the roles of Nup155 and Mel28 in NE assembly were characterized in the *X. laevis* egg extract system and results were applied to the current model of NE reformation.

To achieve this, *X. laevis* Nup155 and Mel28 cDNAs were cloned and antibodies were generated against the corresponding polypeptides. Functional conservation of Nup155 and Mel28 between nematodes and vertebrates was assessed by localization on *Xenopus* XI177 cells. Nup155 localized to the NE of XI177 cells, as expected for a nucleoporin. Mel28 was detected at the NE during interphase and at kinetochores during mitosis in both *C. elegans* embryos and XI177 cells.

In an NE assembly time course experiment, Nup155 was recruited to developing NPCs in the second step, together with a well characterized subset of nucleoporins. Nup107 and Pom121 bound to chromatin prior to Nup155. Their

localization to chromatin was not impaired in the absence of Nup155 but, like all other nucleoporins investigated, they failed to assemble into NPCs at the nuclear periphery under this condition. Nuclei reconstituted *in vitro*, in the absence of Nup155, lacked NPCs as shown by immunofluorescence and electron microscopy. Next, the integrity of nuclear membranes was investigated. It was shown that nuclear membrane vesicles docked to chromatin upon Nup155 depletion but did not fuse to form continuous nuclear membranes. Defects in NPC assembly and nuclear membrane fusion were restored by addition of recombinant Nup155. This demonstrated that the described phenotypes were specifically caused by Nup155 depletion.

Interestingly, the second protein investigated, Mel28, is also linked to nucleoporins. Mel28 and Nup107 co-immunoprecipitated from *X. laevis* egg extracts. Mel28 bound to chromatin in reactions with membrane-free egg cytosol in contrast to nucleoporins. In NE assembly reactions with Mel28-depleted cytosol none of the investigated, soluble nucleoporins were recruited to chromatin templates. Under these conditions, the integral membrane protein Pom121 also failed to be incorporated into an NE.

In summary, this work extended the current model of postmitotic NE assembly by demonstrating that the absence of the soluble nucleoporin Nup155 inhibits NPC formation and nuclear membrane fusion. This was not observed previously for any other soluble nucleoporin. Interestingly, lack of the integral membrane protein Pom121 led to a similar phenotype. Nup155 and Pom121 are suggested to participate in a checkpoint that coordinates NPC assembly and nuclear membrane fusion to form a functional NE. Furthermore, present data indicate that Mel28 is essential for nucleoporin association with chromatin, and therefore, is required for NPC assembly. To place Mel28 into the current model of NE assembly, the defect caused by Mel28 depletion on nuclear membranes remains to be investigated, although, based on the present data, we hypothesize that Mel28 may constitute an anchor for NPCs at chromatin and thereby in the NE.

Zusammenfassung

Ein grundlegendes biologisches Merkmal des Lebens ist die Fähigkeit zur Zellteilung. In mehrzelligen Organismen zerfällt die Kernhülle zu Beginn der Zellteilung und rekonstituiert sich am Ende neu. Die Zielsetzung dieser Arbeit war die funktionelle Charakterisierung von neuen Proteinen, welche an der Errichtung der Kernhülle nach der Mitose beteiligt sind.

Die Reduktion der Expression von Nup155 und Mel28 mittels RNAi in *Caenorhabditis elegans* (*C. elegans*) verursachte starke Defekte bei der Bildung von Zellkernen und in deren Morphologie. Diese Beobachtungen legten nahe, dass Nup155 und Mel28 auch eine essenzielle Funktion bei der Rekonstitution der Kernhülle in Vertebraten einnehmen könnten. Nup155 ist ein Nukleoporin, ein Bestandteil der Kernporenkomplexe. Mel28 ist ein weitgehend unbeschriebenes Protein.

Das *Xenopus laevis* (*X. laevis*) Eiextrakt-System ermöglicht die Bildung von Kernen *in vitro*. Es erlaubt biochemische Manipulationen und somit die Untersuchung von komplexen Prozessen auf molekularer Ebene. Das System ist daher für die funktionelle Charakterisierung von individuellen Proteinen bei der Rekonstitution der Kernhülle geeignet.

Die Bildung der Kernhülle *in vitro* kann in mehrere funktionelle Schritte gegliedert werden. Zu einem frühen Zeitpunkt binden einige Nukleoporine, wie Nup107 und das Membrannukleoporin Pom121 sowie Kernmembranvesikel an Chromatin. Im folgenden Schritt binden weitere Nukleoporine an die bereits vorhandenen und die Membranvesikel fusionieren zu einem Netzwerk. Wenn alle Nukleoporine in Kernporenkomplexe integriert wurden und die Kernmembran sich im letzten Schritt geschlossen hat, liegt ein funktionsfähiger Kern vor. *In vitro* gebildete Kerne sind transportkompetent und können DNA replizieren.

In der vorliegenden Arbeit wurden Nup155 und Mel28 bei der Bildung der Kernhülle in *X. laevis* Eiextrakten charakterisiert und die Ergebnisse in das gegenwärtige Modell integriert.

X. laevis Nup155 und Mel28 cDNAs wurden kloniert und Antikörper gegen die entsprechenden Polypeptide hergestellt. Die funktionelle Konservierung von Nup155 und Mel28 von Nematoden zu Vertebraten wurde mittels ihrer jeweiligen Lokalisierung in einer *Xenopus* Zelllinie überprüft. Nup155 lokalisierte, wie für ein Nukleoporin erwartet, an der Kernhülle. Mel28 wurde in beiden Organismen während der Interphase an der Kernhülle und während der Mitose an den Kinetochoren der

Chromosomen detektiert.

In einer zeitaufgelösten Reaktion der Rekonstitution von Zellkernen *in vitro*, assoziierte Nup155 erst im zweiten funktionellen Schritt nach Nup107 und Pom121 mit dem Chromatin. Bei der Verwendung von Nup155-freiem Eizytosol zur Bildung von Kernen, konnten Nup107 und Pom121 weiterhin an Chromatin binden, allerdings wurden sie nicht im folgenden Verlauf der Kernrekonstitution in Kernporenkomplexe an der Chromatinperipherie integriert. Die Assoziation von Mel28 mit Chromatin war ebenfalls unabhängig von Nup155. Bei der *in vitro* Rekonstituierung von Kernen in Abwesenheit von Nup155 konnten keine Kernporenkomplexe gebildet werden, wie mittels Immunfluoreszenz und Elektronenmikroskopie gezeigt wurde.

Des Weiteren wurde die Integrität der Kernmembranen untersucht. Bei Fehlen von Nup155 konnten Membranvesikel an Chromatin binden, fusionierten aber nicht zu einer geschlossenen Kernmembran. Defekte beim Aufbau von Kernporenkomplexen und der Fusion der Kernmembranen in Abwesenheit von Nup155 konnten durch Zugabe von rekombinantem Nup155 aufgehoben werden. Dies zeigte, dass die beobachteten Phänotypen spezifisch auf das Fehlen von Nup155 und damit auf dessen Funktion zurückzuführen waren.

Interessanter Weise zeigte das zweite zu charakterisierende Protein, Mel28, eine funktionelle Verbindung zu Nukleoporinen. Bei der Immunpräzipitation von Mel28 und Nup107 in *X. laevis* Eizytosol, wurde eine wechselseitige Interaktion der Proteine festgestellt. Mel28 assoziierte ferner mit Chromatin in membranfreiem Zytosol, im Gegensatz zu getesteten Nukleoporinen. Bei der Rekonstitution von Kernen *in vitro* in Mel28-freiem Zytosol, konnte keines der untersuchten Nukleoporine an Chromatin binden. Unter diesen Bedingungen akkumulierte auch das Membrannukleoporin Pom121 nicht an der Kernhülle.

Diese Arbeit erweitert das gegenwärtige Model des Aufbaus der Kernhülle nach der Mitose durch die Entdeckung, dass die Abwesenheit eines löslichen Nukleoporins, Nup155, die Errichtung der Kernporenkomplexe und die Formierung einer geschlossenen Kernmembran inhibiert. Dies wurde zuvor für kein anderes lösliches Nukleoporin beobachtet. Interessanter Weise, führt das Fehlen des Membrannukleoporins Pom121 zu einem ähnlichen Phänotyp. Es wird angenommen, dass Nup155 und Pom121 zu einem Kontrollmechanismus beitragen, der die Bildung von Kernporenkomplexen und Kernmembranen zu einer funktionellen Kernhülle koordiniert. Die derzeitigen Daten legen nahe, dass Mel28 essenziell für

die Assoziation von Nukleoporinen mit dem Chromatin und somit notwendig für den Aufbau von Kernporenkomplexen ist. Um Mel28 im gegenwärtigen Modell zur Bildung der Kernhülle zu platzieren, bedarf es der weiteren Untersuchung, welche Auswirkung die Abwesenheit von Mel28 auf Kernmembranen hat. Die hier gezeigten Ergebnisse legen nahe, dass Mel28 der Anker für Kernporenkomplexe am Chromatin und damit gegebenenfalls in der Kernhülle sein könnte.

Table of contents

<i>Summary</i>	<i>IV</i>
<i>Zusammenfassung</i>	<i>VII</i>
<i>Table of contents</i>	<i>XI</i>
<i>Abbreviations</i>	<i>XV</i>
1 Introduction	1
1.1 The nuclear envelope during cell division	2
1.2 Architecture and composition of the metazoan nuclear envelope	3
1.2.1 The nuclear membrane	4
1.2.2 The nuclear lamina	7
1.2.3 The nuclear pore complex	8
1.2.4 Nucleocytoplasmic transport	17
1.2.5 Regulation of nuclear pore complex assembly	22
1.2.6 <i>X. laevis</i> nuclear reconstitution system	26
1.3 Aim of the project and introduction of Nup155 and Mel28	27
2 Results	31
2.1 Nup155 is essential for nuclear pore complex assembly and nuclear membrane fusion	32
2.1.1 Generating the tools: Cloning and expression of <i>X. laevis</i> Nup155	32
2.1.2 Characterization of anti-Nup155 antiserum	34
2.1.3 Knock down of Nup155 by RNAi in HeLa cells	36
2.1.4 Characterization of Nup155 in <i>X. laevis</i> egg extract fractions	38
2.1.5 Depletion of Nup155 from <i>X. laevis</i> cytosol	39
2.1.6 Nup155 depletion blocks nuclear pore complex assembly	40
2.1.7 In the absence of Nup155 closed nuclear membranes do not form	44
2.1.8 Ultrastructural defects on nuclear membranes	45
2.1.9 Nup155 did not interact with any other nucleoporin investigated	46
2.1.10 Nup155 depletion blocks an early event in nuclear pore complex assembly and nuclear membrane fusion	47
2.2 Mel28, a novel player in nuclear envelope formation	49
2.2.1 Identification of the vertebrate homologue of <i>C. elegans</i> Mel28	49
2.2.2 Cloning of <i>X. laevis</i> Mel28	50
2.2.3 Features of the <i>X. laevis</i> Mel28 protein sequence	51
2.2.4 Conservation of Mel28 among eukaryotes	52
2.2.5 Generation of polyclonal antibodies against <i>X. laevis</i> Mel28	53
2.2.6 Characterization of Mel28 in <i>X. laevis</i> egg extracts and X1177 cells	54

2.2.7	Functional investigation of Mel28 in nuclear envelope assembly _____	58
2.2.8	Time course analysis of Mel28 in nuclear envelope formation _____	60
2.2.9	Recruitment of Mel28 to chromatin _____	61
2.2.10	Mel28 interacts with Nup107 _____	62
2.2.11	Knock down of Mel28 by RNAi in HeLa cells _____	63
3 Discussion _____		65
3.1 Nup155 regulates nuclear envelope and nuclear pore complex formation in vertebrates _____		66
3.1.1	Features of the nucleoporin Nup155 _____	66
3.1.2	Depletion of Nup155 impairs nuclear morphology, segregation and viability _____	66
3.1.3	Nup155 is essential for NPC assembly _____	67
3.1.4	Nup155 is required for nuclear membrane fusion _____	68
3.1.5	Order of events in nuclear envelope assembly _____	69
3.1.6	Nup155 plays a role in a checkpoint mechanism linking nuclear pore complex and nuclear membrane assembly _____	70
3.2 Mel28, a novel factor in postmitotic nuclear envelope reformation _____		73
3.2.1	Sequence analysis of vertebrate Mel28 _____	73
3.2.2	Mel28 localization is conserved from nematodes to vertebrates _____	74
3.2.3	Mel28 is an essential component for nuclear envelope reformation _____	74
3.2.4	Fundamental questions concerning the role of Mel28 _____	75
4 Perspectives _____		77
5 Materials and Methods _____		79
5.1 Materials _____		80
5.1.1	Chemicals and Reagents _____	80
5.1.2	Commonly used buffers, solutions and media _____	82
5.1.3	Commonly used material _____	84
5.1.4	Instrumental equipment _____	85
5.1.5	Nucleotide sequences _____	85
5.1.6	Bacteria strains for cloning and protein expression _____	88
5.1.7	Antibodies _____	88
5.2 Methods _____		89
5.2.1	Molecular biological methods _____	89
5.2.2	Biochemical standard methods _____	92
5.2.3	Biochemical methods related to the <i>X. laevis</i> egg extract system _____	97
5.2.4	Microscopy _____	102
5.2.5	Cell culture _____	102
5.2.6	siRNA knock down of gene expression in HeLa cells _____	102

6	References	104
7	Appendix	116
7.1	Curriculum vitae	117
7.2	Declaration	118
7.3	Publications	119
7.3.1	Publications	119
7.3.2	Poster Presentation	119
7.3.3	Future publication	119
	Acknowledgements	120

Abbreviations

A. nidulans	Aspergillus nidulans
aa	Amino acid
AAA-ATPase	ATPases associated with different cellular activities
AL	Annulate lamellae
ATP	Adenosine triphosphate
BAF	Barrier to autointegration factor
BAPTA	1,2-Bis(2-aminophenoxy) ethane-N,N,N',N'-tetraacetic acid
BMP	Bone morphogenetic proteins
BSA	Bovine serum albumin
C. elegans	Caenorhabditis elegans
Crm1	Chromosome region maintenance 1
D. discoideum	Dictyostelium discoideum
D. melanogaster	Drosophila melanogaster
DAPI	4',6-Diamidino-2-phenylindole
DIC	Differential interference contrast
DNA	Deoxyribonucleic acid
E. coli	Escherichia coli
EDTA	1-(4-Aminobenzyl)ethylenediamine-N,N,N',N'-tetraacetic acid
EGFP	Enhanced green fluorescent protein
EGTA	Ethylene glycol-bis(2-aminoethyl)-N,N,N',N'-tetraacetic acid
ELYS	Embryonic large molecule derived from yolk sac
EM	Electron microscopy
ER	Endoplasmic reticulum
EST	Expressed sequence tag
FG	Phenylalanine glycine dipeptide
GCL	Germ cell-less
GDP	Guanosine diphosphate
GFP	Green fluorescent protein
GST	Glutathione-S-transferase
GTP	Guanosine triphosphate
GTPase	Guanosine triphosphatase
GTP γ S	Guanosine 5'-(γ -thio)triphosphate
hCG	Human chorionic gonadotropin
HEAT	Huntingtin, elongation factor 3, A subunit of protein phosphatase 2A and TOR1
HeLa cells	Henrietta Lack's cells
HP1	Heterochromatin protein1
iFRAP	Invers fluorescence recovery after photobleaching
INM	Inner nuclear membrane
IPTG	Isopropyl- β -D-thiogalactopyranoside
Kb	Kilo base
kDa	Kilo Dalton
LAP	Lamina associated polypeptide
LBR	Lamin B receptor
LEM	Protein domain found in LAP2, emerin and Man1
mAb	Monoclonal antibody
Mel28	Maternal-effect lethality 28

mRNA	Messenger RNA
NCBI	National center for biotechnology information
NE	Nuclear envelope
NES	Nuclear export sequence
Ni-NTA	Nickel-nitrilo triacetic acid
NLS	Nuclear localization signal
NMR	Nuclear magnetic resonance
NPC	Nuclear pore complex
NTF2	Nuclear transport factor 2
Nup	Nucleoporin
OD	Optical density
O-GlcNAc	O-linked N-acetylglucosamines
ONM	Outer nuclear membrane
ORF	Open reading frame
PCR	Polymerase chain reaction
PMSG	Pregnant mare serum gonadotropin
Pom121	Pore membrane protein of 121 kDa
Ran	Ras like nuclear GTPase
RanBP	Ran binding protein
RanGAP	Ran GTPase activating protein
RanGEF	Ran guanine nucleotide exchange factor
Ras	Rous sarcoma virus cellular oncogene
RCC1	Regulator of chromatin condensation
RNA	Ribonucleic acid
RNAi	RNA interference
RT	Room temperature
RT-PCR	Reverse transcriptase polymerase chain reaction
RZPD	Deutsches Ressourcenzentrum für Genomforschung
<i>S. cerevisiae</i>	<i>Saccharomyces cerevisiae</i>
SDS-PAGE	Sodium dodecylsulfate polyacrylamid gel electrophoresis
siRNA	Small interfering RNA
STEM	Scanning transmission electron microscopy
TGF	Transforming (tumor) growth factor
Tpr	Translocated promoter region
tRNA	Transfer RNA
U	Unit
<i>U. maydis</i>	<i>Ustilago maydis</i>
U snRNA	Uridine rich small nuclear RNA
WGA	Wheat germ agglutinin
<i>X. laevis</i>	<i>Xenopus laevis</i>
XI177	<i>Xenopus laevis</i> 177 cell line
YFP	Yellow fluorescent protein

1 Introduction

The cell is the fundamental unit of life. One feature of living systems is the phenomenon of heredity. The cell is the transport device for the heritable information. To maintain life, cell division takes place after the genome has been doubled, resulting in a mother and a daughter cell. In contrast to prokaryotes, the genome of eukaryotes is compartmentalized in the cell nucleus allowing for separation of biochemical processes to take place in specialized membrane bound environments. Eukaryotes face a special challenge during cell division, because their genome is enclosed by the nuclear envelope (NE), the structure that demarcates the nucleus.¹

The following introductory chapters will give a background on different mechanisms of eukaryotic nuclear envelope breakdown and reassembly and the three structural units of the NE: nuclear membrane, nuclear lamina and nuclear pore complexes (NPCs).^{*} The molecular composition of the NPC will be detailed, as one of the proteins studied here is a nucleoporin. Furthermore, comprehensive information about the current knowledge of nuclear membrane and NPC reformation will be provided. This information will be important to integrate the data presented in this work into the current model of vertebrate NE assembly.

The study employs a vertebrate *in vitro* system to functionally characterize the role of two proteins of the NE in postmitotic nuclear reconstitution. In this *Xenopus laevis* (*X. laevis*) egg extract system the NE entirely disassembles during mitosis and has to reform.

1.1 The nuclear envelope during cell division

In single-celled eukaryotes such as *Saccharomyces cerevisiae* (*S. cerevisiae*), the basic components of the NE stay intact during cell division. Tubulin is imported into the nucleus and the mitotic spindle is assembled within the NE to segregate the chromosomes to opposite sides of the dividing cell. The process is called “closed mitosis”, because the NE is not disassembled (Figure 1.1A).² In contrast, “open mitosis” involves the disassembly of the nuclear membrane and NPCs during mitosis. This is the situation in all known multicellular organisms, in which all components of the NE disassemble; the mitotic spindle forms and segregates the chromosomes in the mitotic cytoplasm (Figure 1.1B). There are also intermediate forms of “closed/open mitosis”. For example, in the fungus *Aspergillus nidulans* (*A. nidulans*),

^{*} The term “nuclear membrane” used in this thesis refers to the double membrane bilayer of the NE.

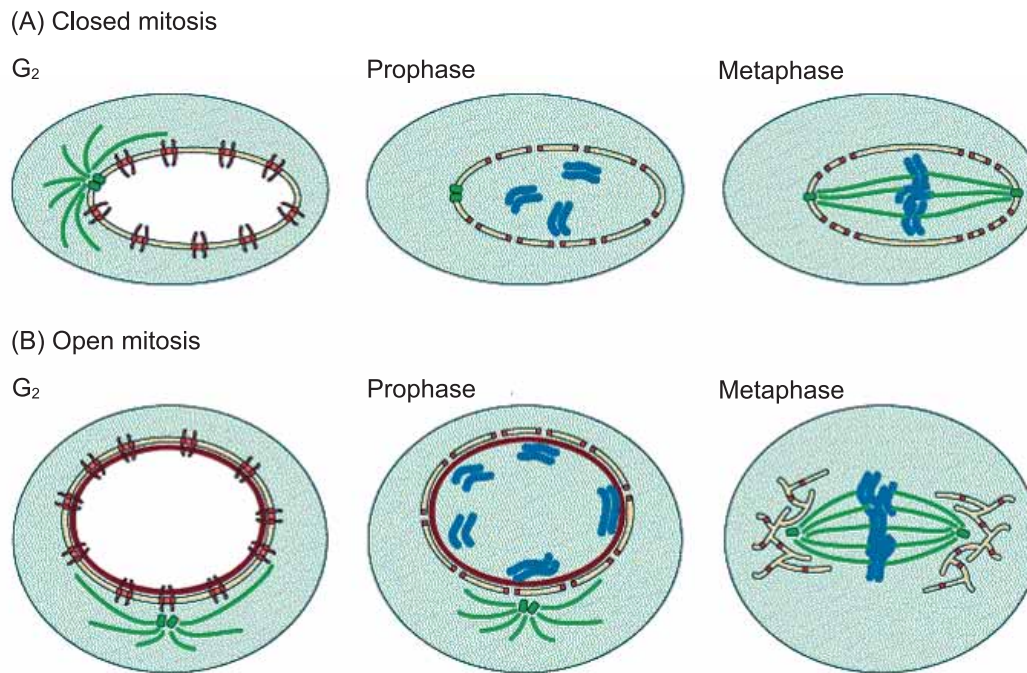


Figure 1.1: Closed and open mitosis. (A) In closed mitosis of some fungi, NPC permeability is remodeled in prophase allowing for mitotic factors and tubulin to enter the nucleus. The NPC scaffold stays intact and NE integrity is preserved. There is no nuclear lamina in single-celled eukaryotes. (B) NE breakdown in metazoan occurs in two steps: partial NPC disassembly accompanied by increased permeability in prophase is followed by complete NE disassembly. NPCs (red/orange), NE (light brown), nuclear lamina (dark brown), chromatin (blue), microtubules (green), soluble tubulin (light green). (Modified from Rabut *et al.*, (2004). *Curr. Opin. Cell Biol.* 16, 314-321.)

cell division occurs as closed mitosis, because the nuclear membrane stays intact, but NPCs partially disassemble.³ An unconventional example for an open mitosis comes from the basidiomycete *Ustilago maydis* (*U. maydis*). Chromosomes and spindle pole bodies migrate into the bud, building up the daughter cell and leave the old NE behind. Some material from this NE is recycled for the formation of the new NEs.⁴ In metazoa like the nematode *Caenorhabditis elegans* (*C. elegans*) and in syncytial embryos of the fruitfly *Drosophila melanogaster* (*D. melanogaster*), the NE disassembles completely but this takes place relatively late during mitosis at mid-late anaphase.⁵ In animal cells NE breakdown starts at prometaphase and reformation occurs around the decondensing chromatin during telophase.²

1.2 Architecture and composition of the metazoan nuclear envelope

The structural composition of the NE is explained next. Three structural elements comprise the metazoan NE and functionally and morphologically demarcate the nucleus from the rest of a cell. Firstly, the nuclear membrane seals off

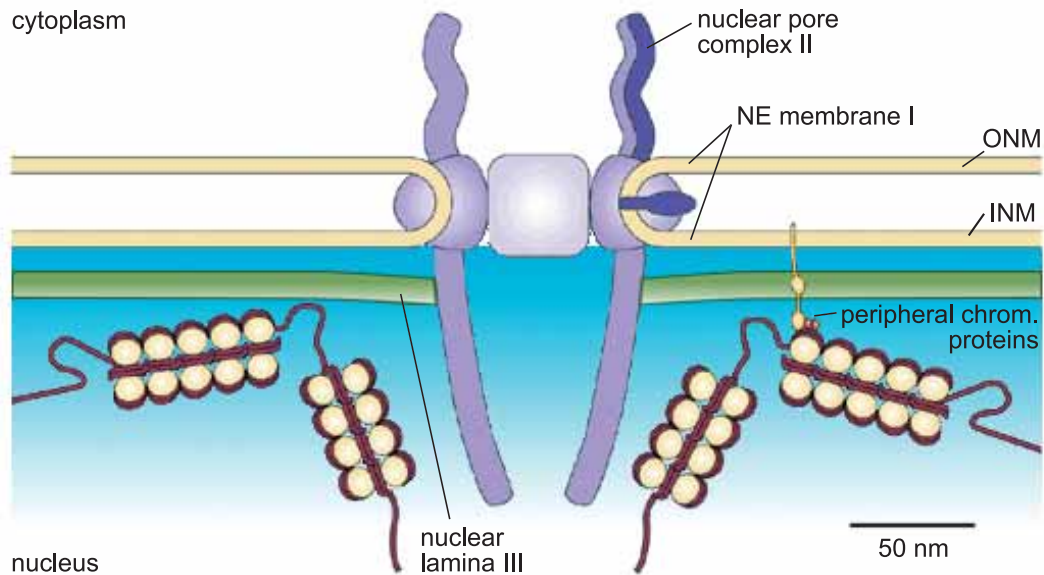


Figure 1.2: *Composition of the metazoan nuclear envelope.* The NE consists of three structural elements; (I) the nuclear membrane (yellow), (II) NPCs (purple), and (III) the nuclear lamina (green). Integral membrane proteins of the INM connect to the nuclear lamina and peripheral chromatin (right side). Nucleoporins with transmembrane domains link NPCs and nuclear membrane (indicated by dark purple component of the NPC which is inserted into the NE membrane at the right side). (Modified from Burke and Ellenberg (2002). *Nat. Rev. Mol. Cell Biol.* 3, 487-497.)

the nucleus from the cytoplasm and establish a distinct environment for nuclear processes. Secondly, NPCs inserted in the double lipid bilayer, allow nucleocytoplasmic transport. Thirdly, the mesh-like nuclear lamina is sandwiched between the inner nuclear membrane (INM) and peripheral chromatin (Figure 1.2). The nuclear lamina confers rigidity to the NE by connecting the INM with underlying chromatin. In addition, the nuclear lamina provides a crucial platform for gene transcription. Chromatin proteins connect to the lamina and/or the INM and thereby contribute to the overall integrity of the NE. These diverse structural components and their mutual interactions define the architecture of the nucleus and execute its function.⁶ Nuclear membrane, nuclear lamina and NPCs will be described in more detail below.

1.2.1 The nuclear membrane

The nuclear membrane comprises two concentric phospholipid bilayers. The outer layer is exposed to the cytoplasm, whereas the inner membrane faces the nucleoplasm. They are separated by a luminal space. The outer nuclear membrane (ONM) is continuous and almost identical in protein composition with the rough endoplasmic reticulum (ER). Exceptions are a few integral membrane proteins

present only in the ONM. Both ER and ONM are decorated with ribosomes engaged in protein synthesis. The NE not only confines processes that occur inside or outside the nucleus, but also plays a structural and functional role in localizing the nucleus within the cell.

Studies in *C. elegans* have identified integral membrane proteins of the NE that link the nucleoskeleton with the cytoskeleton by joining the nuclear lamina with microtubules and actin filaments in the cytosol. One of these, UNC84, localizes either to the ONM or INM, where it binds to UNC83, which interacts with microtubules at the nuclear periphery (Figure 1.3, top right). On the other hand, UNC84 binds directly or indirectly to the lamina and thereby mediates the connection between cytoplasmic intermediary filaments with the nucleoskeleton.^{7, 8} Analysis of *unc83* and *unc84* *C. elegans* mutants suggested that the complex is involved in nuclear migration and positioning by connecting microtubule-dependent motors to the nuclear lamina.⁹

Nesprins are another protein family found to accomplish connections of the lamina to the cytoskeleton. Nesprins are huge membrane proteins, presumably in the ONM, which bind F-actin *in vitro* and colocalize with the actin cytoskeleton by immunofluorescence.^{10, 11} Nesprins have several spectrin repeat domains that serve as molecular scaffolds, mediate protein-protein interactions and interact with actin and microtubules.³⁸ In *C. elegans*, UNC84 binds to ANC-1, a nesprin that is believed to mechanically link the nucleoskeleton to the actin cytoskeleton.¹²

ONM and INM fuse at NPCs that penetrate the double membrane bilayers. Characteristics of the INM are introduced next. Studies of individual proteins as well as proteomic approaches have identified a diverse group of transmembrane proteins residing specifically in the INM (Figure 1.3).^{13, 14, 15} From there, they connect to the nuclear lamina and/or the peripheral chromatin.^{6, 16, 17} By nuclear magnetic resonance (NMR) the structure of one of the nucleoplasmic domains involved in these integrative interactions, the LEM domain, was determined. The LEM domain was first found in three proteins of the INM, LAP2, emerin and MAN1.^{18, 19}

Lamina associated polypeptides (LAPs) attach to lamins and DNA, as well as to a peripheral chromatin protein, called Barrier to Autointegration Factor (BAF).^{20, 21, 22} BAF is an essential dimeric protein that seems to interact with all tested LEM-domain proteins.²³ LAP2 β exemplifies the integration and coordination of NE structure to nuclear processes; this protein contributes to the initiation of DNA

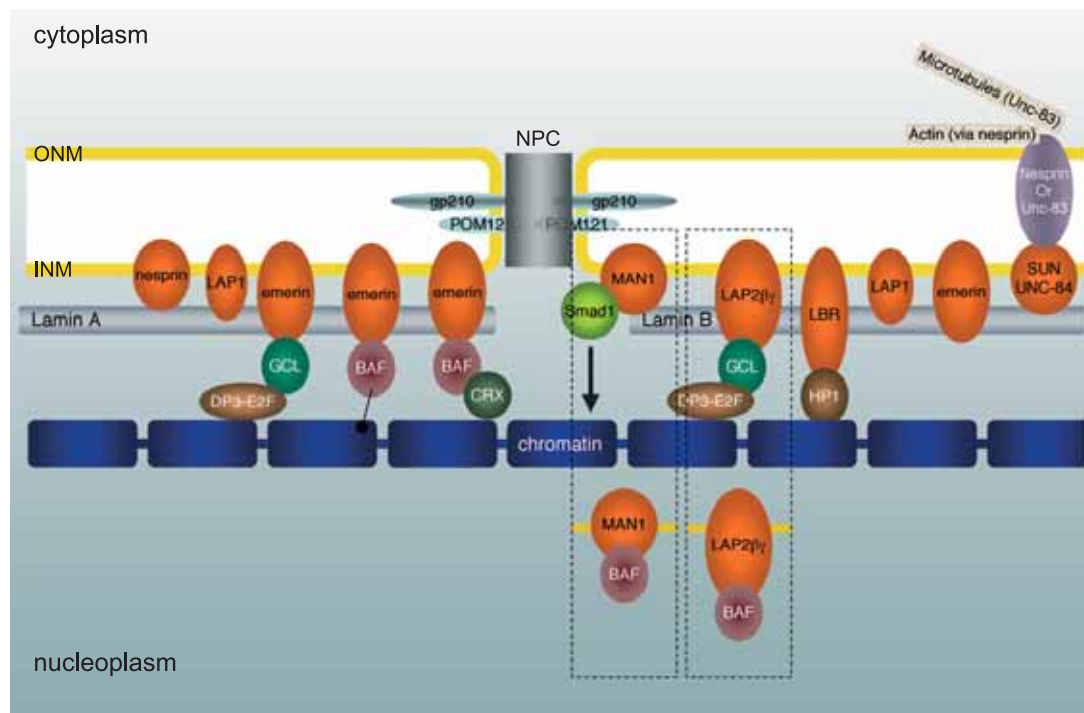


Figure 1.3: *Interdependent interactions between the three structural units of the NE.* Proteins of the NE fulfill diverse roles like: positioning of the NE within the cell by connecting it with the cytoskeleton, association of the nuclear membrane with the nuclear lamina for conferring structural stability, regulation of gene transcription by interaction between proteins of the nuclear lamina and/or INM to peripheral chromatin proteins. Individual components are addressed in the text. (Modified from Hetzer *et al.*, (2005). *Annu. Rev. Cell Dev. Biol.* in press.)

replication and transcription regulation.^{24, 25, 38} LAP2 β binds lamin B and is involved in gene regulation by binding to the transcriptional regulator germ cell-less (GCL).^{26,27,38}

Another LEM-domain containing INM protein is emerin, which functionally overlaps with LAP2 β as it also binds B- and A-type lamins, BAF and at least four gene regulators.^{28, 29} Interestingly, loss of emerin expression or mutations in the gene cause X-linked Emery-Dreifuss muscular dystrophy.^{30, 31}

MAN1, which spans the INM twice also carries a LEM domain. Its C-terminal domain binds to receptor regulated SMAD proteins that mediate signaling downstream of bone morphogenetic proteins (BMPs) and members of the transforming (tumor) growth factor (TGF) β superfamily.^{32, 33, 34} As such, MAN1 could play an important role in regulating vertebrate gene expression at various levels.³⁸

Lamin B receptor (LBR) is an INM integral membrane protein that directly links the underlying nuclear lamina by interacting with lamin B.³⁵ It does not contain a LEM domain. *In vitro*, LBR binds to chromatin-associated proteins like heterochromatin protein 1 (HP1), which mediates gene silencing. HP1 also binds to double stranded DNA and Histone H3-H4 tetramers.^{36, 37, 38}

1.2.2 The nuclear lamina

Enclosing the chromatin periphery underneath the INM, the lamina is a platform for multiple protein-protein interactions. Lamins are involved in DNA replication, RNA polymerase-II-dependent gene expression, RNA synthesis and processing, chromatin organization, spacing of NPCs, positioning of the nucleus in the cell, coupling of nucleoskeleton and cytoskeleton, development and disease, nuclear shape, nuclear size, nuclear deformation capacity, NE organization and NE assembly (for review see 38, 39 and references therein). The lamina's structural features and connections to INM proteins that are important in the context of this study are described below (Figure 1.3).

Lamins, the building blocks of the nuclear lamina, constitute a class of intermediate filaments (type V) and seem to exist only in metazoan cells.⁴⁰ Gene and protein sequence comparisons between mollusk and vertebrate lamins suggest that other intermediate filaments may have evolved from lamins.^{41, 42} Lamins are classified as A- and B-types, encoded by two genes. The tail domain of both classes carries a nuclear localization sequence (NLS).⁴³ Lamin B is posttranslationally modified by isoprenylation at its carboxy-terminal CaaX box.^{44, 45} The fatty acid is inserted into the inner leaflet of the INM and thereby anchors lamin B at the INM, in addition to its binding to LBR and other INM proteins. Class A lamins comprise lamin A and C and are derived from the same transcription unit by alternative splicing.⁴⁶ Lamin A retains an additional C-terminal region which is initially isoprenylated like lamin B but subsequently cleaved off by a specific metalloprotease.⁴⁷ Lamins form dimers with a central rod-like, α -helical coiled-coil domain and globular head and tail domains. Structures of higher organization are established by head to head and tail to tail polymerization.⁴⁸ The nuclear lamina has the form of a two dimensional lattice that permits a structural and functional link between the nuclear membrane, NPCs and chromatin. In *X. laevis* oocyte germinal vesicles the lamina is an interwoven network that links NPCs to each other.⁴⁹ The lamina extends into the nucleoplasm in some somatic cells.⁵⁰ Lamins bind to the INM proteins MAN1, LBR, LAPs, and nesprin-1 α *in vitro*.^{38, 51, 52} Lamins associate with chromatin proteins, for example with Histone2A or H2B dimers and BAF.³⁸ The numerous interactions of lamins with peripheral chromatin proteins and integral membrane proteins of the INM further indicate its functional complexity. Interestingly, depletion of only B-type lamins from

metazoan leads to cell death, whereas lamin A is mainly expressed in differentiated tissues and is thus not essential in all cells.^{53, 54, 55, 56, 57}

1.2.3 The nuclear pore complex

NPCs were initially characterized to understand how transport of a variety of very heterogeneous cargos like RNAs, proteins, or combinations thereof is accomplished. The present study examines the much less known roles of nucleoporins in postmitotic NE reformation. However, this must be put in context. First, the structure and composition of NPCs will be described, and the nucleocytoplasmic transport of diverse substrates discussed. Finally, the function of nucleoporins in NE assembly will be summarized.

1.2.3.1 Organization of the nuclear pore complex

Electron tomography analysis of yeast and *X. laevis* NPCs and very recent, cryoelectron tomography of transport-active nuclei from the protozoan *Dictyostelium discoideum* (*D. discoideum*) revealed the macroscopic structure of NPCs (Figure 1.4).^{58, 59, 60, 61, 62} The central part of the vertebrate NPC, that traverses the ONM and INM, can be subdivided into a cytoplasmic ring, a luminal spoke ring and a nuclear ring. Attached to the cytoplasmic ring are eight cytoplasmic filaments of ~50 nm length, whereas a fishtrap-like nuclear basket of ~100 nm extends from the nuclear ring. This basket is composed of nuclear filaments that are joined by a distal ring. NPCs show an 8-fold rotational symmetry axis that is perpendicular to the membrane plane. NPCs have distinct cytoplasmic and nucleoplasmic faces (for review see 63, 64, 65).

The central framework of the yeast NPC is simpler and smaller (calculated mass of 44 MDa) than a vertebrate NPC (60 MDa). Masses were predicted by proteomic analysis of respective NPCs.^{59, 66, 67} However, mass determination based on quantitative scanning transmission electron microscopy (STEM) determined ~66 MDa for *S. cerevisiae* and ~125 MDa for *X. laevis* NPCs.^{68, 69, 70} Isolated NPCs for mass determination might include transport complexes and other proteins peripherally connected to NPCs, leading to a higher mass prediction. Otherwise, loss of nucleoporins by subcellular fractionation or misprediction of the copy number of single nucleoporins might result in underestimation of NPC mass.

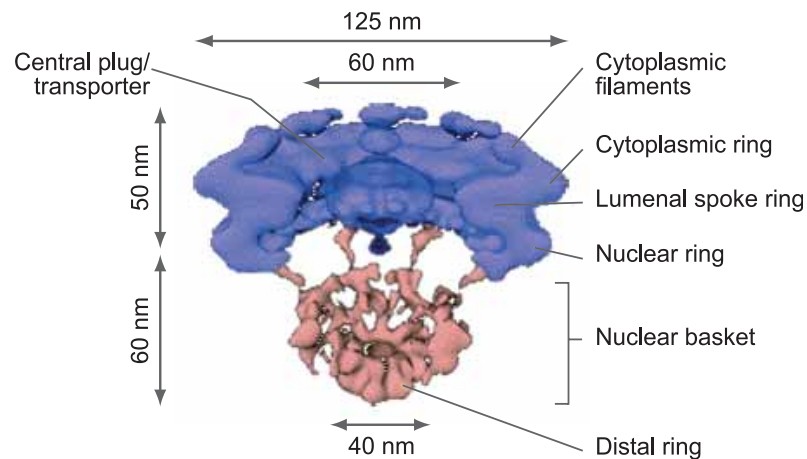


Figure 1.4: *Structure of the nuclear pore complex.* Vertical section through the structure of *Dictyostelium discoideum* NPC determined by cryoelectron tomography. Substructures and dimensions are labeled. Nuclear basket is colored red, central spoke ring complex and cytoplasmic filaments are depicted in purple. (Modified from Schwartz *et al.*, (2005). *Curr. Opin. Struct. Biol.* 15, 221-226.)

The overall dimensions of the *D. discoideum* NPC are 125 nm in diameter at its cytoplasmic face, 40 nm diameter at the distal nucleoplasmic ring and ~110 nm in total length.⁶² The narrowest point in the channel lies within the central pore and measures 45 nm and allows translocation of cargo complexes with a diameter of 35-40 nm (Figure 1.4).^{61, 71} It is currently a controversy whether the putative central plug or transporter in the pore is a well-organized structure. Most likely, the object represents either an integral component of the NPC or a mixture of cargoes caught in transit through the NPC. The shape, size and position of this structure are very dynamic, with two preferred positions along the transport axis. When NPCs are reconstructed with the central plug/transporter in one of these two positions, the resulting structures differ significantly. This indicates that the translocation of cargo through the pore might deform it.^{62, 72}

1.2.3.2 Structural features of nucleoporins

In this chapter structural characteristics of the NPC building blocks are addressed to explain their molecular functions.

NPCs were purified from yeast and rat liver nuclei and subjected to mass spectrometry to identify their protein composition. In both species, NPCs are composed of ~30 different nucleoporins that likely exist in multiples of eight due to the eight-fold rotational symmetry of the NPC.^{66, 67}

Investigation of tagged nucleoporins by immunoelectron microscopy showed that most nucleoporins are distributed symmetrically relative to the plane of the NE.

Some locate asymmetrically either on the cytoplasmic or nucleoplasmic side.^{73, 74, 75} Nucleoporins are very large proteins, often 100 kDa or more. Most are soluble proteins when not incorporated into the NPC, with only two well-characterized exceptions in vertebrates: the integral membrane proteins Pom121 and gp210, and three in yeast: Ndc1, Pom34 and Pom152.^{66, 76, 77, 78, 79, 80} Nucleoporins are mainly composed of four distinct domain structural elements: FG-repeat regions, coiled-coil domains, β -propellers and α -helical repeats (Figure 1.5).^{81, 85}

Eleven nucleoporins in yeast and ten in vertebrates contain FG-repeat regions. These are domains with multiple glycine-leucine-phenylalanine-glycine- (GLFG), FXFG-, and/or FG-repeats interrupted by polar amino acid residues.⁸² FG-repeat nucleoporins are localized at the cytoplasmic and nuclear periphery of the NPC and mediate interactions between nucleoporins and soluble transport receptors.⁶⁵ The FG-domains of eleven FG-nucleoporins in *S. cerevisiae* were systematically deleted in various combinations. It was postulated from these results that a minimal set of FG-domains is essential for nucleocytoplasmic transport through

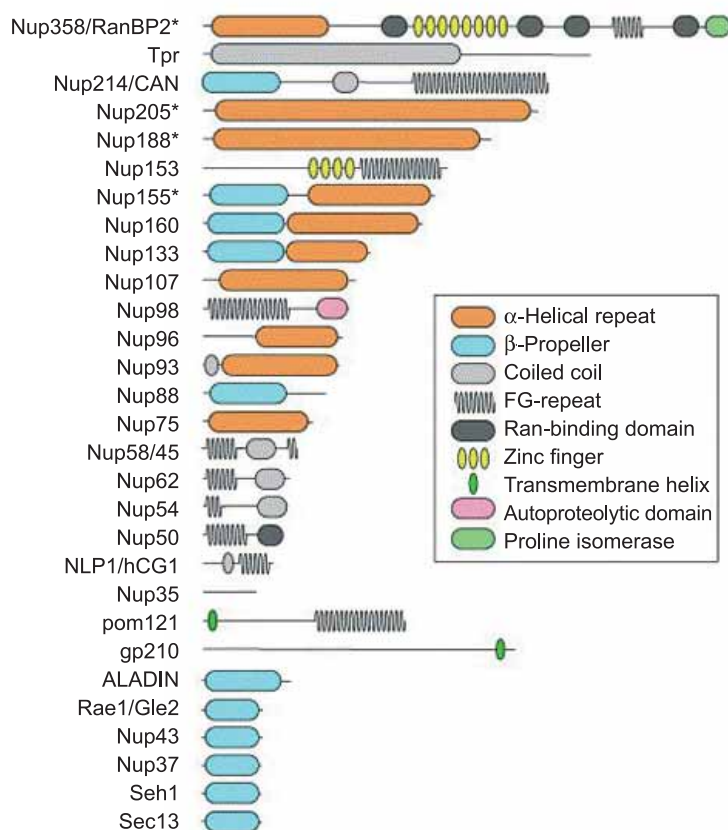


Figure 1.5: *Domain organization of vertebrate nucleoporins.* Structural elements and domains are indicated based on published data and predictions. (Modified from Schwartz *et al.*, (2005). *Curr. Opin. Struct. Biol.* 15, 221-226.)

NPCs. FG-domains on asymmetrically distributed nucleoporins seem dispensable, but specific combinations of symmetrically arranged FG-domains were required. Distinct transport pathways make use of specific FG-nucleoporins.⁸³ It was demonstrated that FG-repeats of nucleoporins in yeast constitute regions that lack an ordered secondary structure and appear “natively unfolded”. They may constitute an amorphous mesh of filaments that form a mechanical barrier for non-cargo proteins. The unfolded and flexible features of FG-repeats could enable multiple, simultaneous, and transient contacts with a variety of interaction partners.⁸⁴

A second structural feature of nucleoporins are coiled-coil domains that commonly mediate protein-protein interactions.⁸⁵

Thirdly, WD-repeats carried by some nucleoporins are predicted to be organized into β -propellers.⁶⁷ Even more domains in nucleoporins build a propeller fold, for example the N-terminal domains of human Nup133 and yeast Nup159 (homologue to human Nup214).^{85, 86, 87} The fourth domain element is constituted by α -helical repeats arranged to higher order structures in many nucleoporins.⁸⁵ Protein complexes that are constituents of the NPC framework, like the Nup107 complex, share the structural element of a β -propeller fold, an α -solenoid fold, or a defined combination of both (Figure 1.5).⁸⁸ Employing recent structure prediction tools and biochemical methods, it was hypothesized about a common progenitor of protein complexes that bends membranes as for example protein coat components in vesicular transport and NPCs.^{81, 89}

1.2.3.3 Molecular composition of the nuclear pore complex

An obvious matter of interest is how a large sophisticated structure like the NPC can be built of ~30 nucleoporins. Current knowledge on the vertebrate NPC is presented below.

Subcomplexes of nucleoporins were isolated from cell extracts and analyzed by mass spectrometry.^{90, 91} They are believed to function as building modules of the NPC. The Nup107 subcomplex is the best characterized.⁸⁸ Proteomic approaches, but also biochemical characterization of individual nucleoporins in addition to immunoelectron microscopy (EM) localization data have contributed to establish a nucleoporin interaction and localization map (Figure 1.6).^{66, 73, 85, 92, 93}

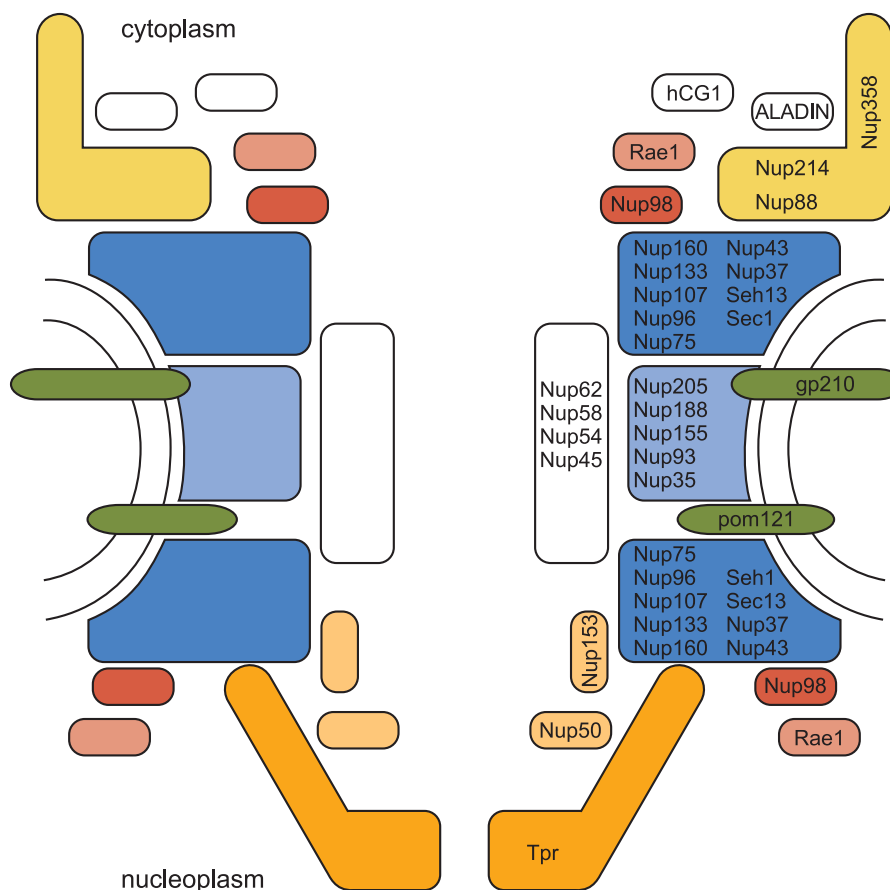


Figure 1.6: Schematic nucleoporin interaction map of a metazoan nuclear pore complex. Biochemically defined subcomplexes are grouped and illustrated in different colors. The illustration summarizes the present data and gives a simplified view of characterized interactions between nucleoporins. (Modified from Schwartz *et al.*, (2005). *Curr. Opin. Struct. Biol.* 15, 221-226.)

Some nucleoporins or nucleoporin subcomplexes that are relevant for the context of this study are introduced in more detail below.

Starting from the cytoplasmic side of the NPC, Nup358, also known as Ran binding protein 2 (RanBP2), is the core component of the long filaments that extend from the cytoplasmic face of the NPC (Figure 1.6).⁹⁴ Nup358 contains FG repeats, provides binding sites for import substrates, and displays SUMO E3 ligase activity.^{95, 96} Ran GTPase activating protein 1 (RanGAP1), an important regulator of the Ran mediated nucleocytoplasmic transport, binds to sumoylated Nup358.^{97, 98, 99} Nup358 has several RanGTP binding sites providing a platform on which RanGTP hydrolysis could take place by interaction with RanGAP.¹⁰⁰ Nuclear export sequence (NES) mediated transport was significantly reduced in the absence of Nup358. It is believed that Nup358 provides a platform for rapid disassembly of such transport complexes by the combined catalytic action of RanGAP and RanBP1 leading to RanGTP hydrolysis and release of the export cargo.^{101, 102} Despite Nup358's putative

role in Ran-driven transport, Nup358 depleted nuclei, reconstituted *in vitro*, were import competent, although NPCs lacked cytoplasmic filaments.¹⁰³ This suggests that the association of import cargo with the filaments might not be necessary to guide transport complexes to the pore. Association of import transport complexes with Nup358 could lead to their sumoylation, rather than being essential for translocation. Concordantly, RNAi against Nup358 in HeLa cells had no profound effect on the uptake of proteins into the nucleus but was essential for kinetochore function. Nup358 depletion severely perturbed chromosome congression and segregation.¹⁰⁴ In mitosis, Nup358 and its interaction partner RanGAP1 relocate to spindle microtubules and kinetochores.¹⁰⁵ Interestingly, further nucleoporins like the Nup107 complex and Rae1 colocalize together with cell cycle regulating checkpoint proteins Mad1 and Mad2 at kinetochores during mitosis.¹⁰⁶

Association of Nup358 with the NPC was found to be dependent on the presence of Nup214 and Nup88. All three nucleoporins co-immunoprecipitated as a subcomplex (Figure 1.6). However, Nup214 and Nup88 localization was not affected by absence of Nup358.¹⁰¹ Nup214 forms a cytoplasmically oriented subcomplex with Nup88/84 near the entrance of the translocation channel and is not part of the cytoplasmic filaments.^{103, 107, 108} Nuclei formed in *X. laevis* egg extracts devoid of Nup214, show only minor reduction in NLS-mediated protein import.¹⁰³

The vertebrate Nup107 complex consists of nine components: Nup107, Nup133, Nup160, Nup96, Nup75, Nup37, Nup43, Seh1 and the coatamer II protein (COPII) Sec13 (Figure 1.6).⁸⁸ The yeast homologue of the Nup107 complex, the Nup84 complex, was reconstituted from seven known subunits *in vitro* and the structure determined by EM showed a Y-shaped multiprotein complex.¹⁰⁹ This complex was estimated to constitute a major part of the octagonal spoke-ring complex by contributing 16 copies of the y-shaped subcomplex localizing symmetrically around the cytoplasmic and the nuclear ring moiety.^{63, 75} One hypothesis is that the conserved Nup107 complex correlates with an early assembly intermediate, the star-ring region, consisting of eight triangular subunits, observed by high resolution scanning EM.^{110, 111} Yeast Nup84 complex and vertebrate Nup107 complex have also been implicated in mRNA export from the nucleus.^{112, 113, 114, 115} As mentioned above, a fraction of the vertebrate Nup107 complex localizes to kinetochores during mitosis.^{88, 111} In contrast to its stable integration into NPCs during interphase, the association with kinetochores is dynamic. It is hypothesized that the

pool of kinetochore associated Nup107 complex might serve as an early platform for NPC formation on chromatin after mitosis.¹¹¹ Nup107 complex function in NE assembly in *X. laevis* egg extracts will be discussed below (chapter 1.2.5).

Two further nucleoporin subcomplexes have been described in vertebrate NPCs. Nup93-Nup205-Nup188 form a subcomplex, of which Nup93 and Nup205 reside in the center of the pore.^{75, 116, 117} Nup35 was recently shown to interact with Nup93, Nup155, Nup205 and lamin B and at least the Nup35-Nup93 interaction was shown to be direct.¹¹⁸ *In vitro* characterization of the Nup93 complex was performed in the *X. laevis* egg extract system by immunodepletion of the complex. These experiments proposed a putative function of Nup93 complex important for nuclear morphology since assembled nuclei were smaller than control nuclei, but still capable of NLS-substrate transport. DNA replication occurred later than in control nuclei. Localization of several other nucleoporins to the nuclear rim was impaired upon Nup93 complex depletion and the number of complete nuclear pores seemed to be reduced. However, the specificity of the observed defects was not confirmed as the restoration of the phenotypes by readdition of recombinant protein was not demonstrated.¹¹⁶ In *C. elegans*, depletion of Nup93 or Nup205 by RNAi resulted in ~100% embryonic lethality and slightly smaller nuclei than in control embryos. Strong and abnormal peripheral condensation of chromosomes was also observed. NPCs aggregated in the NE and allowed passive diffusion of a 70 kDa dextran unlike control NPCs, but a 160 kDa fluorescent reporter molecule was excluded from the nucleus, indicating that the nuclei were enclosed by intact NEs. In addition, protein import was not impaired.¹¹⁹

The Nup62-Nup58-Nup54-Nup45 complex is believed to decorate the pore center symmetrically and possibly to line the transport channel (Figure 1.6).^{120, 121} NPCs devoid of the Nup62 complex were defective in nuclear transport.¹²² Recombinant Nup62, Nup58 and Nup54 were shown to directly interact with transport factors.¹²¹

Little is known about vertebrate Nup155. It was isolated from rat liver nuclei by urea extraction, characterized as a nucleoporin, and localized by immuno EM at the nucleoplasmic and cytoplasmic side of the NPC.¹²³ The relative abundance of Nup155 was estimated at 32 copies per NPC.⁶⁷ In a genome-wide yeast-two-hybrid screen, human Gle1 was found to interact with human Nup155. The binding was confirmed *in vitro* with bacterially expressed Gle1 and Nup155 produced in rabbit

reticulocyte lysate.¹²⁴ Gle1 is required for mRNA export and localizes to NPCs in yeast and human cells.^{63, 125} Human Nup155, Gle1 and CG1 formed a heterotrimeric complex *in vitro*.¹²⁶ Since Nup155 is one of the proteins characterized in this work, a more comprehensive view of its implicated functions is presented in a later chapter of the introduction.

The nuclear filaments emanating from the NPC core structure towards the nuclear interior are composed of Tpr (translocated promoter region) which are suggested to form the main architectural element of the nuclear basket (Figure 1.6).^{75, 127} Wild type and recombinant Tpr are capable of forming homodimers *in vivo* and *in vitro* and are proposed to bind as such to the NPC core. The rod-shaped Tpr coiled-coil region can extend to >100nm.¹²⁸ The C-terminal end of Tpr is assumed to form the terminal ring of the nuclear basket.⁷⁵ It is only peripherally attached to the NPC and does not seem to provide a scaffold for other nucleoporins. Nup153 is part of the nucleoplasmic coaxial ring of the NPC.¹²⁹ It interacts directly with Tpr and has been proposed to connect to the nuclear basket (Figure 1.6).^{75, 130}

In vitro reconstituted nuclei in *X. laevis* egg extracts devoid of Nup153 lack Tpr, Nup93, and Nup98, further components of the nuclear basket. These nucleoporins were not co-depleted with Nup153. Nucleoporins of the cytoplasmic face of the NPC and general FXFG nucleoporins did not seem to be affected upon Nup153 removal. NPCs without these basic components of the nuclear basket and intranuclear filaments are mobile within the plane of the NE. NPC anchoring might thus occur via the nuclear lamina and any of the nucleoporins mislocalized upon Nup153 depletion.¹²⁹ Furthermore, Nup153 has been reported to interact with at least one type of lamin in *X. laevis* egg extracts.¹³¹ Absence of Nup153 leads to a strong reduction of importin α/β mediated import.¹²⁹

Two characterized transmembrane nucleoporins sit in the nuclear membrane. They are components of both NPCs and the nuclear membrane and therefore were believed to be potentially important for NE formation and NPC anchorage. The NPCs penetrate ONM and INM that fuse at the positions of pore insertion. As NPCs are the only known mediators of transport or diffusion between nucleus and cytoplasm, the NE must be otherwise sealed. The tight link between NPCs and the nuclear membrane might be established by two type I integral membrane nucleoporins, the pore membrane protein of 121 kDa (Pom121) and the glycoprotein gp210

(Figure 1.6).^{132, 133, 134} The C-terminus of Pom121 predominantly consists of FXFG-repeats that extend into the nuclear pore. The transmembrane segment is situated at the N-terminal region.¹³² In contrast, gp210 exposes only a short C-terminal tail towards the pore, whereas its main N-terminal section resides in the intraluminal space between ONM and INM (Figure 1.6).¹³⁵ Both pore membrane proteins were believed to be candidates that putatively anchor the NPC in the NE membrane.^{132, 134} gp210 was described to be required for viability in HeLa cells and *C. elegans* embryos, in which its knock down by RNAi led to aberrant membrane structures of the NE and clustered NPCs.¹³⁶ Interestingly, gp210 is the only nucleoporin found to be cell-type specifically expressed during mouse organogenesis.¹³⁷ These observations underline the interesting question of whether NPC composition varies in different cell types and at the same time make gp210 a weaker candidate for an essential function like NPC anchorage. Pom121 is indeed an important player in nuclear reconstitution *in vitro* and will be addressed in detail below (chapters 1.2.1.4 and 1.2.5).

Some nucleoporins, for example Nup214, Nup98, and Nup62 are posttranslationally modified by O-linked N-acetylglucosamines (O-GlcNAc) at levels that remain constant during the cell cycle, whereas phosphorylation of nucleoporins occurs during mitosis.¹³⁸ NPCs devoid of N-acetylglucosamine-bearing nucleoporins show normal morphology, but are defective for import of a reporter substrate carrying an NLS.¹³⁹ The function and regulation of glycosylation and phosphorylation of nucleoporins is largely unknown.^{138, 140}

1.2.3.4 Dynamics of the nuclear pore complex

From the dynamic behavior of individual nucleoporins it can be inferred whether they function as stable core components of the NPC, and thus are likely to play a role in NPC assembly. Several aspects of NPC dynamics in live cells were investigated by confocal microscopy and fluorescence photobleaching techniques, like turnover and mobility of NPCs in the NE.

Monitoring of GFP-tagged Pom121, Nup153, and lamin B in live cells demonstrated that NPCs did not move individually in the plane of the NE. NPCs and nuclear lamina movement is tightly correlated and both form an elastic two dimensional network: NPCs and the lamina move synchronously. This led to the conclusion that lamins and NPCs are part of one stable network in the nuclear

periphery.¹⁴¹ Pursuing initial observations of Pom121 and Nup153 mobility within NPCs, 19 stable cell lines expressing different EGFP-tagged nucleoporins were generated to map the functional dynamics of the entire pore complex. Dissociation rates of individual nucleoporins were measured by inverse fluorescence recovery after photobleaching (iFRAP) and nucleoporins grouped into three categories: scaffold nucleoporins with residence times of more than 35 h, adaptor nucleoporins associating with NPCs for 2.5 h - 30 h, and dynamic nucleoporins with residence times at NPCs below 2.5 h.

All examined members of the Nup107 complex associated very stably with NPCs, indicating that the subcomplex bound as one unit to the NPC and could form a scaffold onto which other nucleoporins associated. Other potential scaffold nucleoporins are Nup214, Nup93 and Aladin. However, NPC integrity was not strongly disturbed in nuclei lacking Nup214 or Aladin.^{103, 142} The second most stable class comprises Pom121, Nup62, Nup58, CG1, Nup35 and Nup98. These nucleoporins were suggested to function as scaffold adaptors by assembling on top of the stable core nucleoporins. gp210 had an average residence time of only 5 min, which argues against a function in NPC anchorage. Nup50 and Nup153 were assigned to the group of dynamic nucleoporins and presumably have regulatory or transport related roles.¹⁴³

1.2.4 Nucleocytoplasmic transport

As mentioned above, transport through the pore has been comprehensively studied. Both NPC assembly and nucleocytoplasmic transport are regulated by the GTPase Ran. This is illustrated in the context of protein import and export.

Proteins functioning in replication, transcription, splicing, and all other nuclear processes must be imported into the nucleus after their synthesis in the cytoplasm. Vice versa, mRNAs, tRNAs, U snRNAs and other components required for protein synthesis must be exported. Soluble transport receptors that specifically recognize and shuttle cargo, mediate most transport events. Three major transport receptor classes are distinguished by their type of cargo: the importin β family of transport receptors, NTF2, and mRNA export receptors. Importin β -like transport receptors can function as importins (transferring cargo into the nucleus) or exportins (out of the nucleus) or even in both directions for protein or RNA cargos. Transport receptors release their load at its destination and recycle back to the opposite site of the NPC,

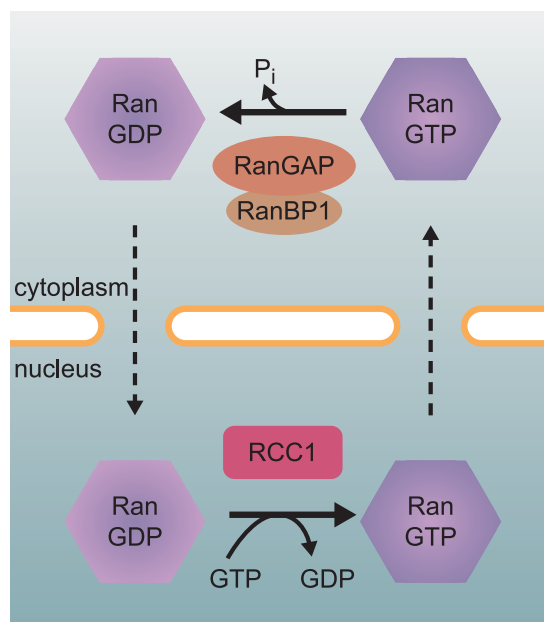


Figure 1.7: *The Ran cycle in nucleocytoplasmic transport.* RanGDP is transported into the nucleus where RCC1 catalyzes the dissociation from GDP and enables GTP binding to Ran. Subsequently, RanGTP-export complexes shuttle back to the cytoplasm. There, GTP-hydrolysis, catalyzed by RanGAP and RanBP1, generates RanGDP. (Modified from Hetzer *et al.*, (2005). *Annu. Rev. Cell Dev. Biol.* in press.)

where they are reloaded with new cargo. How transport occurs is best understood for the family of importin β transport receptors that requires the small GTPase Ran.^{144, 145} The regulatory functions of Ran not only comprise nucleocytoplasmic transport, but also formation of the mitotic spindle as well as NE and NPC assembly.¹⁷ Therefore, the principle of Ran driven processes will be explained by the example of Ran dependent transport. Like all GTPases that mediate energy consuming processes, Ran's function necessitates a guanine nucleotide exchange factor, RanGEF, which promotes GDP dissociation from Ran and subsequent binding of GTP. The GTPase activating protein (RanGAP) catalyzes the hydrolysis of Ran bound GTP to GDP with the help of RanBP1 and RanBP2.¹⁴⁴

Key characteristic of the Ran cycle is that RanGEF (RCC1) and RanGAP are spatially separated (Figure 1.7). RCC1 binds to chromatin through an interaction with core histones and resides in the nucleus, whereas RanGAP and RanBP1/BP2 are restricted to the cytoplasmic side of the NE. In metazoan cells, RanGAP binds in its sumoylated form to cytoplasmic NPC filaments via RanBP2.¹⁴⁶ The local separation of RanGEF and RanGAP generates a RanGTP gradient across the NE, with high RanGTP concentration in the nucleus, that is coupled to nucleocytoplasmic transport (Figures 1.7 and 1.8). Importins bind their substrate in the cytosol either directly or via

an adaptor molecule. Importin α is an adaptor that recognizes cargo carrying a basic, lysine rich nuclear localization signal (NLS). Importin α bridges the association of cargo with the import receptor importin β .^{147, 148} Inside the nucleus, RanGTP binds to importin β and displaces importin α and the imported substrate (Figure 1.8). Importin β -RanGTP leaves the nucleus and the transport receptor is recycled after RanGTP hydrolysis upon interaction with RanGAP and RanBP1/BP2 at the cytoplasmic NPC filaments.

In contrast to importin β -cargo complexes that are destabilized by RanGTP, export complexes are stabilized by RanGTP binding. The exported substrate is released as described above when GTP hydrolysis occurred and the export complex disassembles. The empty exportin recycles back into the nucleus. Importin α is guided back to the cytoplasm by the export receptor CAS and RanGTP (Figure 1.8). Equivalent to importin β , CRM1 is a multivalent export receptor making use of a

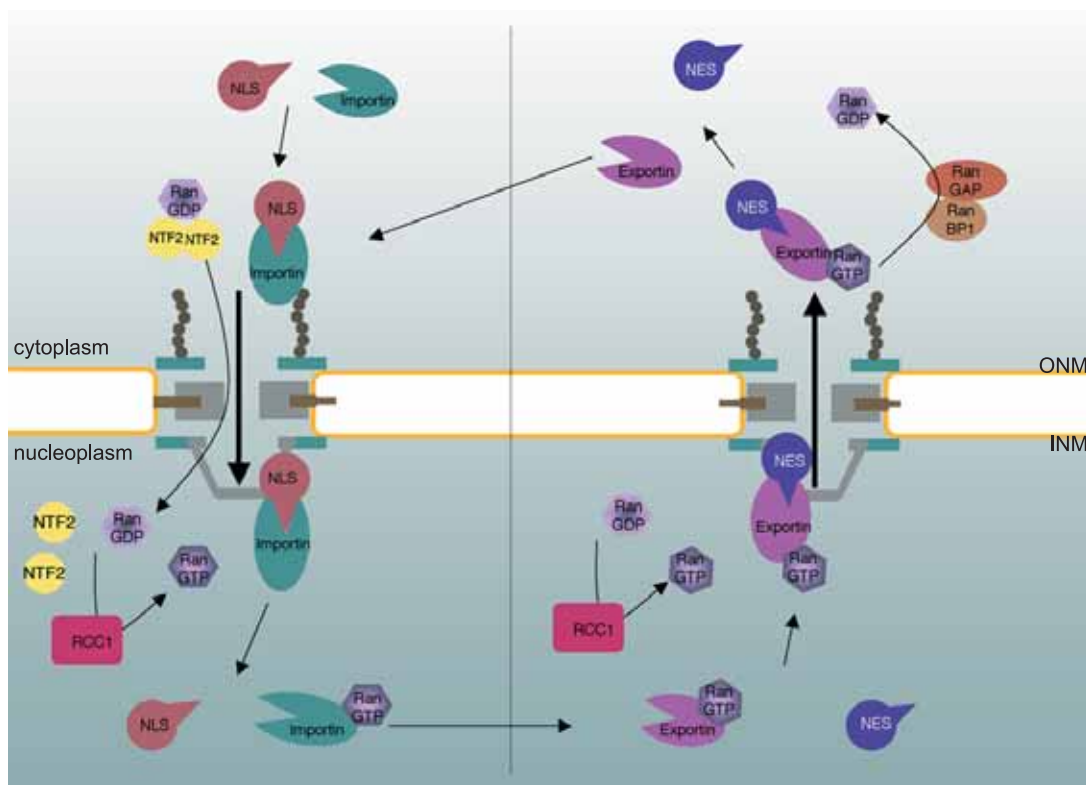


Figure xx: *Ran driven nucleocytoplasmic transport cycle.* A transport receptor of the importin β family associates with an NLS carrying substrate in the cytosol and shuttles through the NPC into the nucleus (left side). The transport cargo is released from its receptor by RanGTP binding to the import receptor which is recycled back to the cytoplasm. Export receptors form a complex with RanGTP and an NES containing export substrate and translocate to the cytoplasm. Hydrolysis of GTP to GDP occurs at the cytoplasmic filaments in the presence of RanGAP and RanBP1. The export complex disassembles (right side). To complete the Ran cycle, NTF2 transports RanGDP back into the nucleus. Chromatin bound RCC1 mediates nucleotide exchange of GDP with GTP on Ran. (Adapted from Hetzer *et al.*, (2005). *Annu. Rev. Cell Dev. Biol.* in press.)

variety of cofactors to shuttle a diverse group of cargoes. A major class of CRM1 substrates are proteins with a leucine-rich nuclear export signal (NES).^{149, 150} To complete a cycle, RanGDP is imported back into the nucleus by the small nuclear transport factor 2 (NTF2).¹⁵¹

NTF2 represents the second class of transport receptors with RanGDP as its only cargo. RanGDP release is imparted by nucleotide exchange on from RanGDP to RanGTP on Ran in the nucleus, leading to dissociation of RanGTP and NTF2 (Figure 1.8). This very efficient trafficking process takes place independently of the RanGTP gradient.^{17, 144, 145}

Members of a third class of nuclear transport receptors export mRNA. These receptors are heterodimers comprised of TAP and p15 in metazoa and Mex67 and Mtr2 in yeast.¹⁵² RanGTP depletion from the nucleus does not seem to have a direct effect on mRNA export but indirectly impairs the recycling of proteins needed for mRNA trafficking.^{153, 154}

Interestingly, Ran also functions as a positional marker for chromatin during mitosis in the absence of an NE. Local generation of RanGTP around chromosomes affects microtubule organization and induces the formation of microtubule asters and spindles.^{155, 156, 157, 158} Importin β sequesters proteins exhibiting an aster-promoting activity during mitosis and renders them inactive. In the vicinity of mitotic chromosomes, RCC1 creates RanGTP that locally releases the aster-promoting factors from importin β , similar to liberating import cargo.^{159, 160, 161} Thereby, Ran regulates the formation of a mitotic microtubule network.

1.2.4.1 Postmitotic reassembly of the nuclear envelope

The introduced structural components of the NE reassemble around the decondensing chromatin and thereby complete “open mitosis” in multicellular organisms. This process constitutes the key event of the presented study. A wealth of data derives from genetic studies in *C. elegans* as well as *in vivo* real time microscopy. Several *in vitro* systems that reconstitute NE assembly, permit biochemical interference. Altogether, the results obtained compose the current model for reformation of the nuclear membrane, assembly of NPCs and organization of the nuclear lamina after mitosis.

Present knowledge about the role of lamins in nuclear reformation proposes that they are not essential, since lamins are transported into the nucleus and

accumulate at the nuclear periphery to form the intranuclear lamina meshwork after the formation of the nuclear membrane and NPCs.^{141, 162, 163}

Next, the behavior of membrane proteins in the process of NE reformation will be discussed. LBR-GFP residing in the INM was monitored by high resolution confocal time-lapse imaging in mitotic cells. LBR redistributed into the interconnected ER membrane system during mitosis, suggesting that ER integrity was maintained.¹⁶⁴ Other live cell imaging studies support the observation that INM proteins are absorbed into the mitotic ER network and diffuse from there back to the INM where they are retained by specific protein-protein interactions established at the end of mitosis.^{141, 164, 165}

In contrast, *in vitro* systems that employ embryonic extracts to reconstitute nuclei, describe distinct membrane vesicle populations that participate in NE assembly. The apparent discrepancy between *in vivo* studies reporting an intact ER network during mitosis that absorbs INM proteins and the characterization of functionally and molecularly distinct vesicle populations in embryonic extract systems could be explained by the existence of ER microdomains in which INM proteins are locally enriched. These would fragment into vesicles during extract preparation, resulting in biochemically diverse membrane vesicle fractions.^{166, 167}

At least two different vesicle groups were discovered that vary slightly during mitosis in their functions depending on the system used and the method of membrane preparation. One vesicle type associates with chromatin and the second is reported to either insert into a closed pre-NE and to support NE growth, or to be necessary for initial NE vesicle fusion.^{168, 169, 170, 171, 172} Importantly, Pom121 and gp210 were identified as specific components of two different vesicle fractions that were recruited to the reforming NE at different time points and that can be depleted independently from *X. laevis* egg extract.¹⁷³ Two distinct protein complexes were characterized that specifically promoted distinct fusion steps required for NE but not for ER formation. Nuclear membranes that dock to chromatin cannot fuse in the absence of a trimeric complex composed of the AAA-ATPase p97 and its adaptors Ufd1 and Npl4. The same fusion step requires the GTPase Ran discussed below. p97-Ufd1-Npl4 and Ran did not play a role in ER formation arguing that ER and NE reconstitution are distinct processes with different molecular requirements *in vitro*.¹⁶⁶ p97's complex with p47 does not participate in the early NE fusion step but is essential for NE growth, involving further insertion of nuclear membrane vesicles into

the initial closed NE. In contrast to p97-Ufd1-Npl4, p97-p47 complex is crucial for ER formation.¹⁷⁴

Distinct membrane vesicle populations are targeted to chromatin by specific protein-protein interactions. As already discussed, several INM proteins bind chromatin associated proteins like HP1 or BAF and thereby likely target membranes to chromatin at the end of mitosis. LBR is capable of targeting NE membranes to chromatin *in vitro* and is known to bind to HP1 and histones.^{37, 175} Nevertheless, none of these interactions was proven to be essential for NE formation.

The importance of Ran in NE assembly was already mentioned and comes into play at the point of membrane vesicle fusion. In the *X. laevis* egg extract *in vitro* system, NE formation necessitates generation of RanGTP from RanGDP by RCC1 and subsequent GTP hydrolysis, in short, a complete Ran cycle. Vesicle fusion to form a closed NE is blocked by GTP γ S and hence, NPCs do not assemble.^{176, 177, 178} Similarly, it is possible to assemble nuclei around RanGDP coated sepharose beads incubated in *X. laevis* egg extracts. These pseudo nuclei possess NPCs, a nuclear lamina and mediate specific transport.¹⁷⁹

Another regulatory element displays dual functions in transport and fusion of nuclear membranes. Employing natural chromatin templates for NE assembly in *X. laevis* egg extracts, importin β seems to negatively regulate membrane fusion. This block can be reversed by RanGTP addition.¹⁸⁰ Finally, the transport cargo adaptor importin α also displays a postmitotic role. An NLS-protein independent function for importin α was described and proposes that membrane association of importin α , regulated by phosphorylation, is required for NE formation.¹⁸¹

The central role of the components of the Ran cycle, as well as importin α and β , in NE formation was confirmed *in vivo* by RNAi in *C. elegans*.^{182, 183}

1.2.5 Regulation of nuclear pore complex assembly

Importin β and Ran affect NPC assembly after mitosis in addition to their roles in nucleocytoplasmic transport and NE membrane formation (see above). Two independent studies by Harel *et al.*, (2003) and Walther *et al.*, (2003) provided evidence that NPC assembly in *X. laevis* egg extracts is regulated via the binding of several nucleoporins to importin β that are released by RanGTP, generated in the vicinity of chromatin at the place of NE reformation.^{180, 189} In NE assembly reactions

without a chromatin template, NPCs formed into annulate lamellae (AL) upon RanGTP stimulation.¹⁸⁴ AL are found in the cytoplasm and consist of flattened membrane cisternae that are perforated by numerous densely packed pore complexes lacking chromatin and lamina. Frequently, these structures are observed in rapidly growing or differentiating cells, such as male and female gametes, tumor cells, and virally infected cells.¹⁸⁵ Harel *et al.*, (2003) described two distinct steps in NE and NPC formation and proposed different functions for importin β . The fusion of docked membranes around a chromatin template was inhibited by importin β and could be triggered by RanGTP. An importin β mutant, deficient in binding to Ran and importin α , enabled membrane fusion to a closed membrane that lacked NPCs. This indicates that the release of nucleoporins bound to importin β upon RanGTP guides NPCs to the NE.¹⁸⁰ Walther *et al.*, (2003) showed that the binding of Nup107, Nup153 and Nup358 to chromatin is triggered by RanGTP or the hydrolysis deficient RanQ69L mutant as a consequence of their release from importin β .¹⁸⁶ In summary, these data suggest that nucleoporins are targeted to chromatin by RCC1 that generates RanGTP. This in turn displaces nucleoporins from importin β . A genetic approach in *S. cerevisiae* also indicated a role for the RanGTPase cycle in yeast NPC assembly *in vivo*.¹⁸⁷

A closed NE membrane devoid of NPCs can be formed under the following conditions: presence of an importin β mutant deficient in RanGTP and importin α binding, addition of the Ca^{2+} chelator BAPTA, or absence of the Nup107 complex. These results indicate that the integrated process of nuclear membrane fusion and NPC assembly can be uncoupled under certain conditions.

Two different models are currently postulated for NPC insertion into the NE. One model postulates that NPCs are always assembled into membranes, either in membrane vesicles or in a closed NE.^{171, 177, 180} Another model distinguishes between postmitotic NPC and NE assembly that initiates isochronically on chromatin and an S-phase situation in that an NE already exists into which additional NPCs are either inserted or existing NPCs are divided by a yet unknown mechanism.^{2, 184, 188, 189}

The following data provide evidence for postmitotic NE formation initiating on chromatin. Assembly of the nuclear membrane and NPCs takes place in an interdependent manner (Figure 1.9, left picture).

After mitosis the Nup107 complex concentrates at the nuclear periphery during

anaphase, well in advance of Nup62 as shown by co-immunofluorescence on fixed HeLa cells.^{111, 190} Its early recruitment to chromatin after mitosis and low mobility make the Nup107 complex a potential scaffold nucleoporin onto which other nucleoporins assemble. This points toward an essential role of the Nup107 complex in NPC formation.¹⁴³ Two independent studies investigated this aspect by RNAi in HeLa cells and *in vitro* in the *X. laevis* egg extract system.^{189, 191} Knock down of components of the Nup107 complex by RNAi reduced other nucleoporins stained by mAb414 and led to nuclei with reduced NPC number. RNAi against Nup133 induced AL formation in the cytoplasm, most likely due to unbalanced nucleoporin levels.¹⁸⁹ Employing Nup107 complex immunodepleted *X. laevis* egg cytosol in nuclear reconstitution reactions led to the formation of sealed nuclear membranes around sperm chromatin that are devoid of NPCs, similar to nuclei assembled in the presence of BAPTA or an importin β mutant (Figure 1.9, right picture).^{189, 191} The BAPTA block of NPC assembly occurs downstream of the Nup107 complex function.¹⁸⁹ The integral membrane nucleoporins Pom121 and gp210 are not concentrated at the rim of the NE in Nup107 complex devoid nuclei.¹⁹¹ The Nup107 complex binds to chromatin earlier than for example mAb414 antigens and before membrane vesicles fuse to enclose the chromatin, suggesting that the nuclear membrane and NPCs assembly occurs isochronically.¹⁸⁹ The processes can be uncoupled in the presence of BAPTA, by an excess of Importin β , or by the absence of Nup107 complex.^{177, 180, 189} Interestingly, in an *in vitro* nuclear assembly time course, Nup107 localizes at the decondensing chromatin template at about the same time as Pom121, but before mAb414 antigens.^{173, 189} However, depletion of the integral membrane nucleoporin Pom121 results in a block of nuclear membrane fusion and NPC assembly (Figure 1.9, middle picture).¹⁷³ The arrest in NE vesicle fusion was restored by readdition of purified Pom121 reconstituted into liposomes and added to the Pom121-depleted detergent extract.¹⁷³ It seems intriguing that Pom121 depletion blocked nuclear membrane vesicle fusion upstream of the function of the Nup107 complex, whose absence led to a closed nuclear membrane lacking NPCs.¹⁸⁹ However, a double depletion of both Pom121 from membranes and Nup107 complex from the cytosol resulted in nuclei with closed nuclear membranes devoid of NPCs, i. e. the “Nup107 phenotype” (Figure 1.9, right image).¹⁷³ In conclusion, in the absence of Nup107 complex, Pom121 is not required for nuclear

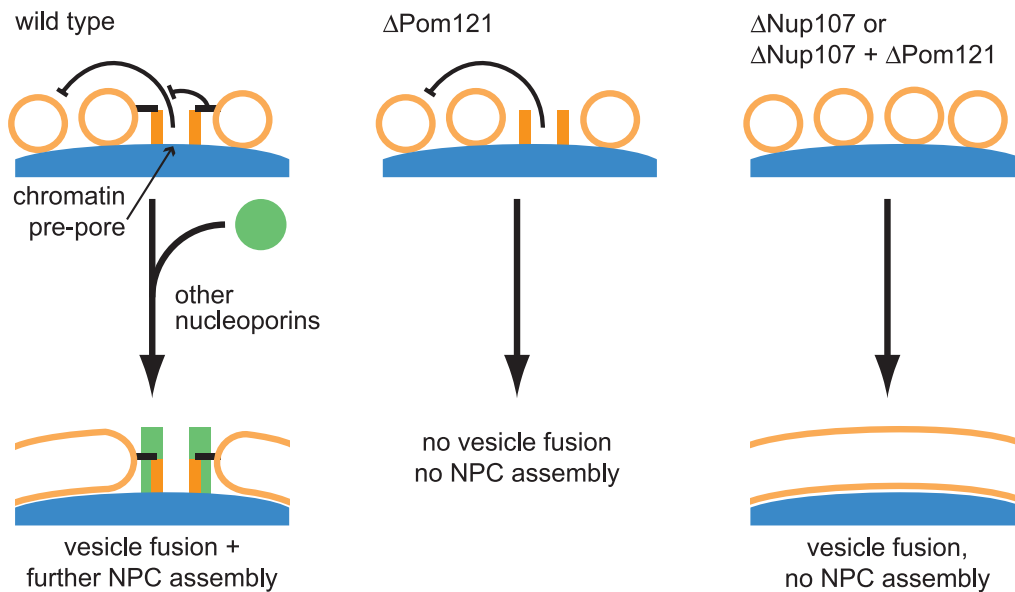


Figure 1.9: *Model for the roles of Nup107 complex and Pom121 in postmitotic NE assembly.* In the wildtype situation (left) at the end of an open mitosis, the Nup107 complex and maybe other nucleoporins are recruited to chromatin forming a “pre-pore”. At the same time, membrane vesicles dock to the chromatin template. Subsequently, additional nucleoporins are recruited to the prepore forming an NPC and in parallel the nuclear membrane seals. In the absence of Pom121 (middle) and in the presence of the “pre-pore”, neither NPC assembly nor nuclear membrane vesicle fusion can proceed. However, depletion of the Nup107 complex alone or in combination with Pom121 (right) releases the block on nuclear membrane fusion transmitted upon the failure of Pom121 and leads to a closed nuclear membrane devoid of NPCs (right). (Modified from Antonin *et al.*, (2005). *Mol. Cell* 17, 83-92.)

membrane vesicle fusion and therefore, Nup107 complex is responsible for the block in membrane fusion upon Pom121 depletion from membranes. Furthermore, nuclear membrane vesicles can fuse in the absence of Pom121 proving that it is not essential for the formation of a closed nuclear membrane. Recruitment of soluble Nup107 complex and Pom121-carrying membrane vesicles to chromatin occurs independently. Removal of the second integral membrane nucleoporin, gp210, from an NE assembly reaction did not lead to a defect in nuclear membrane fusion or NPC assembly.¹⁷³ Moreover, the relatively late recruitment of gp210 to the nucleus after mitosis *in vivo* and *in vitro* rather indicates a function different from NE reformation.^{173, 190} These data clearly argue for a postmitotic NE formation model that is initiated at the chromatin template. Nuclear membrane and NPC formation are functionally linked and both processes seem to be controlled and lead to a block after Pom121 removal.

A whole series of soluble nucleoporins was depleted from *X. laevis* egg extracts so far, like N-acetylglucosamine-modified nucleoporins, the Nup62 complex, Nup98, Nup93 complex, Nup214, Nup358, and Nup153. However, depletion of these

nucleoporins did not lead to a similar inhibition in NPC and/or NE assembly as depletion of Pom121 or the Nup107 complex.^{103, 116, 122, 129, 139, 192}

1.2.6 *X. laevis* nuclear reconstitution system

Addressing the molecular mechanism of a cellular process requires an adequate system that permits dissection and manipulation of the biological activity of interest. Reassembly of the NE around decondensing chromatin represents a fundamental and multifaceted procedure that is difficult to address as a whole.

Yeast genetic screens were successfully employed to identify proteins involved in a wide variety of cell biological processes but cannot be applied to identify candidates that participate in postmitotic NE assembly since yeast undergoes closed mitosis.^{2, 4}

Genome wide systematic RNAi knock down studies in *C. elegans* have described and grouped candidates leading to defects in pronuclear/nuclear appearance that require further biochemical investigation.^{193, 194, 195, 221} Microscopy of fluorescently tagged proteins in living cells gave insight into redistribution of NE proteins during mitosis. However, the process of NE assembly is difficult to manipulate experimentally in intact cells.^{141, 196, 197} For this reason, cell free extracts of vertebrate cells to study NE assembly were developed.^{198, 199} Their disadvantages are that only little material can be recovered and cells must be synchronized in metaphase to obtain disassembled NE precursors. In addition mitotic chromosomes are difficult to remove and to replace with another chromatin source.²⁰⁰

Lohka and Masui established the first *in vitro* nuclear assembly system by preparation of cell-free extracts from eggs of the amphibian *Rana pipiens*.²⁰¹ Eggs of many species possess stockpiles of NE precursors and other nuclear proteins to permit rapid mitotic divisions upon fertilization.²⁰² Protein synthesis does not take place during these early embryonic cell cycles. These qualities make them a rich and therefore, biochemically valuable source of components required for *in vitro* NE formation. When demembrated sperm nuclei were incubated with egg extract, an NE formed, chromatin decondensed, and DNA synthesis was initiated.²⁰¹ Cell-free extract with similar qualities could also be prepared from *X. laevis* eggs employed here.²⁰³

Mitotic and interphase *X. laevis* egg extracts can be prepared depending on how the eggs are manipulated.

An immature oocyte is arrested in interphase. Under native conditions progesterone secretion by follicle cells induces completion of meiosis I. Subsequently, the oocyte enters meiosis II, which primes it for ovulation. This process can also be induced by injecting pregnant mare serum gonadotropin (PMSG). Next, oocytes are arrested at metaphase of meiosis II, ovulate and are ready for fertilization. The ovulation of mature oocytes can be stimulated with human chorionic gonadotropin (hCG). Penetration of the egg by a sperm induces a transient cytoplasmic Ca^{2+} increase, which is the signal for release of the metaphase arrest. The oocyte completes meiosis II, enters interphase, and starts early embryogenesis by a series of rapid mitotic cell divisions. Fertilization can be mimicked *in vitro* by applying an electric shock or adding a calcium ionophore. These treatments release the eggs from metaphase arrest. Extracts of such activated eggs will complete meiosis II and assemble a nucleus.²⁰⁴ The *in vitro* assembled nuclei are able of nucleocytoplasmic transport and DNA replication.^{205, 206}

X. laevis eggs that are maintained in metaphase II arrest are utilised to generate extracts that mimic mitotic events like spindle assembly. During extract preparation eggs are not activated to imitate fertilization and release calcium, on the contrary, calcium chelator EGTA and competitive phosphatase inhibitors are added to prevent dephosphorylation of cell cycle regulators. However, mitotic extracts can be cycled *in vitro* by addition of calcium to complete mitosis and establish an interphase situation.^{207, 208} The extract is thus capable of reproducing an entire embryonic cell cycle.

Therefore, the cell-free *X. laevis* egg extract system is well suited for manipulation and permits the investigation of complex cellular processes. Components can be depleted from the extract, their absence can be examined in a mitotic or interphase process and restored by addition of purified components proving the specificity of observed phenotypes.^{103, 116, 122, 129, 173, 189, 191, 192, 209}

1.3 Aim of the project and introduction of Nup155 and Mel28

This study investigated two proteins with a potential role in postmitotic NE formation: Nup155 and Mel28, employing the *X. laevis* egg extract nuclear reconstitution system. Both candidates caused severe defects in nuclear morphology by RNAi knock down in *C. elegans* but neither was functionally characterized. *In vitro* NE assembly permits depletion of proteins of interest from the system, generating a

genuine loss-of-function situation. Restoration of observed phenotypes by addition of recombinant protein assigns specific functions to the investigated protein. Therefore, the *X. laevis* egg extract system was chosen to functionally characterize Nup155 and Mel28 in their roles in NE formation.

The first candidate examined in this study, Nup155, was selected by Galy *et al.*, (2003) in a screen that assessed twenty nucleoporins by RNAi mediated depletion for defects in early embryonic development in *C. elegans*.¹¹⁹ Twelve nucleoporins were found to be essential for embryonic viability. The strongest phenotypes observed comprised embryos with neither pronuclei nor nuclei detectable by differential interference contrast (DIC) microscopy. Depletion of Nup35, Nup98/96, Nup358, Nup153, Nup155, or Nup160 caused such defects. Of these candidates, Nup155 was chosen for further characterization in the *X. laevis* egg extract system because little was known about this nucleoporin.

The current knowledge about Nup155 in different species will be outlined to facilitate integration of results on Nup155 function obtained in this work. Nup155 is a well conserved nucleoporin among eukaryotes suggesting that it might fulfill an important function.⁸¹ There are only a couple of studies providing information about vertebrate Nup155. In one, Nup155 was purified and localized to the NPC defining it as a nucleoporin, and in two other studies Nup155 was demonstrated to interact with Gle1 *in vitro*.^{123, 124, 210} Hawryluk-Gara and coworkers showed that Nup35 interacts with a NPC subcomplex containing Nup93, Nup155, and Nup205 extracted from rat liver nuclei *in vitro*. However, only a direct binding between Nup35 and Nup93 was demonstrated.

Tertiary structure predictions by biocomputational methods propose β -propellers at the N-terminal third and α -helical repeats at the remaining part of the protein.⁸⁵ In this respect, Nup155 resembles components of the Nup107 complex.

Two Nup155 homologues, Nup170 and Nup157, were found in *S. cerevisiae*. They are 42% identical and show 78% similarity to each other. Alignment of yeast Nup157 and Nup170 versus mammalian Nup155 showed ~22% identity and ~53% similarity.²¹¹ In a Pom152 synthetic lethal screen in *S. cerevisiae*, NUP170-POM152 double mutants were lethal, while the combination of NUP157-POM152 deletion was viable.²¹¹ Mammalian Nup155 could compensate the loss of Nup170 in a Δ POM152 background. Suppression of Nup170 expression in the absence of Nup157 led to

irregularities in the NE, showing massive extension and invaginations with long stretches devoid of NPCs. The outlined data indicate that Nup157 and Nup170 might have a role in NE organization in yeast. Similarly, overexpression of Nup170 in the same background induced the formation of intranuclear annulate lamellae, similar to upregulation of Nup53.²¹² mRNA transport defects were not observed upon up- or downregulation of Nup170 in the absence of Pom152. In a similar study in yeast, it was demonstrated that Nup1 (homologue of Nup153 in vertebrates) and Nup170 double mutants were lethal.²¹³ An interaction of Nup1 and Nup170 was shown *in vitro*. It was postulated that FG-repeat containing nucleoporins showed an altered stoichiometry in a Δ Nup170 strain. In addition, Nup170 interaction partners were detected in yeast: Nup53 and Nup59 which are homologues of vertebrate Nup35.²¹⁴ Mutant screens suggest a role for Nup107 in chromosome segregation and kinetochore function.²¹⁵

The involvement of Nup155 homologues in yeast in NE morphology and segregation is interesting, but cannot directly be transferred to its vertebrate homologue, since the mechanism of cell division in yeast, with its closed mitosis, is different.

The Nup155 homologue of *D. melanogaster*, Nup154, was selected in a screen for female sterile and semi-sterile lines.²¹⁶ Nucleocytoplasmic transport did not seem to be affected but homozygous egg chambers showed morphological alterations and a decrease in mAb414-recognized nucleoporins. In spermatocytes, the NE showed evaginations and distinct vesicles, whereas NPCs looked normal. Nup154 is required for female and male germline growth and development but also in later developmental stages. A second study on *Drosophila* Nup154 described animals with a loss-of-function mutation that died as larvae.²¹⁷ The function of Nup154 was necessary for growth of mitotically proliferating tissues in larvae and adults.

In humans the Nup155 gene was mapped to the short arm of chromosome 5, chromosome band 5p13.²¹⁸ There are two human Nup155 transcripts of 5.4 kb and 4.7 kb described. The size difference could be due to alternative usage of two 3'-polyadenylation signals or an alternative 5'-cryptic splice donor signal in the first intron. The smaller human transcript dominates. In mouse and rat cell lines only the shorter transcript is present.²¹⁹

Mel28 is a novel player in the process of metazoan NE assembly. It was characterized by Galy and Askjaer in *C. elegans* (unpublished data) after earlier work in *C. elegans* had identified it. Gönczy and coworkers screened maternal-effect embryonic lethal mutations on chromosome III to identify components required for cell division in the one cell stage *C. elegans* embryo.²²⁰ Loci essential for specific cell division processes were identified and mapped. A locus named mel28 was grouped together with mutations resulting in poorly visible pronuclei into the category “pronuclear appearance”. This locus is allelic to mel28 (maternal-effect lethality), a natural mutant found by J. Ahringer (unpublished). Throughout this study the name Mel28 is retained for the respective protein investigated in *C. elegans* and *X. laevis* egg extracts.

Moreover, Gönczy *et al.* (2000) performed a functional genomic analysis of cell division in *C. elegans* by RNAi that addressed all genes of chromosome III.²²¹ The phenotypes observed by time-lapse DIC microscopy were assigned to distinct phenotypic categories. One of them is the “pronuclear/nuclear appearance” class consisting of five genes. Deletion of these genes led to pronuclei in the one-cell stage embryo and nuclei in daughter blastomeres that are not or only poorly visible. The mitotic spindle was also affected in these embryos. Interestingly, three of these candidates encode components of the Ran system, essential for nucleocytoplasmic transport, NE assembly, and spindle formation: Ran, RanGAP1, and RanBP2.^{144, 145} Nup98 and a so far uncharacterized gene C38D4.3 comprise the remaining candidates in this group and it is likely that they might fulfill a crucial role in NE formation. The gene was also picked up in other RNAi screens, selecting for genes functioning in early embryonic defects.^{222, 223} Askjaer and Galy mapped the mutation in the mel28 locus to the *C. elegans* gene C38D4.3 (unpublished data).

Its vertebrate homologue was identified and investigated in the work of this thesis.

2 Results

2.1 *Nup155 is essential for nuclear pore complex assembly and nuclear membrane fusion*

2.1.1 Generating the tools: Cloning and expression of *X. laevis* Nup155

X. laevis Nup155 had to be cloned and expressed for polyclonal antibody generation against Nup155 in rabbits. Full length *X. laevis* Nup155 cDNA was received from “Deutsches Ressourcenzentrum für Genomforschung, GmbH” (RZPD) and cloned into several bacterial vectors for protein expression in *E. coli* (chapter 5.1.5.4). By expression and purification under standard conditions (chapter 5.2.2.1.2) of full length Nup155 with an N-terminal His-tag, the recombinant protein aggregated mainly into inclusion bodies and could only be purified in small amounts under native conditions, not sufficient for rabbit immunization (Figure 2.1, band 1).

Fusion of large soluble proteins, like NusA and Ftr to Nup155 did not improve solubility (data not shown) (chapter 5.1.5.4). Extraction of recombinant Nup155 from inclusion bodies under denaturing conditions and subsequent purification via affinity His-tag on Ni-NTA agarose was not successful either. Therefore, inclusion bodies containing predominantly recombinant Nup155 were purified as such (Figure 2.2; chapter 5.2.2.1.4). The yield and purity of Nup155 recovered from inclusion bodies

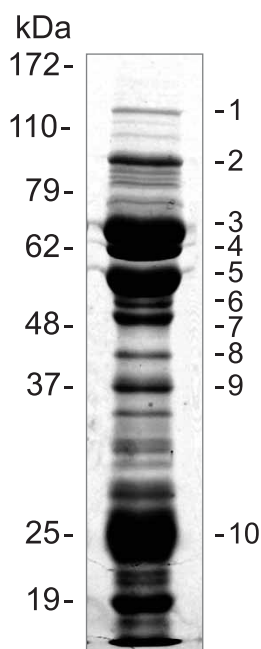


Figure 2.1: *Natively purified recombinant Nup155*. Recombinant His-Nup155 was expressed in *E. coli*, purified on Ni-NTA resin and stained by Coomassie blue after SDS-PAGE. Numbered bands were sequenced by mass spectrometry. Band 1 was identified as full length Nup155 that migrates at ~150 kDa. Bands 2-9 are not Nup155 fragments but contaminating *E. coli* proteins. Molecular weights are indicated at the left.

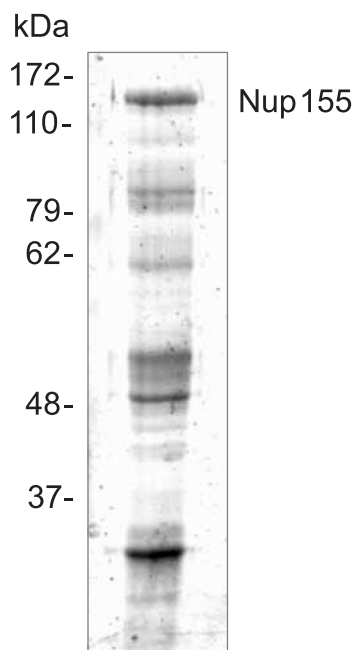


Figure 2.2: *Nup155* purified with inclusion bodies. Inclusion bodies that formed upon *Nup155* expression in *E. coli* were purified, analyzed by SDS-PAGE and stained with Coomassie blue. Full length *Nup155* is indicated. Molecular weights are shown at the left.

was higher than its purification under native conditions, comparing the ratios between full length *Nup155* produced and contaminating *E. coli* proteins in both purifications (compare Figures 2.1 and 2.2). Thus, inclusion bodies formed upon *Nup155* expression were purified and used for polyclonal antibody generation in rabbits.

For affinity purification of the anti-*Nup155* antibodies from serum six *Nup155* fragments were designed and cloned: *Nup155*-N1(aa1-395), *Nup155*-N2(aa392-584), *Nup155*-N1+N2(aa1-584), *Nup155*-C2(aa572-1000) and *Nup155*-C1(aa986-1388). With the help of sequence analysis programs grouped under “The predict protein server” (www.embl-heidelberg.de/predictprotein/predictprotein.html) it was intended to prevent the generation of fragments which might aggregate and precipitate due to disruption of secondary structures. All fragments carried an N-terminal His-tag and were expressed and purified under both native and denaturing conditions (chapters 5.2.2.1.2/3). Eluates of the His-tagged fragments from Ni-NTA affinity resin were separated by SDS-PAGE and stained with Coomassie blue (data not shown). None of the corresponding fragments was abundant enough to be identified by its molecular weight. Immunodetection by anti-*Nup155* antiserum of the purified fragments by Western blot was possible for *Nup155*-N1, -N2, -C1 and -C2 when purified in the presence of urea. For the fragments *Nup155*-N1 and -N2 small amounts were detectable by Western blot when the purification was performed under

native conditions (data not shown). Nevertheless, the yield obtained from all fragments was not sufficient for affinity purification of Nup155 antiserum.

Attempts to further purify the small amounts of soluble full length Nup155 obtained under native conditions (Figure 2.1, band 1) by gel filtration or ion exchange chromatography were not successful, because Nup155 precipitated easily. It was expected that low molecular weight proteins that contaminated the Nup155 purification under native conditions, comprised inefficiently translated Nup155 fragments. We intended to sequence the putative Nup155 fragments to get information about which sections of the protein might be more stably expressed and purified more efficiently. Proteins eluting from the affinity resin upon native purification of Nup155 were separated by SDS-PAGE, stained with Coomassie blue and analyzed by mass spectrometry analysis (Figure 2.1, bands 2-10; chapter 5.2.2.3). Interestingly, only bacterial proteins were identified but no Nup155 fragments deriving from degradation or ineffective translation of full length Nup155 cDNA were found. This seemed to underline the result that only the full length protein was stable when produced in recombinant form. Since no recombinant Nup155 fragment could be expressed to affinity purify the anti-Nup155 antibodies, all subsequent experiments and stainings were performed with the antiserum.

2.1.2 Characterization of anti-Nup155 antiserum

Polyclonal Nup155 antiserum, generated in rabbits, recognized only a single band in *X. laevis* egg cytosol at ~150 kDa on a Western blot, whereas pre immune serum did not interact detectably with any antigen in the cytosol (Figure 2.3A). This indicated that although anti-Nup155 antibodies could not be affinity purified, the antiserum was very specific for its antigen. Moreover, the serum not only recognized *X. laevis* Nup155 in egg cytosol and XI177 cell lysate but also cross-reacted with human Nup155 on a Western blot (Figure 2.3B).

The anti-Nup155 antiserum, when employed in immunofluorescence on *Xenopus* XI177 and HeLa cells, showed an NE rim staining as expected for the localization of a nucleoporin (Figure 2.4). On cells from both species the pre-immune and the anti-Nup155 antiserum caused a weak staining of the nucleoli which was considered to be unspecific as it was also seen with the pre-immune serum.

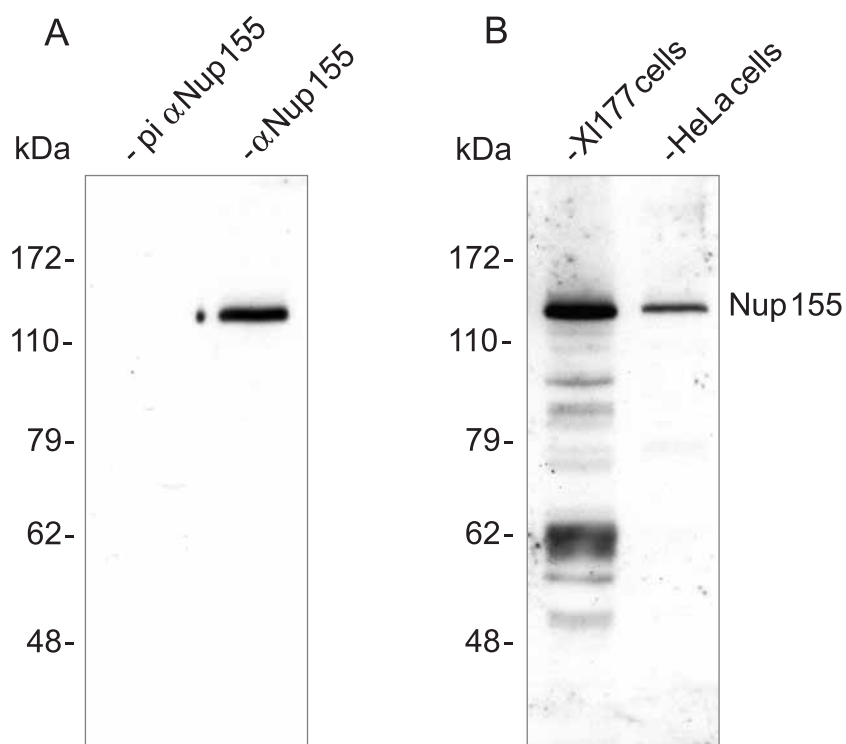


Figure 2.3: *Characterization of anti-Nup155 polyclonal antiserum by Western blot.* (A) The cytosolic fraction of *X. laevis* egg extracts was analyzed by Western blotting with pre-immune (pi α Nup155) or anti-Nup155 antisera (α Nup155). (B) Anti-Nup155 antiserum identified Nup155 in *Xenopus* XI177 cells and human HeLa cells on a Western blot. Molecular weight marks are indicated on the left.

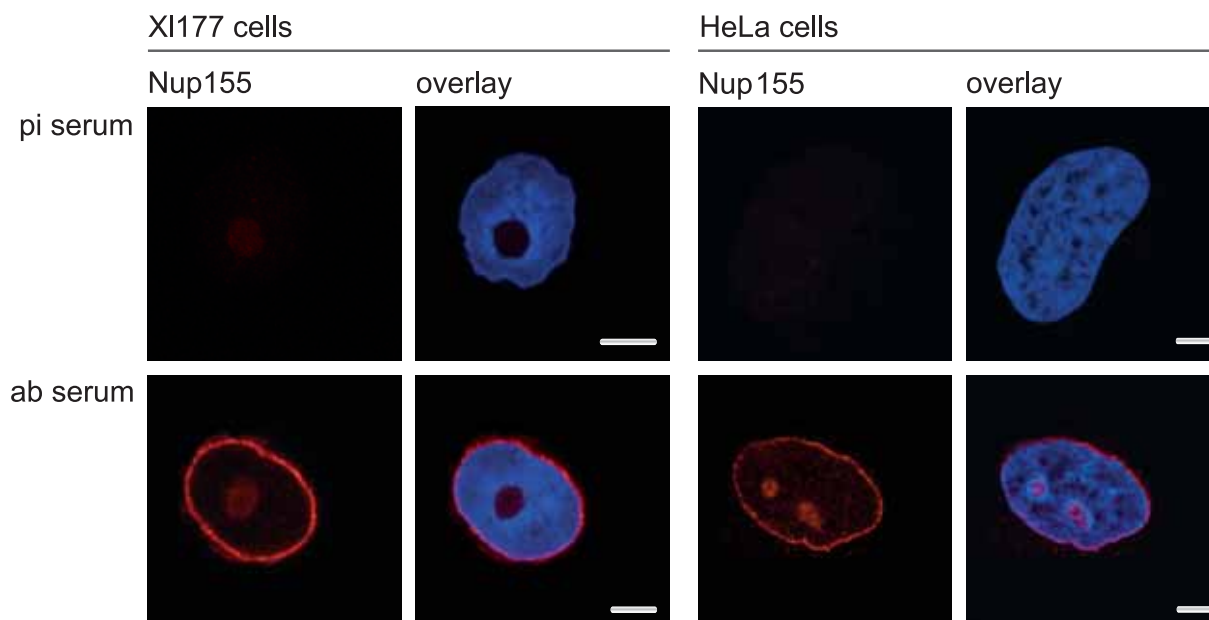


Figure 2.4: *Immunofluorescence of Nup155 on Xenopus XI177 and human HeLa cells.* Cells were pre-extracted with 0,1% Triton X-100 before fixation in paraformaldehyde. Immunofluorescence was performed with Nup155 pre-immune (pi) serum (top row) and anti-Nup155 (ab) serum (bottom row). In the overlaid images chromatin was stained with DAPI (blue). Bar: 5 μ m.

2.1.3 Knock down of Nup155 by RNAi in HeLa cells

Although Nup155 is a well conserved protein from nematodes to vertebrates, initial RNAi experiments in HeLa cells were undertaken to verify its functional conservation, before starting elaborate investigations in *X. laevis* egg extracts. Nup155 knock down efficiency was monitored by immunofluorescence on fixed HeLa cells employing anti-Nup155 antibody and evaluated by confocal microscopy (Figure 2.5). Nup155 was efficiently down regulated 24 h after transfection with small interfering RNA (siRNA) duplexes specific for Nup155, compared to control cells transfected with oligos directed against firefly luciferase (Figure 2.5; chapter 5.2.6). After 48h the NE rim staining of Nup155 was no longer detectable by indirect immunofluorescence (Figure 2.5). Monoclonal antibody 414 (mAb414), recognizing FG-repeats in Nup62, Nup153, Nup214 and Nup358, was used to investigate the behavior of these nucleoporins upon Nup155 depletion by co-immunofluores-

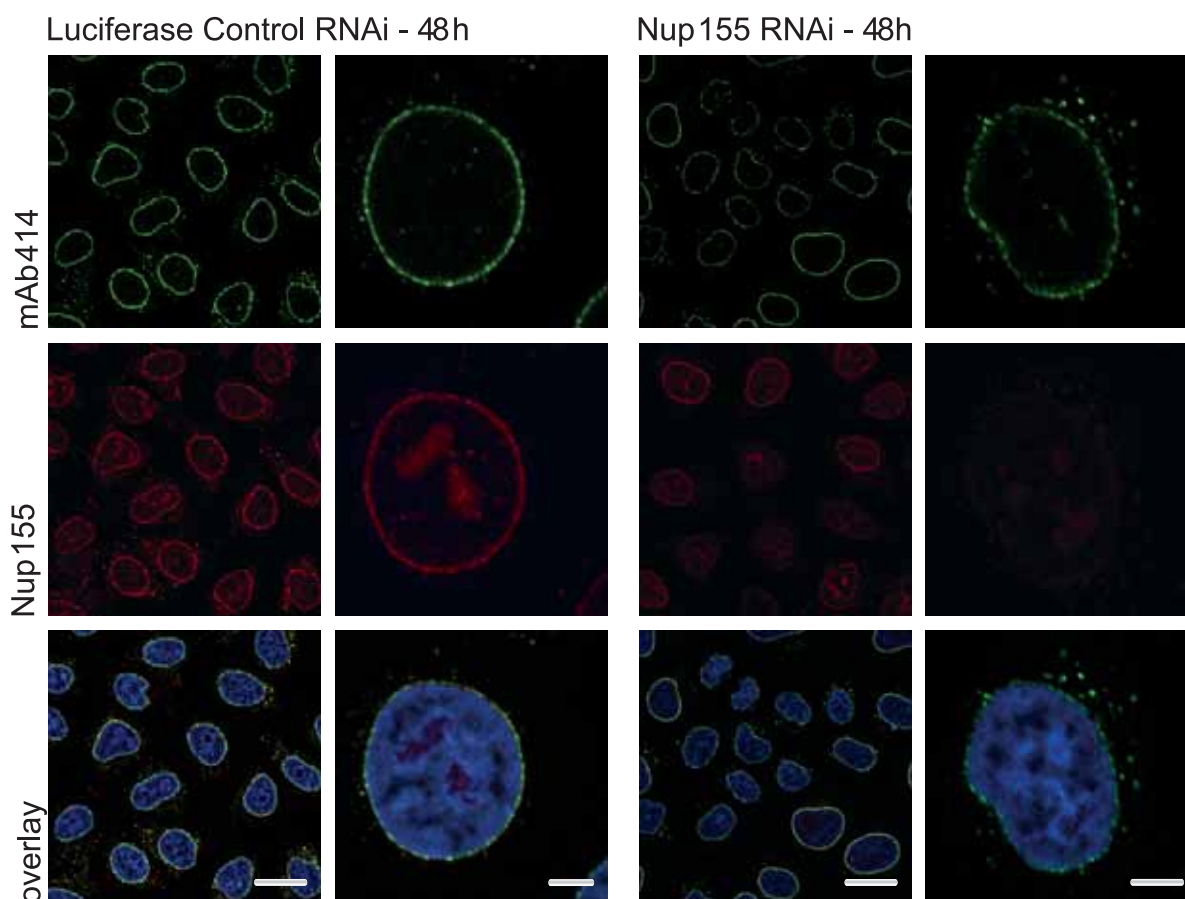


Figure 2.5: *Knock down of Nup155 by RNAi in HeLa cells.* Knock down of Nup155 after 48 h (two right columns) was compared to control samples, transfected with RNAi oligos targeting firefly luciferase (two left columns). mAb414 recognized antigens were monitored by co-immunofluorescence and are depicted in green (upper row), Nup155 is shown in red (middle row) and in the overlaid images chromatin was stained with DAPI (blue). Bar: 20 μ m in low and 5 μ m in high magnifications.

cence.²²⁴ In cells that lacked Nup155, mAb414 signal was also significantly decreased, but still marked the NE (Figure 2.5). The immunofluorescent signal of Nup155 was downregulated in 80-90% of the cells visually screened by confocal microscopy, indicating that the transfection efficiency was high and the Nup155 knock down efficient.

The significant depletion of Nup155 by RNAi judged by immunofluorescence was confirmed by Western blot (Figure 2.6). Equal amounts of total protein were loaded per sample on the gel. The most efficient knock down was detected after 24 h by immunodetection on a Western blot. Cells that were not efficiently transfected with Nup155 siRNA oligos continued to divide as reflected by an increasing Nup155 signal on the Western blot after 48 h compared to 24 h (Figure 2.6). However, the strongest decrease of Nup155 staining was detected after 48 h by immunofluorescence (Figure 2.5). It was concluded that the cells in which Nup155 was depleted most efficiently died and detached from the cover slips during the processing for immunofluorescence. Thus, the most efficient knock down of Nup155 in cells after 24 h could not be visualized by immunofluorescence.

Cell death in Nup155 down regulated samples compared to control reactions was not quantified and investigated further as the RNAi study was meant to give a first hint at Nup155 function in vertebrates only. NPC organization seemed affected due to Nup155 down regulation in HeLa cells, since a reduction of mAb414 recognized nucleoporins by immunofluorescence was observed. Moreover, cell viability was impaired. These strong defects prompted subsequent examination of the role of Nup155 in NE formation in *X. laevis* egg extracts.

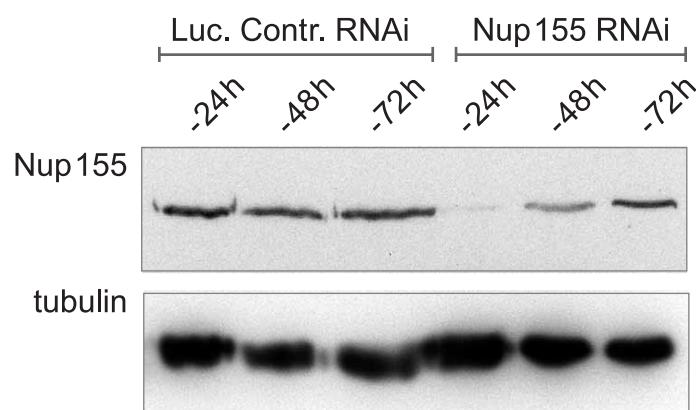


Figure 2.6: *RNAi knock down efficiency of Nup155 analyzed by Western blot.* Cells transfected with siRNA control duplexes (Luc. Contr. RNAi) or siRNA duplexes specific for Nup155 (Nup155 RNAi) were monitored for Nup155. Cells were harvested at the indicated time points, subjected to SDS-PAGE and analyzed by immunodetection on a Western blot for Nup155 protein levels. Equal amounts of total protein were loaded per sample as indicated by tubulin detection.

2.1.4 Characterization of Nup155 in *X. laevis* egg extract fractions

Nup155 was detected in cytosol and total membrane fractions prepared from *X. laevis* eggs on a Western blot (Figure 2.7, Cyt and fMem).

It was investigated whether copurification of Nup155 with the membrane fraction was due to a cytosolic contamination, a peripheral membrane association or its localization in annulate lamellae (AL). First, it was asked whether Nup155 membrane association was peripheral and could be dissociated by washes with high salt containing buffer. Membranes employed were first washed with standard purification buffer S250 to diminish the content of soluble proteins that contaminated the membrane fraction (Figure 2.7A, input). Subsequently, the membranes were homogenized with S250 buffer (Figure 2.7A, buffer) or S250 buffer supplemented with 1M or 2M NaCl, incubated for 30 min on ice and spun down. The integral membrane protein Pom121 was not removed from membranes by high salt washes, as expected (Figure 2.7A).¹⁷³ In contrast, importin α that peripherally associates with

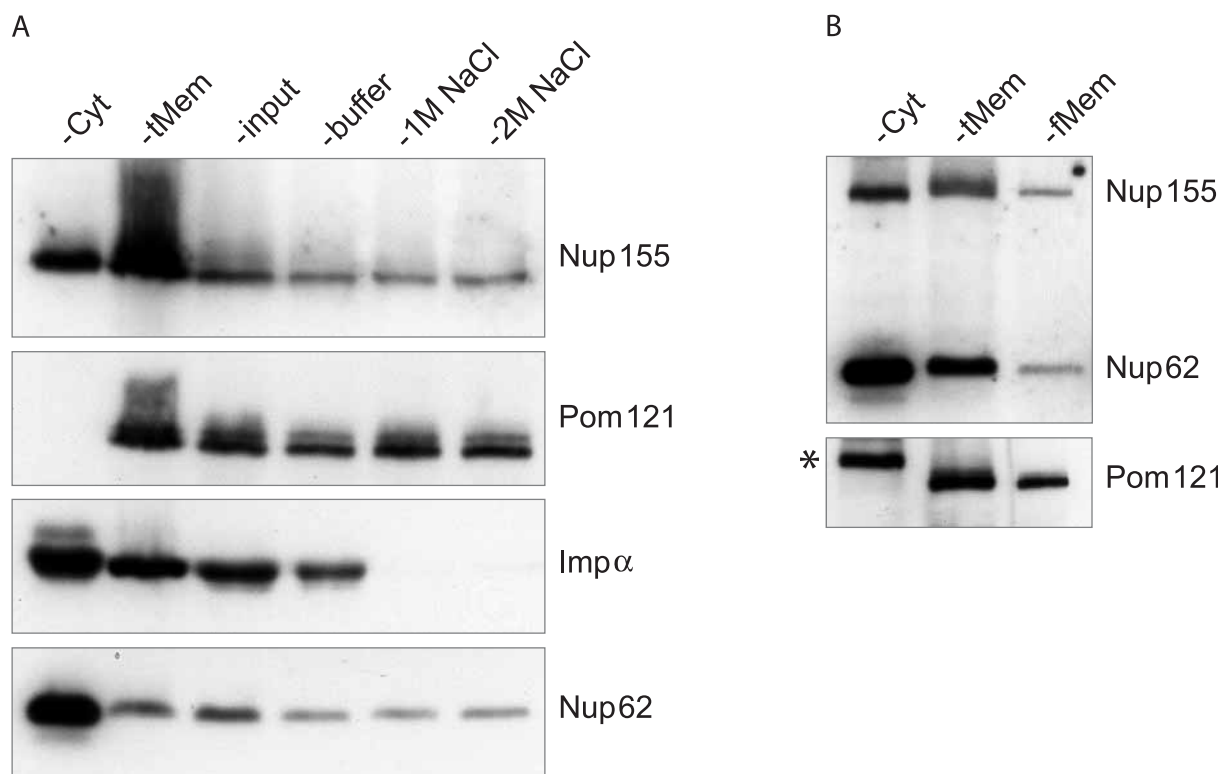


Figure 2.7: Investigation of Nup155 localization in *X. laevis* egg extract fractions. (A) Nup155 was monitored in *X. laevis* egg cytosol (Cyt) and total membrane fractions (tMem) by Western blot. Membranes were subjected to washes with buffer (input) and further treated with either buffer (buffer) or 1M and 2M NaCl. Nup155 behavior was investigated relative to the marker proteins Pom121, Imp α and Nup62 by Western blot. (B) Equal amounts of protein of cytosol (Cyt), total membrane (tMem) and floated membrane (fMem) fractions were probed for the antigens Nup155, Nup62 and Pom121 on a Western blot. The star in the cytosol lane indicates a cross reactivity of the Pom121 antibody.

membranes, was entirely depleted by 1M NaCl in S250 buffer.¹⁸¹ Starting from S250 washed “input” membranes, the Nup155 associated fraction could not be reduced by homogenization with 1M or 2M NaCl but behaved similarly to the integral membrane protein Pom121. Surprisingly, soluble Nup62 behaved alike Nup155 (Figure 2.7A). To exclude the possibility that Nup155 was pelleted with membranes as part of a large, soluble protein complex, membranes were floated through a sucrose step gradient (tMem).¹⁷² The lightest membrane fraction was collected and total (tMem) and floated (fMem) membrane fractions were analyzed by Western blot (Figure 2.7B). Interestingly, Nup155 and Nup62 content was significantly reduced, but not entirely removed after floatation of membranes. The localization of Nup155 and Nup62 after salt treatment of total membrane fractions and floatation was interpreted as evidence that fractions of both proteins were present in annulate lamellae that purified with membrane fractions. Both nucleoporins were indeed detected in isolated *X. laevis* AL.¹¹⁷ It was concluded that Nup155 is a soluble protein, like Nup62.

2.1.5 Depletion of Nup155 from *X. laevis* cytosol

To investigate the role of Nup155 in the *X. laevis* nuclear reconstitution system, it was necessary to deplete Nup155 from the cytosolic extract fraction (chapter 5.2.3). *X. laevis* egg cytosol is highly biologically active and can form about 1000 nuclei per egg. Nuclear proteins and disassembled NE components are stockpiled in *X. laevis* eggs and those of many other species.²⁰⁴ This implies that proteins required for rapid NE formation after fertilization that are wished to be depleted from *X. laevis* egg cytosol are often present in large quantities and require very harsh depletion conditions for their complete removal. Thus, an excess of anti-Nup155 antiserum was crosslinked to protein A sepharose. The column was blocked with bovine serum albumin (BSA) to prevent binding of unspecific proteins. Cytosol was incubated with anti-Nup155 antibody-covered protein A sepharose to deplete Nup155. Mock-depleted cytosol was incubated with beads carrying an unrelated antibody as positive control. After the first round of depletion, the cytosol was incubated a second time with a fresh anti-Nup155 antibody column. 3-5% of Nup155 remained in the cytosol after this procedure (Figure 2.8). In most cases the stringent conditions needed for Nup155 depletion destroyed the activity of the cytosol for *in vitro* NE formation even following mock depletion.

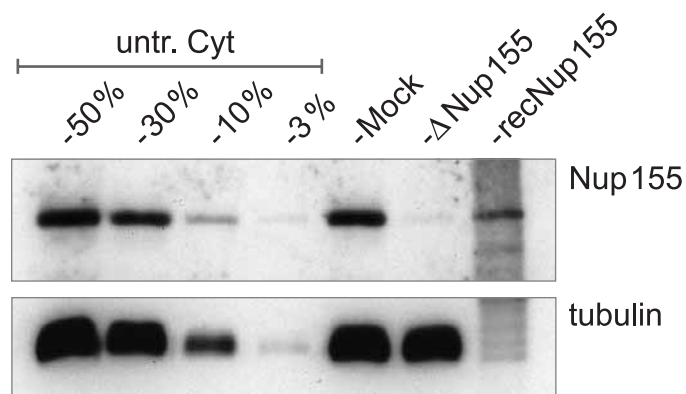


Figure 2.8: Immunodepletion of Nup155 from *X. laevis* egg cytosol was assessed by Western blotting. Amounts of Nup155 in mock-depleted (Mock) and Nup155-depleted (Δ Nup155) cytosol were compared by Western blotting. Equal volumes corresponding to 1/10 of a NE assembly reaction were loaded while varying amounts of untreated cytosol (untr. Cyt) were loaded for comparison. 0.6 μ l cytosol (25 μ g total protein) corresponded to 50% of the sample volume loaded of mock and Nup155 depleted cytosol. Total amount of recombinant Nup155 (recNup 155) used to restore one NE assembly reaction in Nup155-depleted cytosol was loaded. Tubulin served as loading control.

The total protein concentration of *X. laevis* egg cytosol was mostly reduced by roughly 50% after two rounds of depletion due to some dilution that occurs from excess buffer within the resin and unspecific loss of proteins on the sepharose beads (Figure 2.8, [50% untr. Cyt] compared to mock-depleted cytosol [Mock]). To partially overcome this problem, inactive Nup155-depleted extracts were used to preblock antibody columns to diminish unspecific protein binding to the sepharose. Immediately after the blocking step, fresh cytosol was applied to the antibody resin and was depleted of Nup155 in two rounds. If more than 5% endogenous Nup155 remained in the cytosol, no defects were observed in NE formation.

In vitro nuclear reconstitution reactions were performed immediately after the depletion procedure without storage of the treated cytosol to not further impair its activity (chapter 5.2.3.6).

2.1.6 Nup155 depletion blocks nuclear pore complex assembly

It was crucial to employ membranes that lacked any residual Nup155 to examine reconstitution of nuclear membranes and NPCs in the absence of Nup155. To minimize the amount of Nup155 introduced into the system, membranes were purified by a sucrose step gradient.¹⁷² This procedure only copurified nucleoporins assembled into annulate lamellae with floated membrane fractions (Figure 2.7B). The amount of Nup155 that was introduced into the reaction with the light membrane fraction was negligible with respect to remaining 3%-5% Nup155 that was undepletable from cytosol fractions since membranes constitute only 5% of the

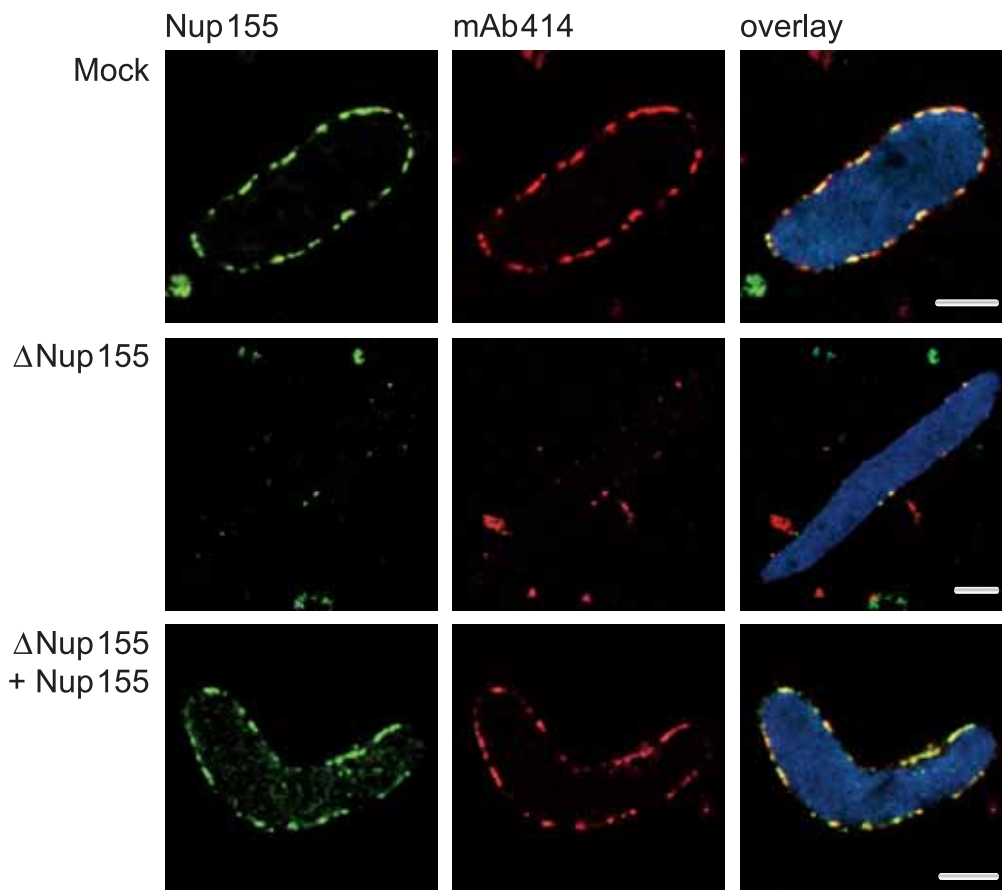


Figure 2.9: *Immunodepletion of Nup155 inhibited NPC formation in vitro.* Nup155 was immunodepleted from cytosol and nuclei were assembled *in vitro*. Nucleoporin localization was analyzed by immunofluorescence in mock-depleted (Mock) and Nup155-depleted reactions (Δ Nup155), or after readdition of recombinant Nup155 (Δ Nup155+Nup155). Nup155 (green), mAb414 (red) and chromatin stained with DAPI (blue) in merged images are costainings of the same nuclei. Bar: 5 μ m.

volume of assembly reactions (Figure 2.8). Floated membranes were incubated together with mock- or Nup155-depleted cytosol, sperm chromatin and an ATP regeneration system to reconstitute nuclei *in vitro* (chapter 5.2.3.5).

When immunofluorescence against Nup155 was performed on mock-depleted nuclei, Nup155 localized at NPCs, resulting in a nuclear rim staining (Figure 2.9, upper row). Nuclei assembled in the absence of Nup155 had entirely lost Nup155 NE staining (Figure 2.9, second row, left image). Examining nucleoporins by mAb414 proved absence of a rim staining, implying that Nup358, Nup214, Nup153, and Nup62 were no longer localized to the nuclear periphery in contrast to control reactions (Figure 2.9, center image). Probing for Nup107 and Pom121 led to a similar observation, but both proteins still stained the entire chromatin templates, whereas their localization at the periphery, marking the NE, was absent (Figure 2.10).

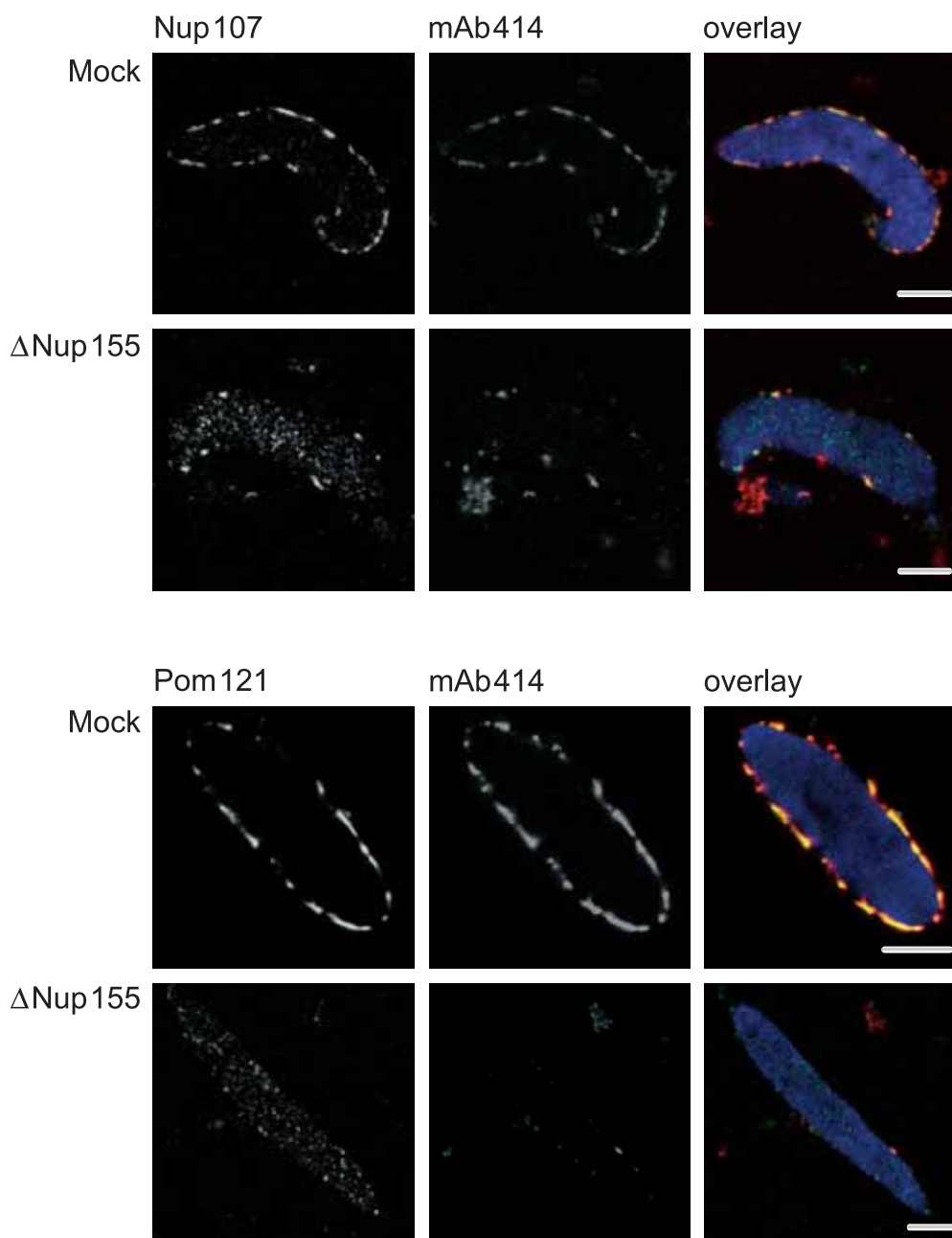


Figure 2.10: *Nup107* and *Pom121* associate with chromatin in nuclei devoid of *Nup155*. *Nup107* (upper, left images) and *Pom121* (bottom, left) recruitment in the absence of *Nup155* was followed by immunofluorescence. In the overlaid images *Pom121* and *Nup107* staining is colored in green, *mAb414* co-labelling is indicated in red and DAPI in blue. Bar: 5 μ m.

Thus, none of the nucleoporins investigated by immunofluorescence concentrated at the NE in the absence of *Nup155* *in vitro*. This finding was concordant with the phenotype obtained in *C. elegans* upon *Nup155* RNAi.²²⁵

To prove that the defects described were caused specifically by removal of *Nup155*, the effect of adding back recombinant *Nup155* on the phenotypes observed in NE formation was tested. Full length recombinant *X. laevis* *Nup155* was expressed and purified under native conditions. *Nup155* was added to *Nup155*- and mock-

depleted cytosol. Recombinant Nup155 was incubated for 10 min with cytosol and sperm chromatin for decondensation and subsequently the NE assembly reaction was started. Recombinant Nup155 was sufficient to achieve reversal of the depletion phenotype, proving that the defect in NPC assembly was specifically caused by Nup155 depletion. All nucleoporins investigated were recruited to the NE again, resulting in NE rim staining. This suggested that readdition of only Nup155 enabled NPCs to assemble again (Figure 2.9, last row). The efficiency of recombinant Nup155 was very high, since readdition of only very little Nup155 was sufficient to complement the depleted extracts. In Figure 2.8 (recNup155) about ten times more recombinant Nup155 was loaded and transferred by Western blotting compared to the volumes of mock- and Nup155-depleted extract employed in a NE assembly reaction.

In mock-depleted reactions nuclei were unperturbed by addition of recombinant Nup155 (data not shown). It seemed that cytoplasmic clusters stained by anti-Nup155 antibodies were induced in mock reactions. This might indicate that excess Nup155 triggered formation of annulate lamellae and incorporated into these structures. This remains speculation as this observation was not investigated further.

The concentration of recombinant Nup155 sufficient to restore NPC assembly was less than the remaining 3-5% cytosolic Nup155 left after depletion. Possibly, this undepletable fraction represented Nup155 organized into annulate lamellae. This could explain why remaining Nup155 appeared inactive and why addition of only small amounts of recombinant Nup155 restored the defects in NE formation. Otherwise, undepleted Nup155 may be restricted in its activity due to binding of other components or because of posttranslational modifications. Except of full size Nup155 only *E. coli* proteins were identified that copurified with recombinant Nup155 rendering it unlikely that proteins other than Nup155 comprise the restoring activity.

By sucrose gradient sedimentation analysis of mitotic HeLa cell extracts, Nup155 sedimented as monomers, suggesting that it is not part of a functional subcomplex which is stable during mitosis.¹²³ This observation fits the results that recombinant Nup155 alone is sufficient to restore the phenotype in NE assembly and indicates that no other components were co-depleted from *X. laevis* egg cytosol.

Immunofluorescence of mAb414 antigens using a different fixation protocol was performed (chapter 5.2.3.6). This fixation method improved preservation of membranes but can cause staining artifacts with some antibodies. However, both

protocols yielded similar results. In the absence of Nup155, mAb414 antigens could not localize to the nuclear periphery which was restored after addition of recombinant Nup155.

2.1.7 In the absence of Nup155 closed nuclear membranes do not form

The absence of any nuclear rim-associated nucleoporins in nuclei devoid of Nup155, including the transmembrane protein Pom121, raised the questions about the integrity of nuclear membranes. Membranes were stained with the lipophilic dye DiI_{C18} after the assembly reaction and before fixation (chapter 5.2.3.7). Confocal microscopy showed that NE membranes were smooth and continuous in the mock-depleted reactions (Figure 2.11, upper row). In contrast, in the absence of Nup155, membrane vesicles associated with chromatin but did not form a continuous membrane. In some cases few vesicles docked to chromatin, in others, membranes were associated with chromatin but did not fuse to form closed nuclear membranes.

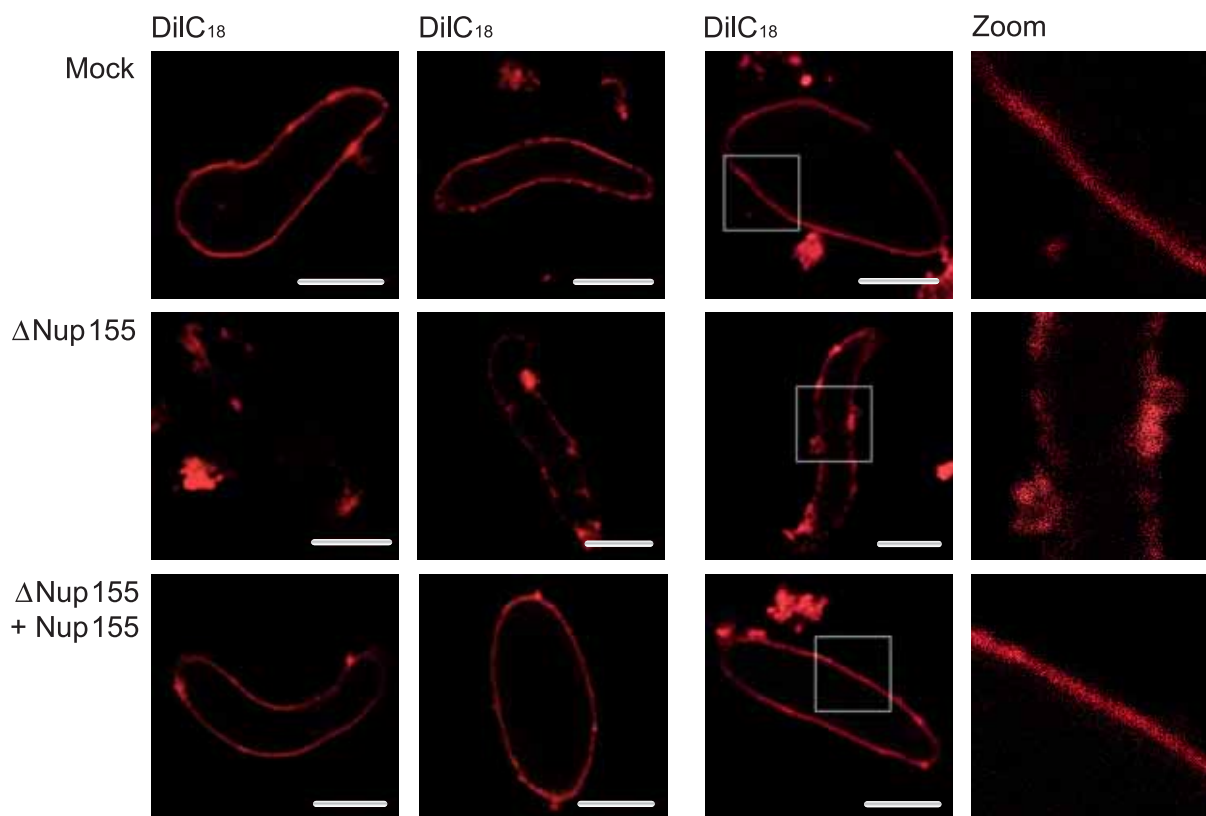


Figure 2.11: *Defects on nuclear membranes upon Nup155 depletion.* Nuclei assembled *in vitro* in mock- (Mock) or Nup155-depleted (Δ Nup155) extracts, or in depleted extracts after addition of recombinant Nup155 (Δ Nup155+Nup155), were labeled with the membrane dye DiI_{C18} before fixation in 2% paraformaldehyde and 0.5% glutaraldehyde and analyzed by confocal microscopy. Left and right image sets derived from independent experiments. The two left image columns are individually adjusted in signal intensity to optimally illustrate membrane structure. Equal exposure times were chosen for right images. Bar: 5 μ m.

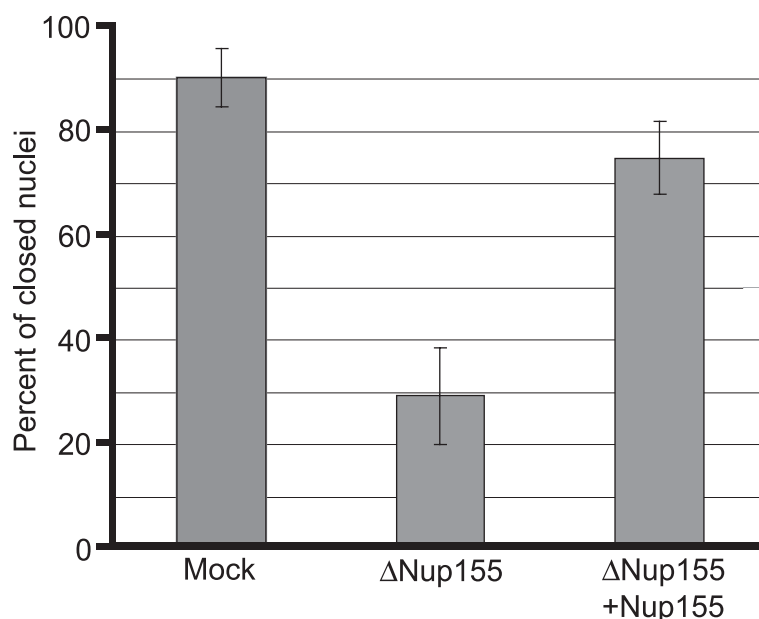


Figure 2.12: *Quantitation of closed nuclear membranes.* In three independent experiments, 100 nuclei from each reaction were examined. The average of the three independent experiments is shown, error bars represent the total variation over the experiments.

The chromatin templates in Nup155 depleted extracts remained condensed, indicating that sealed NEs did not form.

This phenotype was quantified by scanning through one hundred nuclei in each sample of three independent experiments by confocal microscopy. On average, 90% of the nuclei in the mock reactions had a continuous, closed NE. This number was reduced to 29% in Nup155 depleted extracts and could be restored to 75% by addition of recombinant Nup155 (Figure 2.12).

2.1.8 Ultrastructural defects on nuclear membranes

NE assembly reactions were processed for transmission electron microscopy to analyze the membrane phenotype in more detail. In control reactions nuclei exhibited a continuous, homogeneous double membrane bilayer. Electron dense areas spanning the inner and outer nuclear membrane indicated NPCs which were placed at regular intervals (Figure 2.13, Mock, arrows). In the absence of Nup155 no continuous double membrane bilayer was present (Figure 2.13, Δ Nup155). Instead, membrane vesicles interacted with the chromatin surface but remained at this initial docking step without further fusion. In some areas the docked vesicles flattened and formed unconnected patches (Figure 2.13, lower, left image). Importantly, no NPCs were found at the periphery of the chromatin templates in Nup155 depleted samples. These results mirrored observations made by confocal microscopy and confirmed

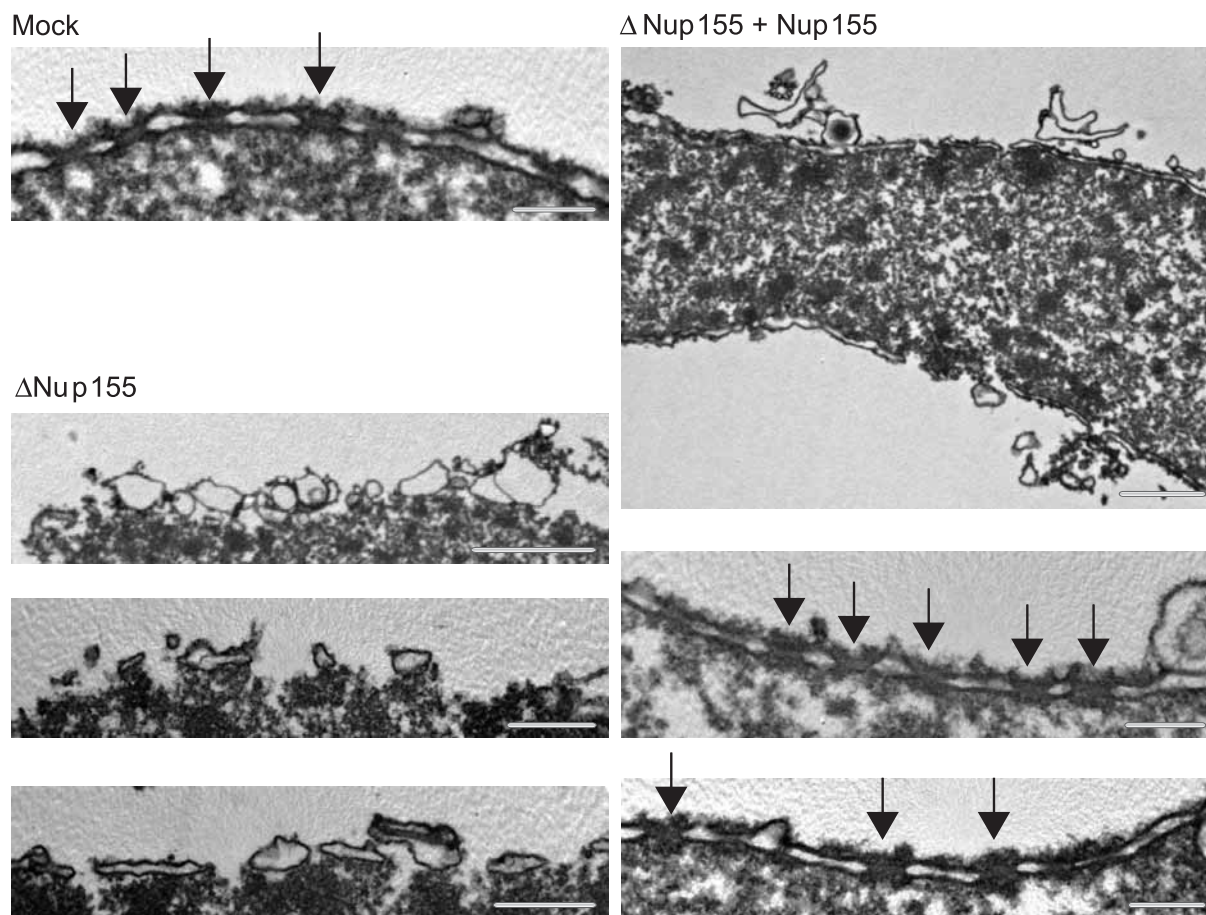


Figure 2.13: *Ultrastructural analysis of nuclear envelope defects in the absence of Nup155.* *In vitro* assembled nuclei were processed for transmission electron microscopy. In mock-depleted (Mock) reactions nuclear membranes were smooth and continues with inserted NPCs. Nuclei devoid of Nup155 (Δ Nup155) exhibited membrane vesicles docking to chromatin inhibited to fuse or little association of membranes with chromatin. NPCs were absent. Readdition of recombinant Nup155 (Δ Nup155+Nup155) restored defects described on nuclear membrane fusion and NPC assembly. Mock-depleted (Mock), bar: 0.2 μ m; Nup155-depleted (Δ Nup155), bar: 2 μ m upper image, 0.5 μ m middle and lower images; Nup155-depleted followed by addition of recombinant Nup155 (Δ Nup155+Nup155), bar: 1 μ m upper image; 0.2 μ m middle and lower images. Arrows mark NPCs.

that neither NPCs nor closed nuclear membranes formed in the absence of Nup155. Both processes were restored upon readdition of recombinant Nup155, membranes fused to continuous bilayers including regularly spaced NPCs (Figure 2.13, Δ Nup155 + Nup155).

2.1.9 Nup155 did not interact with any other nucleoporin investigated

Soluble nucleoporins for which antibody reagents were available could not be detected to interact with Nup155 by co-immunoprecipitation from *X. laevis* cytosol, as shown in Figure 2.14. Neither were the integral membrane nucleoporins gp210 and Pom121 found to bind to Nup155 by co-immunoprecipitation from solubilized

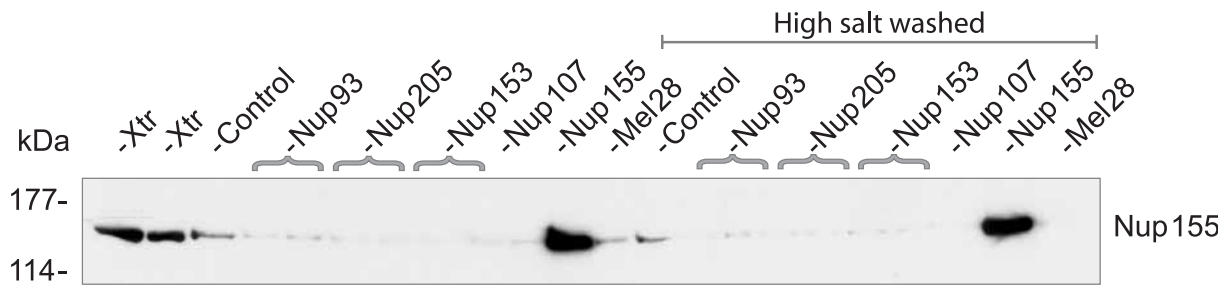


Figure 2.14: *Nup155 did not interact with any other nucleoporins investigated.* Immunoprecipitations from *X. laevis* egg cytosol were performed with the antisera indicated on the top and investigated for co-immunoprecipitation of Nup155 by Western blot.

membranes (data not shown).^{*} Additionally, other proteins that putatively co-immunoprecipitated with Nup155 from cytosol or solubilized membranes were analyzed by SDS-PAGE, stained with silver and subjected to mass spectrometry analysis. However, no specific Nup155 binding proteins were detected (data not shown).

2.1.10 Nup155 depletion blocks an early event in nuclear pore complex assembly and nuclear membrane fusion

The distinct order of events during NE assembly was analyzed *in vitro* to understand the complex effects on NPC formation and nuclear membrane fusion caused by the absence of a soluble nucleoporin.

Nup155, Nup107, mAb414 antigens, DilC₁₈ stained membranes and Pom121 were followed through NPC assembly and formation of nuclear membranes (Figure 2.15 and Antonin *et al.*, (2005)).¹⁷³ Chromatin was decondensed for 10 min in the absence of membranes and the first sample (t = 0 min) was taken immediately after membranes, energy mix and glycogen were added to start the assembly reaction. Nup107 together with Pom121 (data not shown and Antonin *et al.*, (2005))¹⁷³ appeared early relative to mAb414 antigens on the chromatin surface, after approximately 10 min. Nup155 and mAb414 epitopes were visible at the nuclear periphery after ~20 min. Their initial appearance at the chromatin template was different from Nup107 and Pom121 as they were only detected in peripheral foci and did not coat the chromatin surface like Nup107 and Pom121 (Figure 2.15, see also Figure 2.10; Antonin *et al.*, (2005) and Walther *et al.*, (2003)).^{173, 189} Interestingly, Nup155 recruitment to chromatin could not be increased by RanGTP unlike several other soluble nucleoporins (data not shown).¹⁸⁴ Monitoring nuclear membranes by

^{*} Immunoprecipitation experiments were performed by me and in parallel by Dr. Wolfram Antonin. The Western blot presented in Figure 2.14 was kindly provided by Dr. Wolfram Antonin.

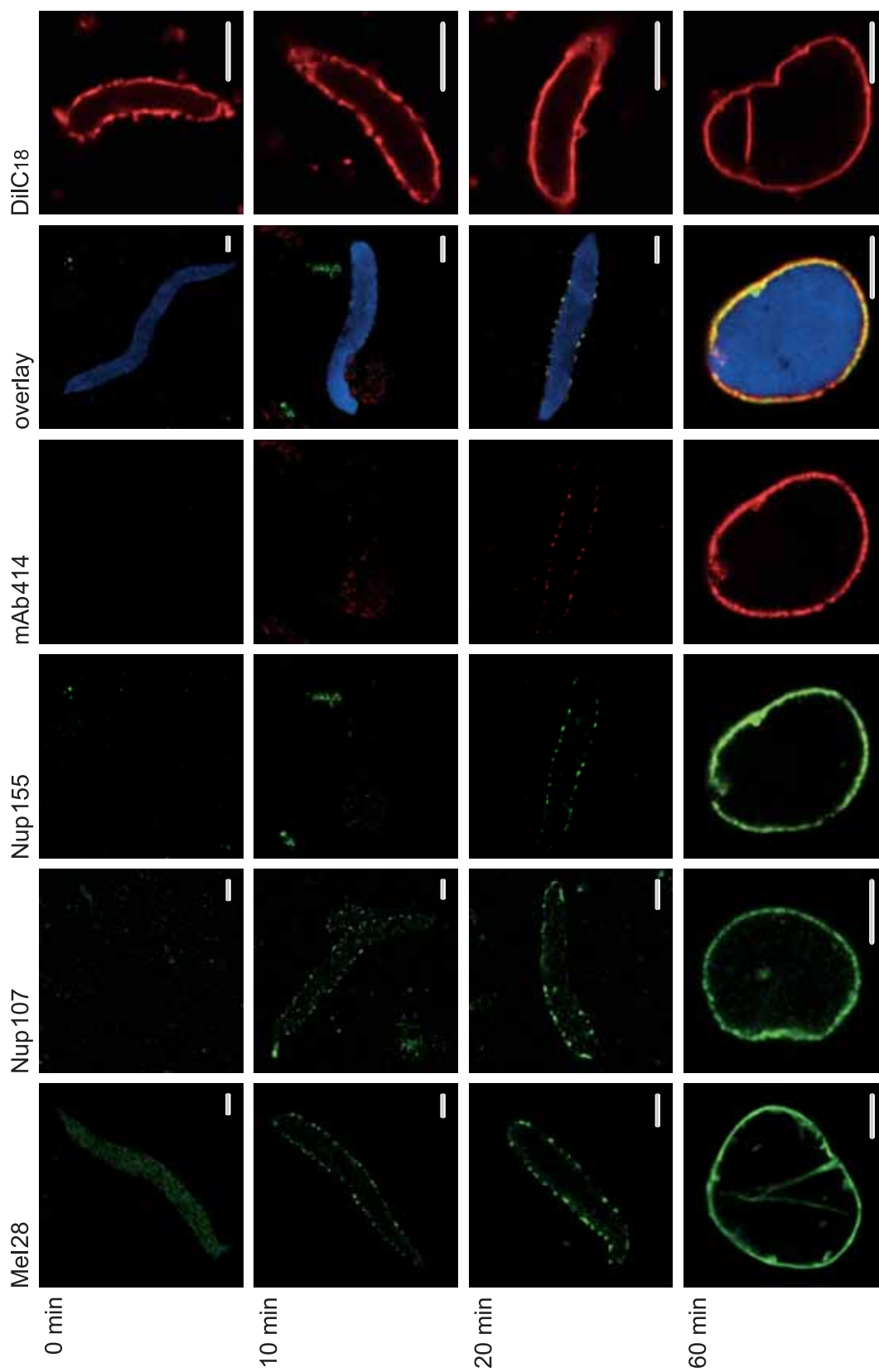


Figure 2.15: Time course of *in vitro* nuclear envelope assembly. NE assembly reactions were fixed in 4% paraformaldehyde at the timepoints indicated. The three columns that show immunodetection of Nup155 (green), mAb414 (red) and DAPI (blue) are identical samples and merged in the overlaid images. Parallel reactions for Mel28 and Nup107 immunodetection (left two columns) and membrane labeling with the dye DiIC₁₈ before fixation (rightmost column) are shown. All bars: 5 μ m.

DiIC₁₈ staining it was found that membranes immediately docked to chromatin when added to assembly reactions. The fusion of vesicles to continuous membranes occurred after approximately 20 min, concomitant with Nup155 and mAb414 antigens accumulating at the nuclear periphery (Figure 2.15, right column of images).

In summary, vertebrate Nup155 is a soluble nucleoporin that recruits late to the postmitotic reforming NPC *in vitro*. Nucleoporins like Nup107 and Pom121, which associate with chromatin early, could not be organized into peripheral foci encircling the NE since later steps in NPC assembly were blocked in the absence of Nup155. In addition, membrane vesicles that docked to the chromatin template *in vitro* were prevented from fusion to form a sealed NE. We conclude that Nup155 is essential for NPC and nuclear membrane formation *in vitro*.

2.2 Mel28, a novel player in nuclear envelope formation

2.2.1 Identification of the vertebrate homologue of *C. elegans* Mel28

Gönczy and coworkers identified an uncharacterized gene that led to severe pronuclear and nuclear appearance defects upon knock down by RNAi in *C. elegans*.²²¹ Galy and Askjaer (unpublished data) mapped the locus of this gene and showed that it is allelic to a mutated gene in a *C. elegans* library clone named mel28.²²⁰ The presence of a Mel28 homologue in vertebrates had to be confirmed prior to its further characterization in the *X. laevis* egg extract system.

Blast searches of *C. elegans* Mel28 at NCBI databases identified a putative mammalian homologue named “Embryonic Large molecule derived from Yolk Sac” (ELYS).²²⁶ It was described as a gene critical for haematopoiesis and was specifically expressed in the yolk sac. At later stages of mouse embryonic development, Mel28 was prominent in fetal haematopoietic tissues: liver, spleen and thymus. ELYS was reported to localize in the nucleus and cytoplasm in a mouse stromal cell line by immunofluorescence. Fragments of ELYS were fused to GAL4 DNA-binding domains and cotransfected with a pFR-luciferase reporter plasmid into HeLa or COS7 cells. The intrinsic stimulatory and inhibitory function of ELYS fusion proteins was assayed by GAL4-binding site dependent transactivation of the luciferase reporter plasmid. The authors hypothesized that ELYS might function as a transcription regulatory factor. The ELYS gene resides on chromosome I in mouse.²²⁷ Homozygous ELYS knock out mouse embryos died at an early stage of development.²²⁸

2.2.2 Cloning of *X. laevis* Mel28

The mouse ELYS sequence was used to search for *X. laevis* expressed sequence tags (ESTs; chapter 5.1.5.1). According to the sequence fragments found, specific primers were designed. Employing those, Mel28 was cloned by RT-PCR from total RNA purified from *X. laevis* oocytes and subsequent PCR amplification of the obtained sequenced DNA fragments. Cloning of a cDNA comprising approximately 6600 base pairs (bp) was hampered by *X. laevis* being a tetraploid organism. For this reason, RT-PCR transcripts derived from different expressed alleles were detected. Splice variants of the gene and sequence polymorphisms further complicated the identification of a transcript that constitutes the corresponding functional *C. elegans* homologue. Because of its size, Mel28 cDNA could not be

```

1  MQNLKAQITG SLVAFPDVTQ KALQEDEINL ESVLHGKFST GRTGLAWLAC GPQLEVTNSV
61  TGERISAYHF SGFTERPPVV VAVKEFTWQK KTGLLVGLVE TEGSVLCLYD IGISKVVKAI
121 VLPGLVTVVE PIINHGGASA STQHLHQSLR WLFVGTAVAT DVGHVLLIDL CLDDLSSNQD
181 ELDASDLEVM SGIPAKIPKL REGATKERRH LSLQLAAPTG TTVSCLSYIS RTNQLAVGYS
241 DGYFSLWNMK TLRRDYHVQI EGSRI PVC AV TFQEPENDPR NCCYLWVVS SESGGDVS LH
301 LLQLAFSERK CLASGQIMYE LLEYCEERY S LDLSGSTLSL RGQKNNTKFL GCQTIEKFRV
361 HGEREDGVHE VTSPDTSVSV FSWQVNTYQ G GKPSVYLG V F DINRWYQAQM PDSLRPGQFL
421 RNCSYFAFWS LEAVVNILTQ DIFDILVHER SLSRGMSPSY PPPEQFYPS TYNFDATCLL
481 NSGLIHFACT GFQKETLHFL KKSQTSLNEA IPDGYNRCLV AGLLSPKFTD VQPSSLSQEE
541 QLQAMFSAAV ETSSLGLLTS CIKRWTAEEQ PRSAANLRFV LEWTWNNVTL TKQEFDRLCF
601 CLFDGSCNFI DPHTLQSLQQ CHLHFSNLTA ILNCFIAQAK EVTYQGAVDL ENKQSVTRLL
661 SLYASVVLWF CRSGLLPDSS DETVQLTRPF YNYQVIQQYY SDQRKKLKRL ARGKWDTSSL
721 MIDGLINQFG DRVQQLWSRD DNGTGKYPPA NLHALLDVYL LENADEMSKH AII IYFLLDI
781 MYSFPDKPDS SIESFPTAFS VPASLIKLIQ GFWLLDHNDY QNSVDCILNP ASSRVMWQH
841 SQI IETLMCQ G DPRQALRYI QVMKPVAATS KEVKLHMSVL LANRSILEAW NLQRLHSSRL
901 NVEELLKHYM ETCQEMGLIE ELFKLTFTDF EQDY LHKFLQ TTGVQNQELL LVHHLQRANY
961 IPALQLNQSL KTNHLNNSER SMARNAILDQ YGKILPRVQQ TLARERAKPY SLPSLVWREV
1021 ARPQPLSTSA KEAAPGSIIT KANFICNVLS KIKEVSSANE KQEEYSPYKS MVSEEPTAAL
1081 LQGIDVPDAF FGTPIKNSRR VSRLLDSPVH PVLMEPTSLV SSDTDNHHQT PHKSPLLKTS
1141 SPLQSSLRM AHMRSFAKAS EFSLLETPLV VRKAKALATN TASSGYTSVT PQSTRSSVR
1201 TTPLVSPSVS PGRSLTPPLR PKETKISFME LSVTRHTKAA HSSEVDLLEM SPVLRSSPDA
1261 AWSGKGKFTS FAQITPVKKI EVNASSGIQ TESPDEMEVS KEASNISVRS EQASLEYHDA
1321 PTPEDLENDE ISETNNVQPQ VIEVHHQMEA GHLTEKPAEL PLTEIQKAMQ EEFKDYEEKE
1381 IEHISVLSNG PSALECTTAL PDIDLLEAAQ C ISETPAGSA VSVTGEQECA ASAKDSESVI
1441 SIHSDSDVHS NLSENDQDGE EVEENILLVD QPVLTMELQL VETADLEVEL EETGSEKTN
1501 KELYPDAAVP LGFTVESIEQ HYTCELARR ETPNEIDEIE AEHF EAENNF SLVLEGDAVE
1561 EEILQPPSSK TDPELTRPPI AHQKHCSEIR ENCEKMTENI PANVSPVGS DLESKILEAL
1621 PSEAEQTVVF VSEKVEDTE EKEVPSEIHG EVLSENKPVR NAMMSLDPSE SQEDKIRQSD
1681 NIISVEKIRM TEEKIYG EKT EKGLQVSPNS DQSAGVRPVT PRRSIRNSSK TNDSSAIIA
1741 NITLPTTPKR GQKKAKENVG ALSVPEEEL TGSTRITRK ATLTALENPE PPQIKEPAVG
1801 EALQVQPSTP TRGRRGRVIT SDGKDYECL EKTALPLTPT RITRSKNILE HEKGIGQIED
1861 TGETEHEVVT PKRGRRSKRV VNESVTHFVH NSSQPDIKTD TSPPKVSLR WTRTGSDNQI
1921 INATEEQVVK MQEDITDTPR KRYKKSNNKL GFEE TADAVS EATIVEDVQE FLIISRPGKN
1981 PNTSVVRSAR KATLPPVIED HSEQPLRSPE SNSKVHSSLL AIAEEIKATN TRTWFGSKSS
2041 VADVSTITFE FSTPKARTKK TVKGSAVQTE LIPPTS YVFS PPSTRTRRAT RANVSETVTE
2101 PELQVQESHE IAETEVP EVG PSKPRGRPPK HKAKITVTRVL KKT SWSTPPV EIKLISPPE
2161 PTVSETDTKK DSAEAKGAEK NSVWRTRRR I MSKPVMR RKM I*

```

Figure 2.16: *Amino acid sequence of xMel28*. Computational analysis predicted an NLS (bright gray; aa 1748-1758) and an AT-hook (dark gray; 2122-2134), but no larger domains.

obtained in one piece but had to be assembled from overlapping PCR fragments cloned, deriving from the same transcribed allele. Parallel sequences of multiple fragments of two different alleles and finally a clone obtained from RZPD was found to cover the entire open reading frame (ORF). The cDNA was 6603 bp, corresponding to a 245 kDa protein (Figure 2.16).

2.2.3 Features of the *X. laevis* Mel28 protein sequence

The Mel28 protein sequence was analyzed for domains and other protein features by several sequence predictions programs (<http://www.embl-heidelberg.de/predictprotein/predictprotein.html>). The protein was calculated to consist of only one domain (Globplot) and to be a non globular protein (GLOBE, see “predict protein”).²³¹ The N-terminal half of the protein (aa1-1000) was calculated to be rather hydrophobic. Multiple HEAT (huntingtin, elongation factor 3, A subunit of protein phosphatase 2A and IOR1) -like repeats were envisaged for the N-terminal part (Dr. Tobias Doerks, personal communication).²²⁹ A single HEAT repeat unit is a pair of interacting anti-parallel helices linked by a flexible “intraunit” loop. HEAT-repeats occur in series forming domains that serve as superhelical scaffolding matrices.²³⁰ In the Mel28 sequence HEAT-like repeats appear as hydrophobic blocks of ~40aa interrupted by charged amino acids. α -Helical repeat domains as found for example in nucleoporins, can be built from HEAT repeats.⁸⁵ However, because of the hydrophobicity of the Mel28 sequence repeats, it can not be excluded that they might organize into β -strands (Dr. Tobias Doerks, personal communication).

The C-terminus of Mel28 was predicted to be more hydrophilic and rich in sequence repeats, possibly indicating that it can form homodimers (Globplot, exploring protein sequences for globularity and disorder).²³¹ Standard domain prediction programs (“The predict protein server”) revealed only an NLS sequence, starting from aa1748 (KRGQKKAKEN) and an AT-hook (aa2122-2134; Figure 2.16). This DNA binding domain is characterized by a central glycine-arginine-proline (GRP) tripeptide surrounded by basic residues and shows a preference to bind A/T rich DNA regions.^{226, 232}

2.2.4 Conservation of Mel28 among eukaryotes

Data base searches for proteins related to *X. laevis* Mel28, as well as homologues, revealed that Mel28 is conserved through the eukaryotic kingdom.²³³ In fungi, proteins with significant similarity are rather small, comprising ~300aa compared to the vertebrate protein with ~2200aa (data not shown). *D. discoideum* is an exception among single celled eukaryotes with a predicted Mel28 relative of the same size as insects and vertebrates (~2200aa). Plants, like *Arabidopsis thaliana* and *Oryza sativa*, possess a Mel28 homologue of ~900aa. Mel28 sequences of nematodes, insects, amphibian, birds and mammals are well conserved at the N- and C-terminal ends, but less in the mid-regions (data not shown). Mel28 is very well conserved among mammals. All homologous proteins identified in fungi and plants are only predicted and none of them is characterized. The only functional data available so far derived from mutation and knock down screens in *C. elegans*, indicating that Mel28 is essential for normal nuclear morphology.^{220, 221, 222, 223} In addition, vertebrate Mel28, named ELYS, was implicated in haematopoiesis in mouse.²²⁶ In conclusion, very little is currently known about Mel28 present in most eukaryotes.

To obtain further indications for the functional conservation of Mel28 between nematodes and vertebrates, full length Mel28 cDNA was fused to EGFP and expressed in the *Xenopus* cell line, XI177.* Mel28 was confined to the NE, concordant with the localization observed for its homologue in *C. elegans* by confocal microscopy (Figure 2.17 and data not shown). This was a first indication that the correct vertebrate homologue had been identified and cloned.

EGFP-Mel28

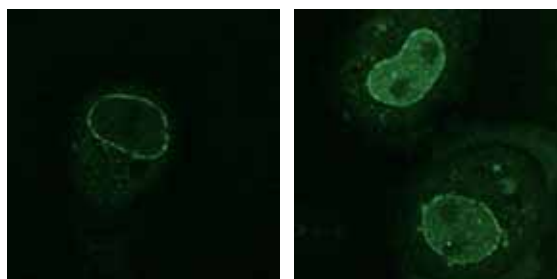


Figure 2.17: *X. laevis* Mel28 localization in XI177 cells. EGFP was fused to the annotated *X. laevis* cDNA sequence and transfected into XI177 cells.

* Dr. Peter Askjaer fused xMel28 cDNA to EGFP and transfected it into XI177 cells. The images shown in Figure 2.17 were kindly provided by him.

2.2.5 Generation of polyclonal antibodies against *X. laevis* Mel28

Mel28 fragments were designed according to secondary structure predictions based on the protein sequence in “The predict protein server” and “NCBI-psi blast” to avoid interruption of secondary structure motifs.^{234, 235, 236}

Seven fragments were cloned and N-terminally fused to GST (Figure 2.18): F1(aa1-195), F2(aa189-1026), F3(aa1918-2201), F4(aa1661-1924), F5(aa1388-1667), F6(aa1661-1924) and F7(aa1602-2120). Fragments F2, F3 and F7 were additionally fused to an N-terminal His-tag.

The constructs were expressed and purified according to their fusion-tags under standard conditions (chapter 5.2.2.1.1/2). N-terminal GST-F1 (21 kDa without tag) and the C-terminal section, His-F7 (57 kDa without tag) were successfully expressed and purified (Figure 2.18, fragments depicted in blue). Neither protein was stable when the affinity-tags were removed by Thrombin cleavage under several conditions tested. It was tried to further purify the Mel28 sections by ion exchange chromatography, but the fragments appeared to precipitate on the column. Gelfiltration was tested to remove smaller, contaminating proteins in the Ni-NTA xMel28-F7 eluate (chapter 5.2.2.2). However, separation of the contained proteins by size did not significantly improve the purity of the target protein (data not shown).

Instead, the purification of the fragments GST-F1 and His-F7 on respective affinity resins was optimised. Both fragments were injected into rabbits for polyclonal antibody generation against the N-terminus and a C-terminal section of *X. laevis* Mel28 (Figure 2.19).

Xenopus Mel28

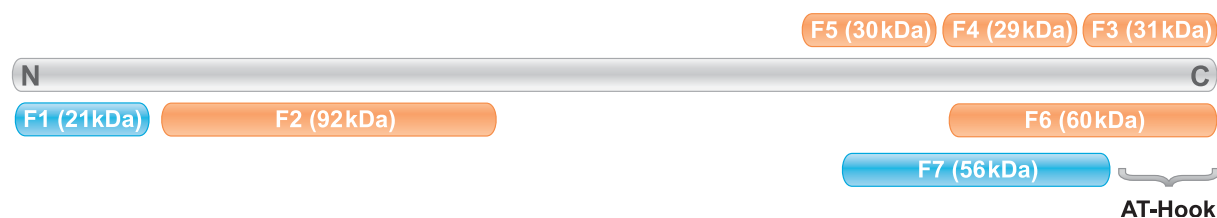


Figure 2.18: Schematic illustration of the distribution of cloned *X. laevis* Mel28 fragments. The shown fragments were fused to GST- and His-tags and expressed in *E. coli*. Fragments used for antibody generation are depicted in blue.

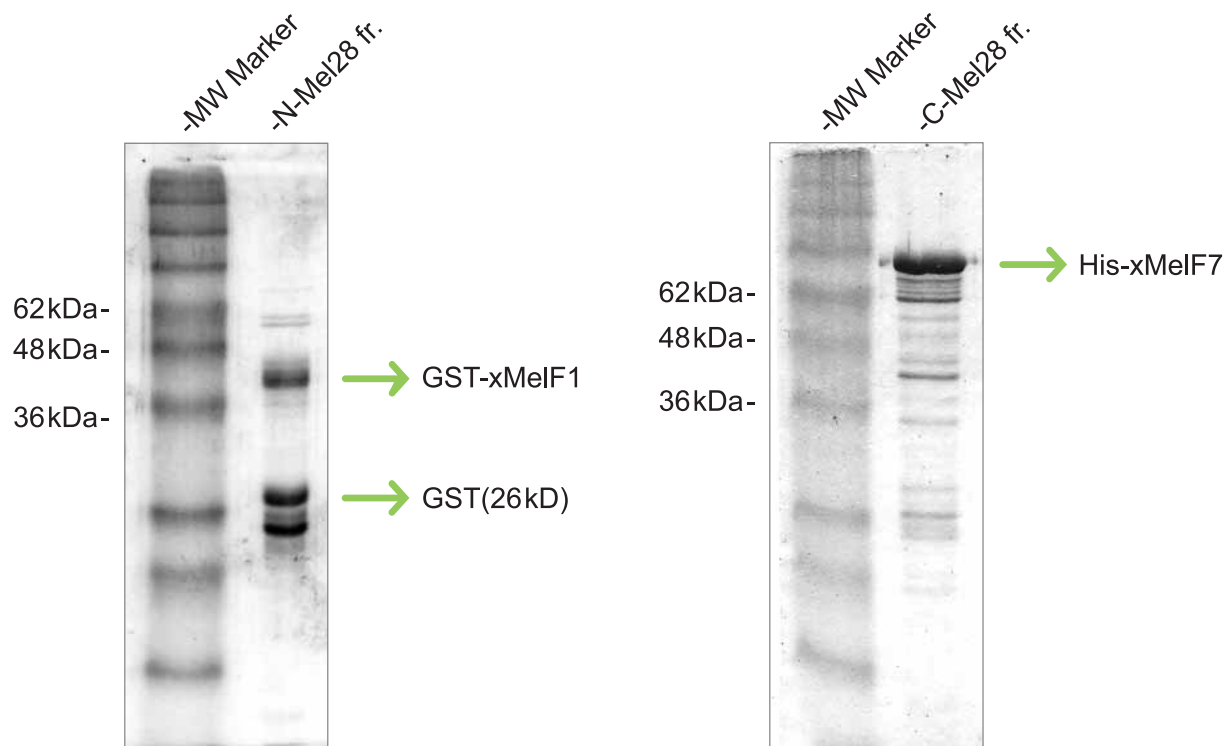


Figure 2.19: *Mel28* fragments purified for antibody generation. GST-xMelF1 and His-xMelF7 were expressed in *E. coli* and purified on affinity resins. Eluates (N-Mel28 fr. and C-Mel28 fr.) were separated by SDS-PAGE and stained with Coomassie blue. Molecular weight markers are indicated on the left lane in each image.

2.2.6 Characterization of Mel28 in *X. laevis* egg extracts and XI177 cells

N- and C-termini of Mel28 were recognized by the respective polyclonal antisera in the cytosol fraction of *X. laevis* eggs on a Western blot (Figure 2.20 and data not shown). The anti-C-terminal antiserum showed a higher affinity for its antigen than the antibodies generated against the N-terminus of Mel28. Therefore, anti-C-terminal Mel28 antiserum was employed for immunodetection of Mel28 on Western blots and for immunofluorescence staining of Mel28 on *in vitro* assembled nuclei and XI177 cells.

Western blots of *X. laevis* egg extract fractions demonstrated that Mel28 was predominantly cytosolic (Figure 2.20, Cyt and tMem). Its migration behavior in SDS-PAGE reflected the molecular weight prediction of ~250 kDa. The antiserum recognized exclusively Mel28 in cytosol fractions on a Western blot demonstrating its specificity (Figure 2.20, $\text{p}\alpha\text{Mel28}$ serum). A small amount of Mel28 was detected in the total membrane fraction but was completely removed by flotation of membranes through a discontinuous sucrose step gradient (see Figure 2.7B and Figure 2.20, fMem). Mel28 was virtually absent from sperm chromatin as judged by Western blot

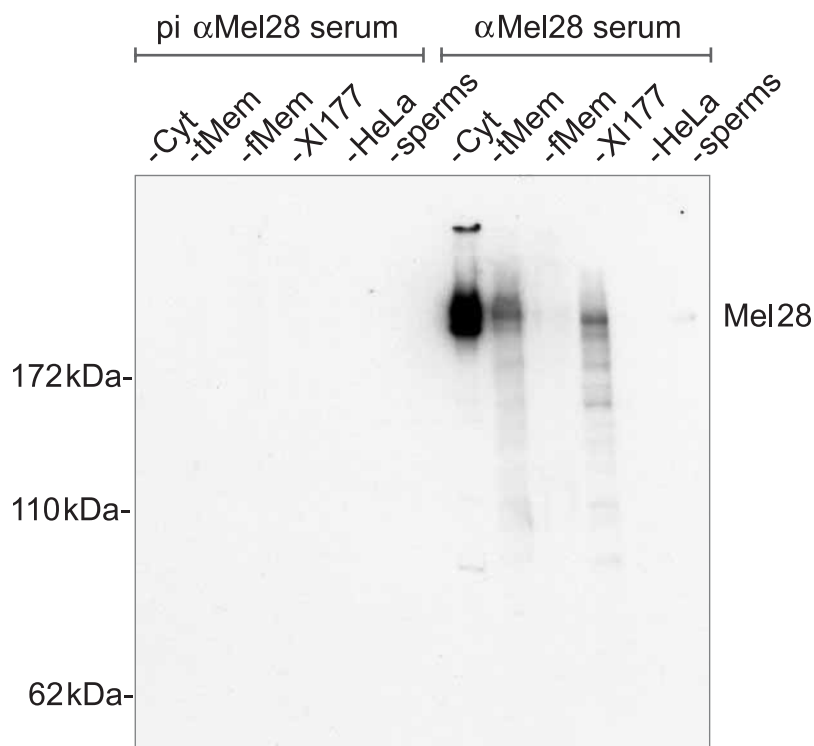


Figure 2.20: Characterization of anti-C-terminal Mel28 antiserum by Western blot. 25 μ g total protein was loaded from each sample: Cytosol (Cyt), total membrane fraction (tMem), floated membrane fraction (fMem), XI177 and HeLa cells, and sperm chromatin (sperm). Pre-immune serum did not show unspecific cross reactivity. Molecular weight marks are indicated on the left.

(Figure 2.20, sperms). Mel28 could not be localized on sperm chromatin when investigated by immunofluorescence. Instead, Mel28 was a component of the NE surrounding the sperm heads in cases where the NE membrane had not been removed entirely during chromatin preparation (data not shown). These results show that the chromatin source employed in *X. laevis* NE assembly assays did not introduce significant amounts of Mel28 into the system. Mel28 displays properties expected from a soluble protein in *X. laevis* egg extract fractions.

Anti-C-Mel28 antibodies did not cross-react with proteins in HeLa cells, on Western blots (Figure 2.20, lane HeLa) or by immunofluorescence (data not shown).

Mel28 was detected in *Xenopus* XI177 cells by Western blot (Figure 2.20, lane XI177) and by immunofluorescence (Figure 2.21A and B). Reflecting the localization of EGFP-Mel28 in XI177 cells, anti-Mel28 antibodies produced a bright NE rim staining in interphase cells, whereas the pre-immune serum did not yield any signal during interphase or mitosis (Figure 2.21A and B). Cells were followed through cell cycle. Interestingly, Mel28 staining disappeared from the nuclear rim upon NE breakdown and localized to the kinetochores in early prophase (Figure 2.21B, second column). The nucleoporin marker mAb414 dissociated from the NE during

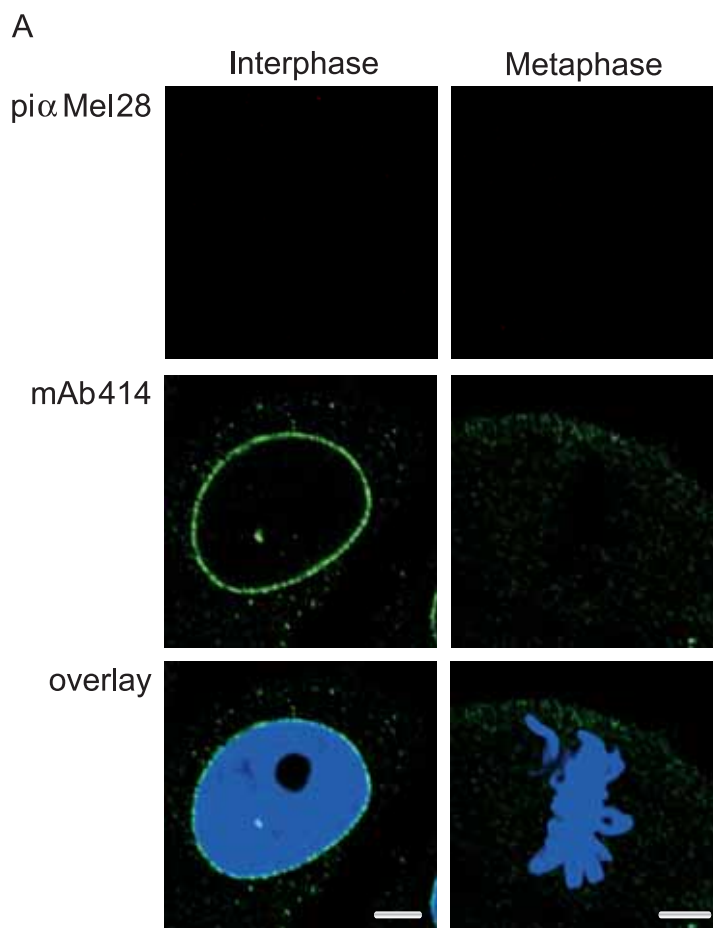


Figure 2.21A: Rabbit pre-immune serum in immunofluorescence on fixed XI177 cells. No background staining is caused by pre-immune serum ($\text{pi}\alpha\text{Mel28}$) in cells in interphase or metaphase ($\text{pi}\alpha\text{Mel28}$, red channel). mAb414 labeling stained the nuclear rim in interphase (green). In the overlaid images DAPI is depicted in blue. Bar: 5 μm .

mitosis. Most soluble nucleoporins distribute throughout the cytoplasm at this stage. Mel28 marked the kinetochores from prophase to anaphase and started to enclose decondensing chromosomes at telophase. At this cell cycle stage mAb414 recognized antigens also reappeared at the surface of the chromatin and an NE started to reform (Figure 2.21B, telophase). Interestingly, Mel28 association with kinetochores during mitosis was also observed in *C. elegans* embryos by Galy and Askjaer (unpublished data).

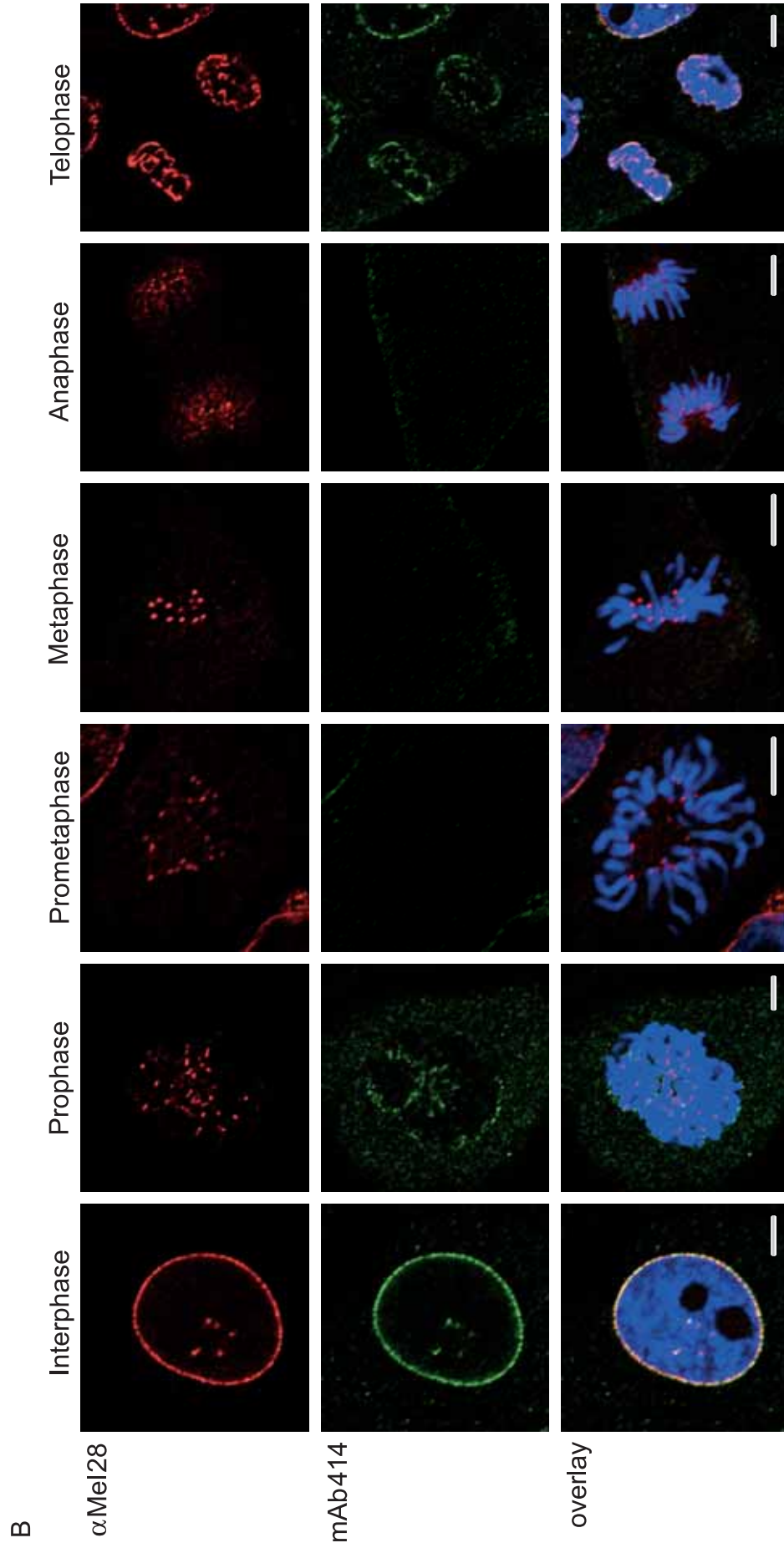


Figure 2.21B: Immunofluorescence of anti-Mei28 antiserum in X1177 cells during mitosis. Mei28 (red channel) resided at the NE during interphase. In prophase, Mei28 dissociated from the NE and marked the kinetochores of forming chromosomes, where it resided until anaphase. In telophase, the NE reformed and Mei28 started to encircle the decondensing chromatin. mAb414 antigens were monitored as reference (green). In the overlaid images, the state of the chromatin can be followed by labeling with DAPI (blue). Bar: 5 μ m.

2.2.7 Functional investigation of Mel28 in nuclear envelope assembly

Mel28 was immunodepleted from *X. laevis* cytosol under the same experimental conditions as Nup155 (chapter 5.2.3.4). Two rounds of depletion eliminated Mel28 to more than 97% from cytosolic extract fractions (Figure 2.22). As mentioned above, Mel28 was not detected in floated membranes prepared from *X. laevis* egg extracts (Figures 2.20 and 2.22, fMem). Therefore, membranes employed in the assembly reactions were not a source of Mel28. Nuclei were reconstituted from mock-depleted cytosol and processed for immunofluorescence. Mel28 localization at the NE was confirmed and additionally some Mel28 associated with chromatin, similarly to Nup107 and Pom121 staining (Figure 2.23, upper section, and Figure 2.10). Mel28 was completely absent from the NE and chromatin when nuclei were reconstituted from depleted cytosol (Figure 2.23, upper section, Δ Mel28). After Mel28 depletion no NE association of any soluble nucleoporin investigated, Nup358, Nup214, Nup153, Nup62, Nup107 or the integral membrane nucleoporin Pom121 could be detected at the rim of the decondensing chromatin (Figure 2.23, middle and lower sections, Δ Mel28). Interestingly, Nup107 chromatin staining was

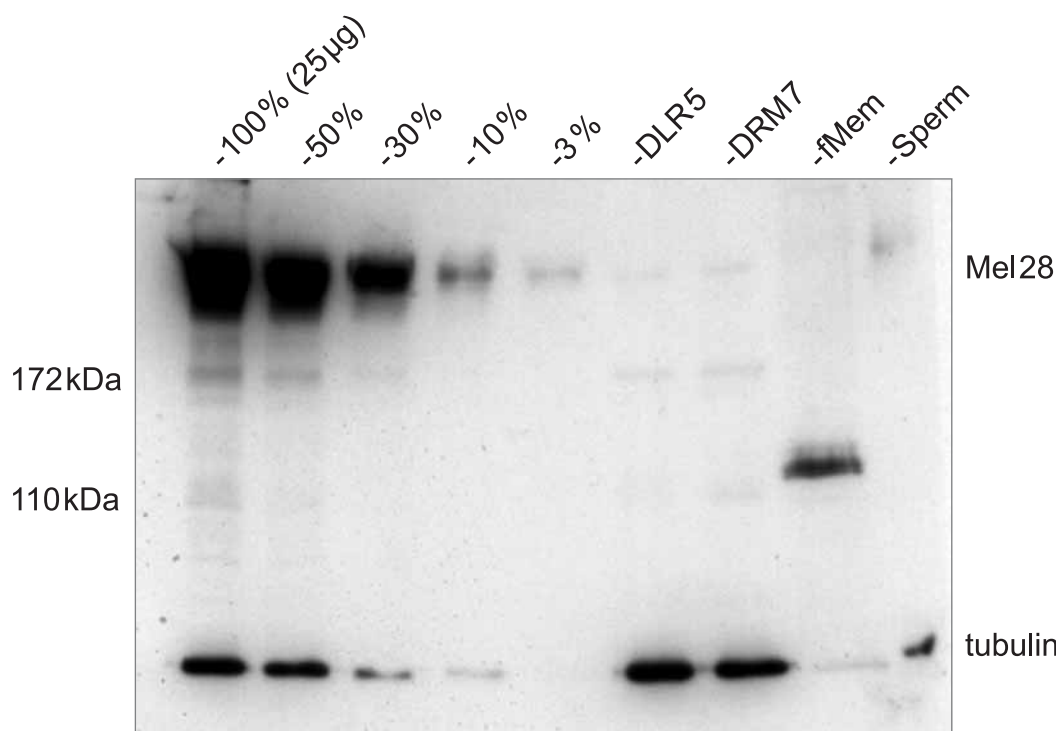


Figure 2.22: *Immunodepletion of Mel28 from X. laevis* egg cytosol. Two different anti-C-Mel28 antisera were used for depletion: DRL5 and DRM7. 25 µg depleted cytosol was loaded and compared to mock depleted cytosol (25 µg = 100%). By titration of mock-depleted cytosol the remaining amount of Mel28 after depletion can be estimated to be less than 3%. Floated membranes (fMem) and sperm chromatin (sperm) represent 25 µg protein loaded. Tubulin served as a loading control.

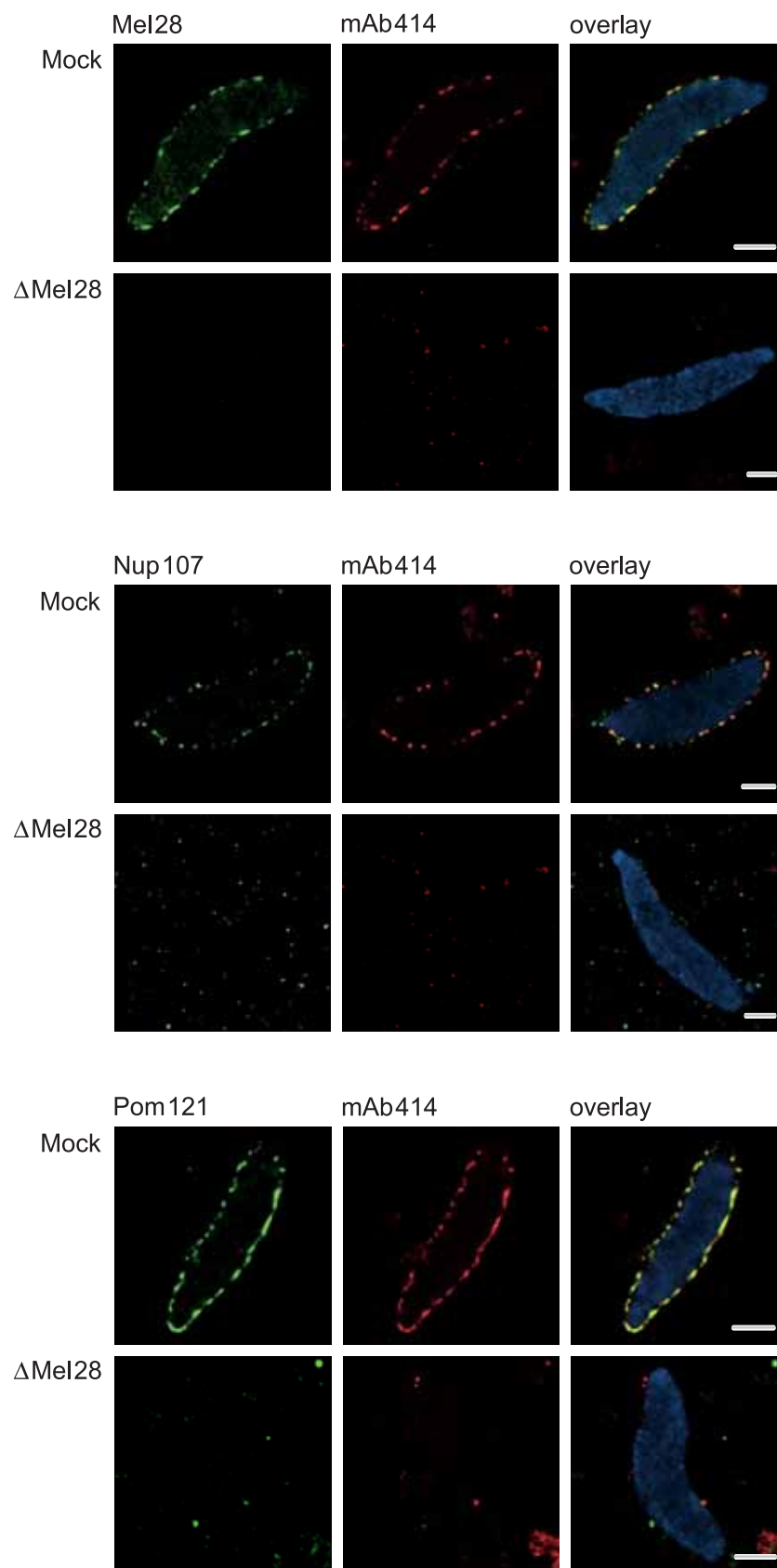


Figure 2.23: *In vitro* reconstituted nuclei devoid of Mel28. Co-immunostainings of mock- (Mock) and Mel28-depleted (Δ Mel28) nuclei were performed, visualizing Mel28 (upper images), Nup107 (middle images), and Pom121 (bottom images) in green and mAb414 recognized antigens (middle column of images) in red. In overlaid images DAPI is represented in blue. Bar: 5 μ m.

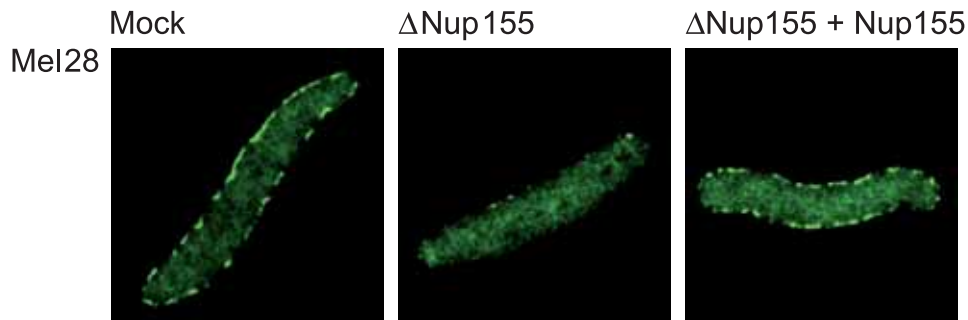


Figure 2.24: *Mel28 remained associated with chromatin upon Nup155 depletion.* Nuclei were reconstituted in the absence of Nup155 (Δ Nup155) and examined for Mel28 localization (green). In mock-depleted cytosol (Mock) and Nup155-depleted cytosol restored by addition of recombinant Nup155 (Δ Nup155+Nup155) Mel28 marks the NE. Mel28 association with chromatin was not impaired by Nup155 depletion.

also not detectable after Mel28 depletion, in contrast to the case when Nup155 was depleted (Figure 2.10).

These data were similar to the phenotype observed upon Nup155 depletion which prevented the accumulation of any nucleoporin investigated at the NE (Figures 2.9 and 2.10). A remarkable difference was that Nup107 and Pom121 could still associate with the chromatin template upon Nup155 elimination but were unable to be organized into NPCs residing in an NE rim staining. In contrast, removal of Mel28, a relatively uncharacterized candidate in NE formation, abolished Nup107 chromatin interaction as well (Figure 2.23, middle section). It is currently under investigation whether Pom121 carrying vesicles can still dock to chromatin lacking Mel28. The specificity of the described phenotype has yet to be proved by readdition of recombinant Mel28 to the depleted extract.

Mel28 recruitment to chromatin and NE was analyzed in Nup155 depleted extracts on reconstituted nuclei by immunofluorescence (Figure 2.24). Absence of Nup155 prevented organization of Mel28 to the NE, but Mel28 association with the chromatin template was not perturbed, similar to Nup107 and Pom121 (Figure 2.24, center image). This observation suggests that Mel28, like Nup107 and Pom121, is recruited early to the chromatin template in the process of NE assembly.

2.2.8 Time course analysis of Mel28 in nuclear envelope formation

NE assembly time course experiments were performed to monitor the behavior of Mel28 relative to Nup155, Nup107, Pom121, mAb414 antigens and nuclear membranes (Figure 2.15). Mel28 covered the chromatin templates after decondensation but before the assembly reaction had been started by addition of

membranes and energy mix (t = 0 min; Figure 2.15, first image column). All other nucleoporins examined in this study required addition of membranes to localize to chromatin (Figure 2.15). In summary, in the NE *in vitro* assembly time course Mel28 bound to the chromatin template first, like Nup107 and Pom121, to be then organized to a continuous rim staining encircling the nuclear periphery during later steps in NE formation (Figure 2.15, t = 60 min, first image column). Surprisingly, Mel28 covered the chromatin template earlier than all other nucleoporins investigated here (t = 0 min). However, Walther *et al.*, (2003) observed Nup107 and Nup133 recruitment to chromatin, similarly to Mel28 before addition of membranes to the NE assembly reaction.¹⁸⁹ The discrepancy between the observations of these two studies might originate in the use of different antisera displaying unequal sensitivities for their antigen. Nup133 and Nup107 antibodies employed by Walther *et al.*, (2003) were generated against human Nup107 and Nup133 and affinity purified.¹¹¹ In this work, polyclonal antiserum directed against a fragment of *X. laevis* Nup107 was used (chapter 5.1.7.1). The recruitment of Nup107 complex to chromatin will be addressed further by monitoring several different nucleoporin constituents of the complex.

2.2.9 Recruitment of Mel28 to chromatin

The recruitment of Mel28 to chromatin templates in *X. laevis* cytosol was investigated further to see whether this behavior was functionally different from Nup107 association with chromatin. The cytosol employed routinely in assembly reactions was not completely free of membrane contaminations due to the preparation procedure. To address the question, whether membranes were required for Mel28 binding to chromatin, membrane-free cytosol was generated, by dilution and high speed ultracentrifugation.¹⁸⁴ Sperm chromatin was incubated with membrane-free cytosol under the same conditions as for NE assembly reactions and processed for immunofluorescence (chapter 5.2.3.6). Nup107 and mAb414 antigens could not be detected on sperm chromatin in this experimental setup as previously reported by Walther and coworkers, whereas Mel28 covered the entire template (Figure 2.25).¹⁸⁴

The data suggested that Mel28 recruitment to chromatin was distinct from Nup107. The results presented in Figure 2.25 support the hypothesis that Mel28 association with chromatin was upstream of Nup107 localization but this requires further investigation.

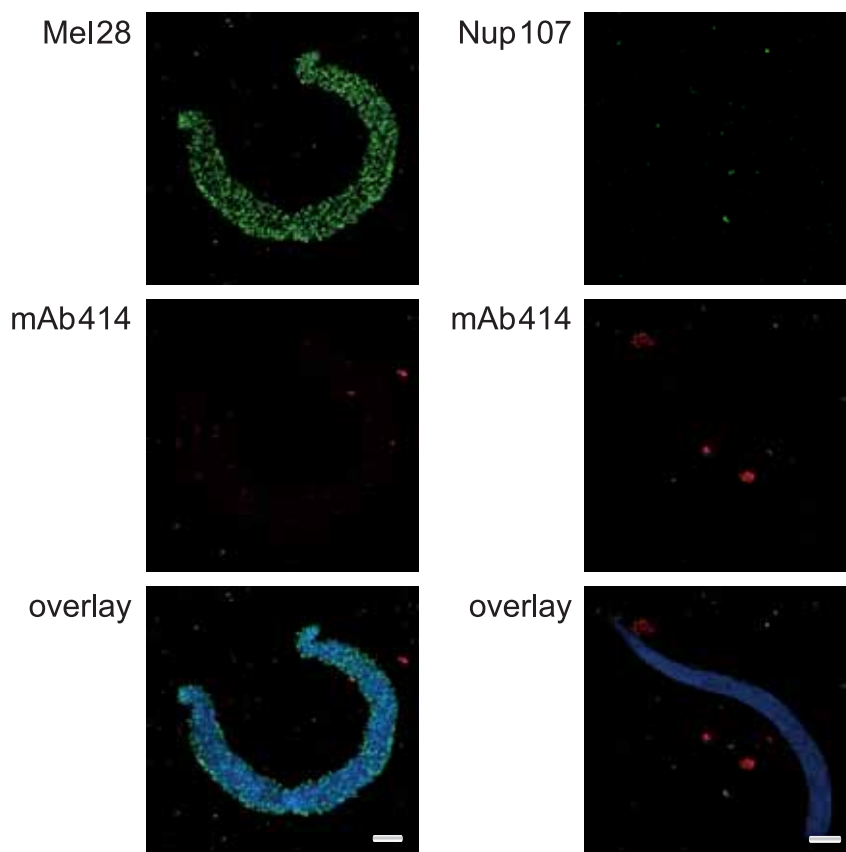


Figure 2.25: Membranes were not required for Mel28 recruitment to chromatin. Sperm chromatin was incubated in virtually membrane-free cytosol and examined for recruitment of Mel28 and Nup107 (green channel) and co-stained for mAb414 antigens (red channel). Chromatin was labeled with DAPI and is shown in blue in the merged images. Bar: 5 μ m.

2.2.10 Mel28 interacts with Nup107

Mel28 depletion from *X. laevis* egg cytosol prevented nucleoporin binding to the NE and chromatin templates. Moreover, Mel28 was the earliest factor recruited to chromatin in NE assembly time course experiments. Therefore, it was obvious to address whether Mel28 might be a platform on chromatin to which subsequent nucleoporins bind. To test this hypothesis, it was investigated whether Mel28 interactions with nucleoporins could be detected *in vitro*. Co-immunoprecipitation experiments of Mel28 and several other nucleoporins were carried out using *X. laevis* egg cytosol (Figure 2.26; chapter 5.2.3.8) and solubilized membranes (data not shown). Nup107 antiserum co-precipitated Mel28 in contrast to a control serum and Nup93, Nup205, Nup155, Nup35, Nup153 as well as Pom121 and gp210 antisera (data not shown). Vice versa, Mel28-Nup107 interaction was confirmed by anti-C-Mel28 antiserum pulling down Nup107 (Figure 2.26). Immunoprecipitations with anti-N-Mel28 antibody yielded similar results (data not shown). Mel28-Nup107 interaction was resistant to high salt washes and the presence of detergents. It persisted

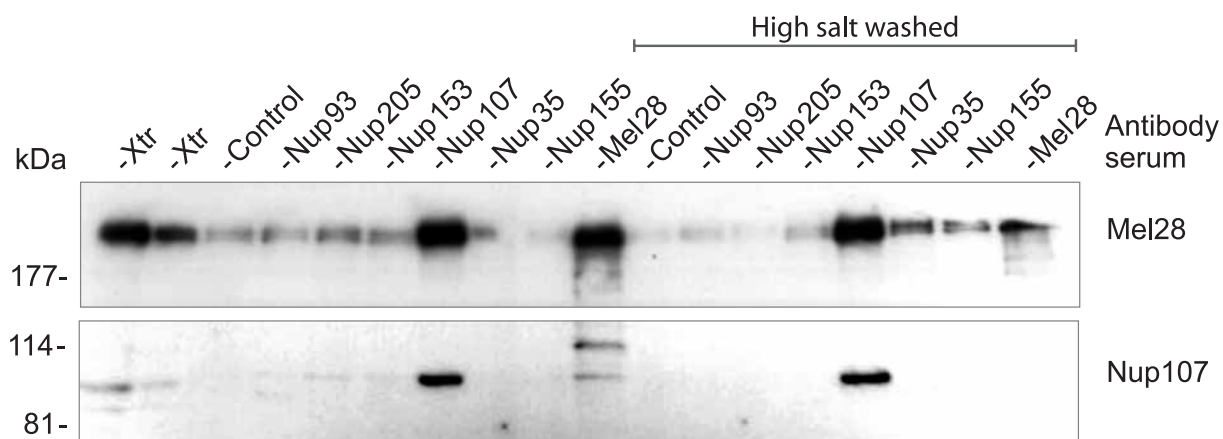


Figure 2.26: *Mel28 and Nup107 co-immunoprecipitate*. Antisera depicted at the top were incubated with *X. laevis* egg cytosol and bound to protein A sepharose. Precipitated proteins were eluted and probed for the presence of Nup107 and Mel28 by Western blot.

throughout mitosis as observed by co-immunoprecipitations from mitotic *X. laevis* egg cytosol (data not shown).*

2.2.11 Knock down of Mel28 by RNAi in HeLa cells

The function of Mel28 in living cells was investigated by RNAi (Figure 2.27). HeLa cells were transfected with either control siRNA oligos targeting a gene that is not present in HeLa cells, or with two different siRNA duplexes matching the human Mel28 mRNA sequence. Cells were fixed after 24 h and 48 h and subjected to immunofluorescence. Schnickschnack, an integral membrane protein of the inner nuclear membrane (Dr. Wolfram Antonin, unpublished data), was chosen to monitor effects on nuclear membranes upon Mel28 knock down. Several nucleoporins were followed by mAb414 staining in Mel28 down regulated cells. Mel28 levels could not be monitored, because antibodies generated against *X. laevis* Mel28 did not cross react with the human homologue.

Accumulation of mAb414 stainable clusters was observed after 24 h in the cytosol in Mel28 downregulated cells but not in control cells (Figure 2.27). The nuclear membrane appeared unaffected as judged by immunofluorescence of schnickschnack (Figure 2.27). It was striking that over time mAb414 labelling at the NE became weaker. Nucleoporins seemed to be lost from the NE, either by cell division or by inhibition of insertion of newly synthesized nucleoporins into existing

* Immunoprecipitation experiments were performed by me and in parallel by Dr. Wolfram Antonin. He investigated the stability of the Mel28-Nup107 interaction under conditions of high salt and detergent and during mitosis. The Western blot presented in Figure 2.26 was kindly provided by Dr. Wolfram Antonin.

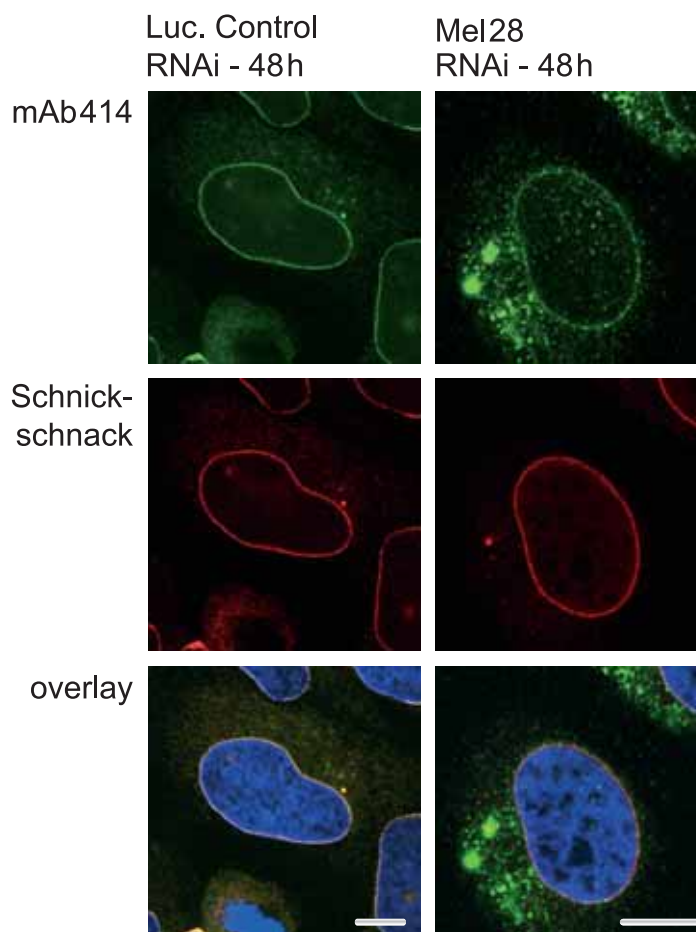


Figure 2.27: Knock down of *Mel28* in living cells caused clustering of *mAb414* antigens in the cytosol. HeLa cells were transfected with siRNA duplexes targeting firefly luciferase (Luc. Control RNAi) or *Mel28* (*Mel28* RNAi). Fixed cells were stained with *mAb414* (green) and *schnickschnack* (red) for immunofluorescence. In the merged images chromatin was labeled with DAPI and is shown in blue. Bar: 10 μ m.

NEs. Effects on the nuclear membrane staining were not noticed at later time points.

In summary, the homologue of *C. elegans* *Mel28* was cloned from *X. laevis* and characterized for its function in NE formation *in vitro*. Localization of *Mel28* in *C. elegans* and *Xenopus* XI177 cells at the NE and kinetochores was concordant. *Mel28* interacts with Nup107 and shares structural features with nucleoporins, like α -helical repeats. *Mel28* could be recruited to chromatin from membrane depleted cytosol in contrast to other nucleoporins and upon *Mel28* depletion from *X. laevis* egg cytosol, nucleoporins investigated could not bind to chromatin or accumulate at the nuclear rim. In conclusion, *Mel28* is a novel, essential player in NE formation. It might be a putative candidate for mediating the anchorage of NPCs to chromatin.

3 Discussion

3.1 *Nup155 regulates nuclear envelope and nuclear pore complex formation in vertebrates*

3.1.1 Features of the nucleoporin Nup155

Although rat Nup155 was characterized as a nucleoporin more than ten years ago, this work presents the first functional analysis of vertebrate Nup155. Radu *et al.*, (1993) identified Nup155 as a nucleoporin and localized it symmetrically at the pore center.¹²³ Nup155 is conserved throughout the eukaryotic kingdom.⁸¹ Analysis of its protein sequence did not reveal the presence of FG-repeats commonly found in nucleoporins that participate in nucleocytoplasmic transport. Nup155 did not bind to wheat germ agglutinin sepharose, a lectin that allows the isolation of nucleoporins modified by O-linked N-acetylglucosamine residues.²³⁷ Nup160, Nup133 and Nup155 contain an N-terminal β -propeller domain whereas the C-terminal sections are predicted to organize into α -helical repeats.⁸⁵ Thus, Nup155 domain architecture resembles nucleoporins of the Nup107 complex that comprises an important architectural unit of the NPC.¹⁴³ Numerous consensus sites for kinases are predicted for Nup155 and reduced migration of Nup155 in mitotic *X. laevis* egg extracts during mitosis was most likely due to phosphorylation (data not shown).¹²³

3.1.2 Depletion of Nup155 impairs nuclear morphology, segregation and viability

Galy *et al.*, (2003) described Nup155 as being essential for viability and normal nuclear morphology during early embryonic development in *C. elegans*.¹¹⁹ In agreement with these results, down regulation of Nup155 by RNAi in HeLa cells also led to cell death. The role of Nup155 for nuclear appearance was further addressed by RNAi in *C. elegans* in parallel to this study.²²⁵

Nematode strains that co-expressed fluorescent β -tubulin and lamin were monitored by time-lapse confocal microscopy. Embryos devoid of Nup155 had no detectable pronuclei visible by DIC microscopy or by lamin staining. Centrosomes separated prematurely, probably because of lack of anchoring to the pronuclear envelopes. Following mitosis, the embryos failed to assemble a visible nucleus or nuclear lamina, suggesting severe defects in NE formation. To further analyze pronuclear appearance *in vivo*, the chromatin was examined in a *C. elegans* strain

expressing histone H2B fused to GFP. Whereas the chromatin in control embryos behaved normally throughout mitosis, pronuclei in Nup155-depleted embryos were dramatically reduced in size and individual chromosomes could not be recognized. Severe mitotic defects were observed. No mitotic spindle formed and chromosome segregation was impaired, leading to non-disjunction of chromosomes.²²⁵ In analogy to segregation defects in *C. elegans*, one of the Nup155 homologues in yeast, Nup170, was reported to have a role in chromosome segregation and kinetochore function.²¹⁵ DNA segregation depends on coordinated events of DNA replication and condensation, sister chromatid cohesion and incorporation into the mitotic spindle via kinetochore fibers. Since pronuclear formation was abnormal in the absence of Nup155 it is likely that one or more of these processes were perturbed, arguing that the defects in DNA segregation upon Nup155 depletion might be indirect. Therefore, it was necessary to directly address Nup155 functions.

3.1.3 Nup155 is essential for NPC assembly

This work shows that Nup155 depletion inhibited NPC formation, as judged by electron microscopy and immunofluorescence analysis on *in vitro* reconstituted nuclei. Early recruitment of Nup107 and Pom121 to the chromatin surface still occurred, but both proteins failed to undergo later accumulation at the chromatin periphery in the NE. Thus, the initial targeting of Nup107 and Pom121 to chromatin in the *in vitro* system appeared independent of Nup155. However, downstream recruitment steps involving additional NPC components and their organization into NPCs was inhibited. Electron microscopy of these nuclei confirmed the absence of any NPCs (Figure 2.13).

In HeLa cells nuclear rim staining of the mAb414 antigens Nup62, Nup153, Nup214 and Nup358 was significantly reduced upon Nup155 knock down (Figure 2.5). This suggests that vertebrate Nup155 might also be essential for NPC formation *in vivo*.

In *C. elegans* Nup35, Nup96, Nup153, Nup98 and Nup358 all failed to accumulate at the NE in the absence of Nup155. The most dramatic phenotype was obtained with Nup35, that was completely absent from the chromatin of Nup155 RNAi embryos. In the absence of Nup155, Nup153 still associated with chromatin but no longer accumulated at the nuclear periphery. Other nucleoporins investigated showed an irregular staining with prominent foci in the cytoplasm.²²⁵

The Nup107 complex assembles early during postmitotic NE reconstitution.^{111, 189} Its association with chromatin prior to NPC assembly and nuclear membrane fusion was not impaired in the absence of Nup155 *in vitro*. Similarly, in a *C. elegans* strain expressing YFP-Nup107 pronuclear rim staining was abolished in Nup155 depleted embryos, but a diffuse localization on the chromatin of the pronuclei remained visible.²²⁵

3.1.4 Nup155 is required for nuclear membrane fusion

The severe effects on pronuclei in *C. elegans* embryos depleted of Nup155 prompted us to address the fate of the nuclear membrane. GFP-Man1, an integral membrane protein of the INM, was visualized through mitosis in *C. elegans* embryos. GFP-MAN1 staining appeared very diffuse, whereas in control embryos GFP-MAN1 marked the NE as a distinct rim staining. Although GFP-MAN1 was recruited to chromatin at the end of mitosis, the distribution was not as homogenous as in control embryos and nuclear membrane morphology was clearly abnormal.

These observations were consistent with the defects on nuclear membrane sealing found on *in vitro* assembled nuclei (Figure 2.11). While docking of membranes to the chromatin surface seemed to occur normally, subsequent fusion steps did not advance to completion, and integration of NPCs into the membranes was not detected. Inhibition of NE membrane fusion in *C. elegans* embryos and in nuclei assembled in *X. laevis* egg extracts were analyzed at ultrastructural levels by EM. This confirmed the conclusion drawn by confocal microscopy. In both systems, three different types of chromatin-membrane associations were noted: chromatin regions free of membranes, flattened membrane patches associated with chromatin but devoid of NPCs, and areas with docked membrane vesicles that had not fused (Figure 2.13).²²⁵

Importantly, the inhibition of NPC and NE assembly was efficiently reversed by addition of purified, recombinant Nup155. Therefore, the *in vitro* system allowed to directly assign the observed defects to Nup155 function.

Previously, such dramatic inhibition of NE assembly was only observed for the membranenucleoporin Pom121.¹⁷³ In contrast to Pom121, no evidence was found that Nup155 is an integral membrane protein, consistent with work by Hawryluk-Gara and coworkers in cultured mammalian cells.¹¹⁸ Therefore, Nup155 is the first soluble nucleoporin that caused a complete block in nuclear membrane fusion and NPC

assembly and its essential function is conserved from nematodes to vertebrates.²²⁵

Interestingly, the two Nup155 homologues in yeast, Nup170 and Nup157 were also implicated in NE morphology. Repression of Nup170 expression in a Δ Pom152 background, revealed an irregularly shaped NE with massive extensions and invaginations. Long stretches of NE devoid of NPCs were described. Vice versa, overexpression of Nup170 in a Pom152 mutant background caused structures resembling intranuclear annulate lamellae, which lied parallel to and beneath the INM and contained regularly spaced NPCs.²¹¹ Taken together, these results argue for a role of yeast Nup170 in nuclear membrane and NPC assembly. Similar membrane extensions originating from the INM were induced by overexpression of Nup53 (homologue of vertebrate Nup35) in yeast. These tubular structures gave rise to flattened double membrane-enclosed cisternae containing empty pores, without incorporated NPCs. Only the yeast integral pore membrane proteins Pom152 and Ndc1 localized to these pores, suggest that these structures marked intermediates in NPC assembly.²¹² Again, a link to the yeast homologue of Nup155 can be drawn, because Nup170 acts as a binding site for Nup53 at the NPC in yeast.²¹⁴ Interestingly, investigating the mislocalization of several nucleoporins upon Nup155 knock down in *C. elegans*, Nup35 was most dramatically affected being completely absent from chromatin.²²⁵ However, co-immunoprecipitation from *X. laevis* egg cytosol employing Nup155 and Nup35 antibodies revealed no direct interaction between Nup155 and Nup35 (data not shown).

3.1.5 Order of events in nuclear envelope assembly

GFP-Nup155 dissociated completely from chromatin during mitosis in *C. elegans* embryos and reflected initial observations of Nup155 in mammalian cells.^{123, 225} In worms, GFP-Nup155 was recruited to chromatin approximately 1 min after anaphase onset. Because of the very rapid divisions in early *C. elegans* embryos this timing cannot be directly compared to nucleoporin recruitment in other organisms, but can be interpreted in relation to similar marker proteins in worms and vertebrates. However, similar behavior was observed for two other nucleoporins that are predicted to be soluble in mitosis, Nup35 and Nup45/Nup58. In vertebrate cells, the products of the alternatively spliced Nup45/Nup58 gene, form an NPC subcomplex together with Nup54 and Nup62.²³⁸ This complex is recruited to the reforming NE later than Pom121 but earlier than gp210 and Tpr, which are the

nucleoporins currently known to assemble last during the process of NPC formation *in vivo*.^{190, 239} Monitoring nuclear reconstitution *in vitro* and *in vivo* confirmed the relative order of recruitment of several nucleoporins. Nup155 was placed isochronically with Nup62 and other mAb414 antigens and significantly later than Nup107 and Pom121.^{173, 189, 190, 239} Moreover, although membranes dock to chromatin very early during nuclear assembly, fusion to closed membranes occurs only concomitantly with Nup155 accumulation (Figure 2.15). Thus, a similar relative timing of Nup155 recruitment was observed *in vivo* and *in vitro*. Further, results from both systems reflected an interdependent process of NPC and nuclear membrane assembly into a functional NE after mitosis.

3.1.6 Nup155 plays a role in a checkpoint mechanism linking nuclear pore complex and nuclear membrane assembly

Integrating the Nup155 depletion phenotype in the order of events taking place during nuclear reconstitution in *X. laevis* egg extracts with previous observations by Walther *et al.*, (2003) and Antonin *et al.*, (2005), we conclude that the Nup107 complex is recruited to the chromatin template for the formation of a “prepore”, even in the absence of Nup155.^{110, 173, 188, 189} In Nup155 depleted *in vitro* reactions Nup107 was present on the chromatin surface but failed to proceed further into NPC formation. Similarly, YFP-Nup107 associated with chromatin throughout mitosis in the absence of Nup155 in *C. elegans* embryos did not organize into a prominent peripheral nuclear staining. Nup107 was recruited to chromatin earlier than Nup155 in the NE assembly time course *in vitro*. Furthermore, membrane vesicles containing Pom121 docked to chromatin in extracts devoid of Nup155. Although Pom121 rim staining was abolished in Nup155 depleted reactions, a dim signal was still detectable on the chromatin surface, most likely deriving from the presence of membrane vesicles carrying Pom121. In a wildtype situation, other nucleoporins would then be recruited, such as mAb414 antigens, Nup155, Nup205 and Nup93. This did not occur in the absence of Nup155. At about the same time as Nup155 bound to chromatin nuclear membranes normally sealed and gp210 was detectable at the NE. In the absence of Nup155 the process was blocked at the stage of nuclear membrane fusion and the recruitment of further nucleoporins, arguing for an interactive process of NPC and nuclear membrane formation.

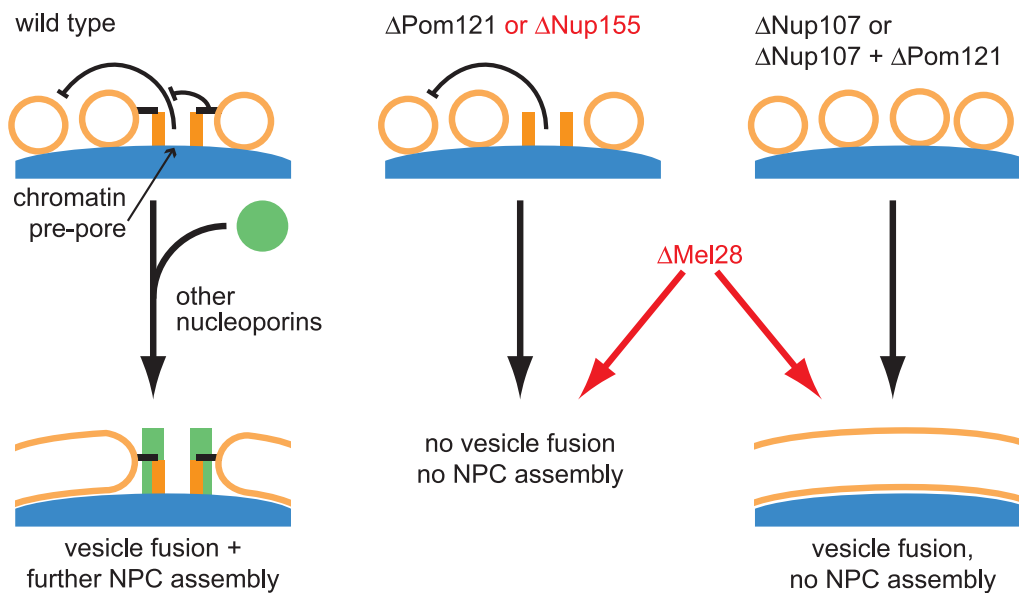


Figure 3.1: *Current model for postmitotic nuclear envelope reformation.* Pom121 and Nup155 depletion led to an inhibition of NPC assembly and membrane vesicle fusion (middle). The block on nuclear membrane formation was overcome by Nup107-Pom121 double depletion, which resulted in a sealed nuclear membrane devoid of NPCs (right). Mel28 was essential for nucleoporin recruitment to chromatin and thus for NPC assembly. The role of Mel28 on nuclear membrane fusion is currently not known. (Modified from Antonin *et al.*, (2005). *Mol. Cell* 17, 83-92.)

Unexpectedly, absence of the soluble nucleoporin Nup155 yielded a very similar inhibition in nuclear membrane and NPC formation as did depletion of the integral membranenucleoporin Pom121, supporting the hypothesis of a quality control mechanism, a checkpoint (Figure 3.1).¹⁷³

For Pom121 it was shown that the block in nuclear membrane fusion could be released upon Nup107-Pom121 double depletion, resulting in a sealed membrane devoid of pores.¹⁷³ The scenario might be similar in Nup155 depleted extracts since Nup107 is present at the chromatin and might block vesicle fusion due to a role in sensing defective NPC formation. Unfortunately, for technical reasons related to the stringency of the conditions needed for Nup155 depletion, we were unable to test the effect of co-depleting Nup155 and the Nup107 complex preventing a direct experimental check of this hypothesis.

Current data suggest that the presence of the Nup107 complex on the chromatin template, presumably forming a “prepore” structure, is responsible for the subsequent block in NPC assembly and nuclear membrane fusion when essential structural components of the pore, like Pom121 and Nup155, are missing. To verify this conclusion it would be interesting to investigate the molecular effect of the calcium chelator BAPTA on NE formation in that context. Although Nup107 complex

is present at chromatin in the presence of the drug integration of NPC assembly and nuclear membrane fusion, otherwise kept under surveillance, seems to be uncoupled and a closed NE devoid of NPCs can be formed.¹⁷⁷ This indicates that BAPTA might interfere with NPC assembly at the point where Nup107 complex controls subsequent NPC assembly and NE membrane fusion. In future, it will be interesting to address whether BAPTA can overcome this inhibition induced in the absence of Pom121 or Nup155. This would further support the hypothesis that both nucleoporins are surveyed by the same checkpoint.

In yeast a direct interaction between Nup157 and the yeast homologue of a component of the Nup107 complex, Nup120, was recently demonstrated. This suggests that metazoan Nup155 might also bind to the Nup107 complex.¹⁰⁹ However, despite several attempts, it was not possible to identify any Nup155 interaction partners by co-immunoprecipitation from *X. laevis* egg cytosol, leaving this possibility open.

In conclusion, this study of Nup155 strengthens the evidence for the recently proposed checkpoint model that links the interconnected processes of nuclear membrane and NPC assembly in the *X. laevis* egg extract system.^{173, 225} Further, it extends this concept by demonstrating that Nup155, a soluble nucleoporin that is recruited at a late step in NPC assembly, must be present for nuclear membrane assembly to proceed to completion. Given that assembly of an NE lacking NPCs would be lethal, the existence of such a checkpoint is reasonable. Except for Nup155, none of the other soluble nucleoporins that have been tested by depletion from *X. laevis* cytosol so far led to a similar phenotype.^{103, 116, 122, 129, 139, 189, 192} Our data may either suggest that rather late steps in NPC assembly are monitored prior to nuclear membrane formation or that Nup155, the Nup107 complex and Pom121 have a direct role in controlling nuclear membrane and NPC assembly. The consistent results obtained from *C. elegans* and the *X. laevis in vitro* system suggest that the NPC-nuclear-membrane-assembly checkpoint is conserved. The presented results suggest the existence of either a protein or a signalling event that brings together the chromatin-associated Nup107 complex, membrane-bound Pom121 and soluble Nup155 (Figure 3.1). An important challenge is now to determine the nature of such a control mechanism and to understand how integration of NPC and nuclear membrane assembly is achieved.

Moreover, it will be crucial to scrutinize how a series of proteins with very diverse functions, like the GTPase Ran and components of the Ran cycle, importin β , the AAA-ATPase p97 and its adaptors Npl4-Ufd1, the nucleoporins Pom121 and Nup155 all display sensitivity for these initial steps of NE formation, leading to inhibition of nuclear membrane fusion when perturbed.^{173, 174, 178, 179, 180, 182, 183, 225} The molecular mechanisms required for NE formation will be only understood when the diverse proteins participating are characterized.

3.2 *Mel28, a novel factor in postmitotic nuclear envelope assembly*

3.2.1 Sequence analysis of vertebrate Mel28

A more detailed analysis of Mel28 in *C. elegans* embryos employing NE specific markers revealed that Mel28 is essential for pronuclear appearance, similarly to Nup155. To address the molecular function of Mel28, the *X. laevis* homologue was identified and cloned. Its functional conservation between nematodes and vertebrates was demonstrated and ongoing experiments investigate this novel candidate essential for NE assembly *in vitro* and *in vivo*.

Among vertebrates, conservation of the N-terminal half of Mel28 (aa1-1000) is good, whereas the C-terminal half exhibits low homology between species, except for the C-terminal ~40aa surrounding an AT-hook. Two expressed alleles were identified in *X. laevis* and the DNA sequence of one was completely annotated and a full length construct was cloned. An IMAGE clone (gi|49903665) that contained the complete ORF was sequenced in parallel to cloned EST fragments deriving from the same allele. The sequence of the IMAGE clone contained two internal stop codons and the presented sequence was therefore composed from two fragments. The full length ORF was confirmed by the sequence contig assembled from individual fragments. Recently, a *X. laevis* Mel28 sequence of 2408aa was submitted to NCBI that is 86% identical to the protein sequence annotated in this work. An additional stretch of ~200aa is inserted in the C-terminal half of the sequence found under the accession number gi|55250537.²⁴⁰ Both sequences are equally identical to the mouse Mel28 (ELYS) sequence. Most likely they derive from different Mel28 alleles. The additionally inserted sequence stretch might be a mispredicted splicing site as none of the vertebrate homologues aligns with this region.

Anti-C-terminal antibodies recognized a doublet at ~250 kDa in *X. laevis* egg cytosol. Doublet bands are quite common for proteins from *X. laevis* because it is a tetraploid organism. Upon immunodepletion of Mel28 from the cytosol both bands disappeared.

3.2.2 Mel28 localization is conserved from nematodes to vertebrates

Localization of vertebrate Mel28 at the NE and at kinetochores during mitosis was demonstrated (Figure 2.21B). This reflected observations of Mel28 localization in *C. elegans* (Galy and Askjaer, unpublished data). Identical localization of Mel28 in both systems was considered as weak evidence for a functional conservation of Mel28 between nematodes and vertebrates. Interestingly, kinetochore localization during mitosis was also described for several nucleoporins, like the Nup107 complex, Rae1 and RanBP2.^{88, 104, 111} One model suggests that factors required early in postmitotic NE reformation are stored at kinetochores during mitosis from where they distribute over the decondensing chromatin and function as binding partners for other proteins recruited from the cytosol.¹¹¹ Furthermore, the localization of NPCs at kinetochores together with checkpoint proteins could link chromosome segregation with NE breakdown and reformation and presents an important function in cell cycle regulation.¹⁰⁶

3.2.3 Mel28 is an essential component for nuclear envelope reformation

During mitosis Mel28 behaved similarly to nucleoporins that leave the NE in prophase and reaccumulate at the decondensing chromatin in telophase *in vitro* and *in vivo* (Galy and Askjaer, unpublished data).²²⁵ Time course experiments performed on *in vitro* assembled nuclei showed that Mel28 was early (Figure 2.15). After preincubation of sperm chromatin with membrane-free cytosol, Mel28 covered the entire chromatin template in contrast to Nup107 or other nucleoporins tested. It was concluded that Mel28 is a soluble protein recruited from membrane-free cytosol to decondensing chromatin (Figure 2.25). Consistent with these results, Mel28 depletion from *X. laevis* cytosol inhibited chromatin localization of Nup107 and any other soluble nucleoporin investigated. The integral membrane protein Pom121 did not accumulate at the nuclear periphery in the absence of Mel28. Whether Pom121 vesicles still dock to chromatin under this condition is currently under investigation. Interestingly, upon depletion of Nup155, which is assembled later into NPCs,

Nup107, Pom121 and Mel28 all still localized at chromatin, but failed to be organized into the NE.

Mel28 was demonstrated to interact with Nup107 by co-immunoprecipitation from *X. laevis* egg cytosol (Figure 2.26). Interestingly, YFP-Nup107 overexpression in a *C. elegans* strain depleted of Mel28 seemed to compensate the phenotypic defects to some extent caused by Mel28 depletion (Galy and Askjaer, unpublished data). This indicates that a functional interaction between Nup107 and Mel28 also takes place in nematodes. Preliminary data proposed that Nup153 and Nup62 co-immunoprecipitate with anti-C-Mel28 antiserum in *X. laevis* egg cytosol (data not shown). Considering the putative interactions with several nucleoporins and the structural features predicted for Mel28 it may be that Mel28 functions as a scaffold, anchoring NPCs to chromatin.

In vivo, depletion of Mel28 by RNAi in *C. elegans* affected nucleoporin localization. mAb414 antigens clustered in the cytosol of early embryos and were visible as aggregated dots on the chromatin surface, suggesting a role for Mel28 in NPC organization and/or localization *in vivo*. RNAi knock down of Mel28 in HeLa cells resulted in prominent mAb414 stainable clusters in the cytosol, while mAb414 staining at the NE became weaker.

In summary, our current data suggest that Mel28 is an early factor that localizes to chromatin during NE reformation and is essential for subsequent recruitment of soluble nucleoporins to the reforming NE.

3.2.4 Fundamental questions concerning the role of Mel28

Two central questions arise from the described observations: First, is Mel28 a so far unidentified nucleoporin and second, how does Mel28 depletion impair nuclear membranes?

Investigations by co-immunofluorescence stainings of Mel28 and other nucleoporins on *XI177* cells resulted in identical punctuated staining patterns surrounding the nucleus, indicating a colocalization of Mel28 with nucleoporins. In contrast, co-staining of Mel28 and mAb414 on fixed *C. elegans* embryos revealed a smooth NE rim labeling of Mel28 and a dotted staining of nucleoporins. In these embryos, Mel28 NE staining is on the nucleoplasmic side relative to mAb414 NE staining, suggesting that Mel28 might not colocalize with nucleoporins (Galy and Askjaer, unpublished data). This question must be addressed by immunoelectron

microscopy of Mel28. However, if Mel28 is a nucleoporin, an obvious question is why it was not identified in biochemical and proteomic approaches, which isolated 30 currently known nucleoporins and even NPC associated proteins?^{66, 67}

Irrespective of whether Mel28 is a nucleoporin or an NE protein, there is accumulating evidence for Mel28 function in NPC anchorage. For example, upon RNAi knock down of Mel28 from HeLa cells, major mAb414-stainable clusters were found in the cytosol and in parallel nuclear rim staining became weaker. This result suggests that Mel28 maybe necessary for nucleoporins to incorporate into NPCs or to be required to anchor NPCs in the NE. The loss of NPCs from the NE in these cells is in agreement with the data obtained from the *X. laevis in vitro* nuclear reconstitution system and in Mel28 depleted *C. elegans* embryos. Considering that Nup107 interacts with Mel28 and that in egg cytosol devoid of Mel28, Nup107 is not recruited to chromatin, Mel28 maybe essential for NPC localization at chromatin. It will be interesting to see whether in the absence of Mel28 a “Nup107-phenotype” exists in which closed nuclear membranes form devoid of pores (Figure 3.1).¹⁸⁹

Concerning the nature of nuclear membranes in the absence of Mel28, only indirect evidence can be provided, hitherto. When Mel28 was knocked down by RNAi in HeLa cells and phenotypic analysis of nuclear membranes was performed, the INM protein schnickschnack seemed unaffected.

4 Perspectives

Before a complete picture of Nup155 and Mel28 function in NE formation is available, several questions remain to be addressed.

It is not understood which mechanism leads to an inhibition of NPC assembly and nuclear membrane fusion in the absence of Nup155. An obvious question is whether Pom121 and Nup155 participate in the same checkpoint mechanism as their individual depletion leads to a very similar inhibition in NE assembly (Figure 3.1). Identification of interaction partners of Nup155 could help to elucidate the mechanistic details but, thus far such partners have not been identified. Double depletion of the Nup107 complex and Pom121 overcame the block in nuclear membrane fusion caused by single depletion of Pom121, leading to formation of nuclei sealed by membranes devoid of NPCs. Double depletion of Nup155 and Nup107 complex could help to pinpoint whether Pom121 and Nup155 participate in the same checkpoint mechanism but this experiment is currently technically impossible.

It was shown that Mel28 binds to chromatin in membrane-free cytosol and interacts with the Nup107 complex. When nuclei were assembled in the absence of Mel28, Nup107 did not bind to chromatin, suggesting that Mel28 might be necessary for Nup107 complex recruitment. Thus, if Mel28 was the earliest protein required for NPC assembly on chromatin, Mel28 might constitute the anchor for NPCs at the chromatin and thereby in the NE. To verify this model, Mel28 localization upon Nup107 complex depletion has to be investigated. If Mel28 still binds to chromatin under this condition but Nup107 is missing in the absence of Mel28, this would suggest a role for Mel28 upstream of Nup107. The presented data are all consistent with this hypothesis but more work will be required to provide definitive evidence. Importantly, the effect of Mel28 depletion on nuclear membranes needs to be investigated to assign it to either a “Pom121 & Nup155” or “Nup107” phenotype upon depletion (Figure 3.1).

5 Materials and Methods

5.1 Materials

5.1.1 Chemicals and Reagents

Acetic acid	Merck (Darmstadt, Germany)
30% Acrylamide/bisacrylamide solution, 37.5:1	Biorad (München, Germany)
Adenosine 5'-triphosphate (ATP)	Sigma-Aldrich (Steinheim, Germany)
Agar-agar	Serva (Heidelberg, Germany)
Agarose	Invitrogen (Karlsruhe, Germany)
Alexa Fluor® 546 goat anti-mouse/rabbit IgG	Invitrogen (Karlsruhe, Germany)
Alexa Fluor® 488 goat anti-mouse/rabbit IgG	Invitrogen (Karlsruhe, Germany)
Ampicillin	Grünenthal (Aachen, Germany)
Ammonium chloride	Merck (Darmstadt, Germany)
Ammonium sulfate	Gibco BRL (Eggstein, Germany)
Ammonium peroxydisulfate	Sigma-Aldrich (Steinheim, Germany)
Bacto tryptone	Difco (Detroit, USA)
Bacto yeast extract	Difco (Detroit, USA)
BAPTA 1,2-bis(2-aminophenoxy) ethane-N,N,N',N'-tetraacetic acid	Invitrogen (Karlsruhe, Germany)
BCA™ Protein Assay Kit	Pierce (Rockford, USA)
Bench Mark™ Prestained Protein Ladder	Invitrogen (Karlsruhe, Germany)
Bovine serum albumin (BSA)	Fluka (Steinheim, Germany)
Bromophenol blue (3',3'',5',5''-tetrabromophenolsulfonephthalein)	Sigma-Aldrich (Steinheim, Germany)
Calcium chlorid	Merck (Darmstadt, Germany)
CNBr-activated Sepharose™ 4B	Amersham Biosciences (Braunschweig, Germany)
Complete™ EDTA-free Protease Inhibitor Cocktail	Roche (Mannheim, Germany)
Coomassie brilliant blue G-250	Sigma-Aldrich (Steinheim, Germany)
Creatine phosphate	Roche (Mannheim, Germany)
Cycloheximid (3-(2-(3,5-dimethyl 2-oxocyclohexyl) 2-hydroxyethyl)glutarimide)	Simar-Aldrich (Steinheim, Germany)
L-Cysteine	Merck (Darmstadt, Germany)
Cytochalasin B	Sigma-Aldrich (Steinheim, Germany)
4',6-Diamidino 2-phenylindole (DAPI)	Sigma-Aldrich (Steinheim, Germany)
1-(4,5-Dimethoxy 2-nitrophenyl)ethyl ester (A23187)	Invitrogen (Karlsruhe, Germany)
Dimethyl sulfoxid (DMSO)	Merck (Darmstadt, Germany)
DNA oligos	MWG Biotech (Ebersberg, Germany)
1,1'-Diocadecyl-3,3,3',3'-tetramethylindocarbocyanine perchlorate (DiIC ₁₈)	Invitrogen (Karlsruhe, Germany)
1,4-Dithio L-threitol (DTT)	Merck (Darmstadt, Germany)
Dulbecco modified Eagle's medium (DMEM)	Invitrogen (Karlsruhe, Germany)
ECL™ anti-rabbit IgG Horseradishperoxidase	
Linked whole antibody (from donkey)	Amersham Bioscience (Braunschweig, Germany)
ECL™ anti-mouse IgG, Horseradishperoxidase	
Linked whole antibody (from sheep)	Amersham Bioscience (Braunschweig, Germany)
Ethanol	Merck (Darmstadt, Germany)
Ethidium bromide	Serva (Heidelberg, Germany)
Ethylenediamine-N,N,N',N'-tetraacetic acid (EDTA)	Sigma-Alrich (Steinheim, Germany)
Ethylene glycol-bis(2-aminoethylether)-N,N,N',N'-tetraacetic acid (EGTA)	Sima-Aldrich (Steinheim, Germany)
Fetal calf serum (FCS)	PAA Laboratories (Cölbe, Germany)
Gene Racer™ Kit	Invitrogen (Karlsruhe, Germany)
L-Glutamine	Invitrogen (Karlsruhe, Germany)
Glutaraldehyde (50% aqueous solution)	Sigma-Aldrich (Steinheim, Germany)
Glutathione Sepharose 4 Fast Flow	Amersham Bioscience (Braunschweig, Germany)

Glycerol (87% aqueous solution)	Merck (Darmstadt, Germany)
Glycine	Merck (Darmstadt, Germany)
Glycogen (source: oyster)	Amersham Bioscience (Braunschweig, Germany)
Guanosine 5'-diphosphate (GDP)	Sigma-Aldrich (Steinheim, Germany)
Guanosine 5'-triphosphate (GTP)	Merck (Darmstadt, Germany)
Hydrochloric acid, 37% (HCl)	Merck (Darmstadt, Germany)
HeLa CCL-2 (human) cell line	LGC Promochem GmbH (Wesel, Germany)
Human chorionic gonadotropin (hCG)	Sigma-Aldrich (Steinheim, Germany)
4-(2-Hydroxyethyl)piperazine-1-ethansulfonic acid (HEPES)	Sigma-Aldrich (Steinheim, Germany)
Igepal CA-630 (NP-40)	Sigma-Aldrich (Steinheim, Germany)
Imidazole	Sigma-Aldrich (Steinheim, Germany)
Immersion oil	Leica (Heidelberg, Germany)
Intergonan (PMSG)	Intervet (Unterschleißheim, Germany)
Isopropyl β -D-thiogalactopyranoside (IPTG)	Sigma-Aldrich (Steinheim, Germany)
Kalium chloride	Merck (Darmstadt, Germany)
Kanamycin	Serva (Heidelberg, Germany)
Lysolecithin	Sigma-Aldrich (Steinheim, Germany)
Magnesium chloride	Merck (Darmstadt, Germany)
Magnesium acetate	Merck (Darmstadt, Germany)
2-Mercaptoethanol	Sigma-Aldrich (Steinheim, Germany)
Methanol	Merck (Darmstadt, Germany)
Milk powder	Frema Reform (Lüneburg, Germany)
MiniElute™ Gel Extraction Kit	QIAgen (Hilden, Germany)
Ni-NTA	QIAgen (Hilden, Germany)
Nucleotides (dNTP)	PEQlab (Erlangen, Germany)
Oligofectamine	Invitrogen (Karlsruhe, Germany)
OptiMEM	Invitrogen (Karlsruhe, Germany)
pEGFP	Clontech (Carlsbad, USA)
pET28a vector	Novagen (Darmstadt, Germany)
pETM90 vector	EMBL, Protein Expression and Purification Facility
pET60 vector	EMBL, Protein Expression and Purification Facility
pGEX-KG vector	EMBL, Protein Expression and Purification Facility
Paraformaldehyde	Sigma-Aldrich (Steinheim, Germany)
Penicillin/Streptomycin	Invitrogen (Karlsruhe, Germany)
PFU polymerase	Stratagene (La Jolla, USA)
Piperazine 1,4-bis(2-ethanesulfonic acid) (PIPES)	Sigma-Aldrich (Steinheim, Germany)
Phenylmethylsulfonyl fluoride (PMSF)	Sigma-Aldrich (Steinheim, Germany)
Poly-L-Lysine solution	Sigma-Aldrich (Steinheim, Germany)
Potassium acetate	Merck (Darmstadt, Germany)
Protein A Sepharose™ CL-4B	Amersham Bioscience (Braunschweig, Germany)
QIAquick® PCR Purification Kit	QIAgen (Hilden, Germany)
QIAquick Gel Extraction Kit	QIAgen (Hilden, Germany)
Restriction enzymes	New England Biolabs (Ipswich, USA)
Reverse transcriptase (RT AMV)	Stratagene (La Jolla, USA)
RNAsin	Promega (Mannheim, Germany)
RNAseH	Invitrogen (Karlsruhe, Germany)
Shrimp alkaline phosphatase (SAP)	Amersham Bioscience (Braunschweig, Germany)
Silver nitrate	Sigma-Aldrich (Steinheim, Germany)
Sodium borate	Merck (Darmstadt, Germany)
Sodium borohydride	Sigma-Aldrich (Steinheim, Germany)
Sodium chloride	Merck (Darmstadt, Germany)
Sodium dodecylsulfate	Serva (Heidelberg, Germany)
Sodium thiosulfat	Merck (Darmstadt, Germany)

Spermidine tetrachloride	Sigma-Aldrich (Steinheim, Germany)
Spermine	Sigma-Aldrich (Steinheim, Germany)
Sucrose	Merck (Darmstadt, Germany)
T4-DNA ligase	Fermentas (St. Leon-Roth, Germany)
Taq polymerase	Roche (Mannheim, Germany)
N,N,N',N'-Tetramethylethylenediamine (TEMED)	Sigma-Aldrich (Steinheim, Germany)
Thrombin	Novagen (Darmstadt, Germany)
Titer Max Gold adjuvant	Sigma-Aldrich (Steinheim, Germany)
Tris(hydroxymethyl)amino methane (Tris)	Sigma-Aldrich (Steinheim, Germany)
Triton X-100	Sigma-Aldrich (Steinheim, Germany)
Trypan blue	Invitrogen (Karlsruhe, Germany)
Trypsin EDTA 1x Gibco™	Invitrogen (Karlsruhe, Germany)
Tween®-20, Sigma-Ultra	Sigma-Aldrich (Steinheim, Germany)
Urea	Merck (Darmstadt, Germany)
Vectashield® mounting medium H-1000	Vector Laboratories (Grünberg, Germany)
Western Lightning™ Chemiluminescence reagent	PerkinElmer Life Science (Boston, USA)

5.1.2 Commonly used buffers, solutions and media

AB (acetate buffer)	20 mM HEPES, pH 7.4 100 mM KOAc 3 mM KCl 50 mM EGTA 150 mM Sucrose
Coomassie staining for SDS gels	0.2% (w/v) Coomassie brilliant blue 40% (v/v) Methanol 10% (v/v) Acetic acid
Cysteine buffer	2% (w/v) Cysteine in 0.25x MMR adjusted to pH 7.8 with NaOH
Coomassie destain solution	40% (v/v) Methanol 10% (v/v) Acetic acid
DMEM + Glucose	DMEM (Sigma) was prepared according to manufacturers instructions and supplemented with : 44 mM NaHCO ₃ 17 mM Glucose
Laemmli sample buffer	10% (v/v) Glycerol 50 mM Tris, pH 6.8 10% (w/v) SDS 1 mM DTT 0.1% (w/v) Bromphenol blue
10x Energy mix	100 mM Creatine phosphate 5 mM GTP 5 mM ATP 0.5 mg/ml Creatine kinase
6x DNA loading buffer	0.25% (w/v) Bromphenol blue 0.25% (w/v) Xylene cyanol FF 40% (w/v) Sucrose in H ₂ O

LB-agar (autoclaved)	1.5% (w/v) Bacto agar in LB medium
LB-media (autoclaved)	1% (w/v) Bacto tryptone 0.5% (w/v) Bacto yeast extract 170 mM NaCl adjusted to pH 7.6 with NaOH
MMR buffer	50 mM HEPES, pH 7.9 100 mM NaCl 10 mM MgCl ₂ 20 mM CaCl ₂ 1 mM EDTA
Paraformaldehyde fix	4% (w/v) Paraformaldehyde in H ₂ O, pH 7.1
PBS (phosphate buffered saline)	130 mM NaCl 100 mM Na ₂ HPO ₄ , pH 7.0
PBS blocking solution for immunofluorescence	PBS 3% (w/v) BSA 0.1% (v/v) Triton X-100
PBS washing buffer for immunofluorescence	PBS 0.1% (v/v) Triton X-100
PBS washing buffer for Western blots	PBS 0.05% (v/v) Tween20
PBS blocking buffer	PBS 0.1% (v/v) Triton X-100 5% (w/v) Milk powder
S250 buffer	20 mM HEPES, pH 7.5 250 mM Sucrose 50 mM KCl 2.5 mM MgCl ₂
S500 buffer	500 mM Sucrose 20 mM HEPES, pH 7.5 50 mM KCl 2.5 mM MgCl ₂
S250+/S500+ buffer	S250/S500 buffer supplemented with: 1 mM DTT 1x Complete™ EDTA-free Proteinase Inhibitor Cocktail
Standard protein purification buffer	20 mM HEPES, pH 7.5 300 mM NaCl 5% (v/v) Glycerol 2 mM MgCl ₂ 2 mM β-Mercaptoethanol 1x Complete™ EDTA-free Proteinase Inhibitor Cocktail (10 mM Imidazole, only for His-fusions)

SDS running buffer	25 mM Tris 192 mM Glycine 0.1% (w/v) SDS
SDS polyacrylamide gel stacking solution	4% (v/v) Acrylamide/bisacrylamide 130 mM Tris, pH 6.8 0.01% (w/v) SDS 0.01% (w/v) Ammonium persulfate 0.001% (v/v) TEMED
Resolving SDS-polyacrylamide solution (8%) (modified accordingly for other percentages of resolving gels)	8% (v/v) Acrylamide/bisacrylamide 260 mM Tris, pH 8.8 0.1% (w/v) SDS 0.1% (w/v) Ammonium persulfate 0.0006% (v/v) TEMED
Wet blot transfer buffer	25 mM Tris 200 mM Glycine 10% (v/v) Methanol
Viki-fix	80 mM Pipes pH 6.8 1 mM MgCl ₂ 150 mM Sucrose 0.5% (v/v) Glutaraldehyde 2% (w/v) Paraformaldehyde

5.1.3 Commonly used material

0.2 ml reaction tubes (Thermo Tube™)	PEQlab (Erlangen, Germany)
0.5 ml micro tubes	Sarstedt (Nümbrecht, Germany)
1.5 ml reaction tubes	Eppendorf (Hamburg, Germany)
10 ml chromatography columns	Biorad (München, Germany)
24-well plates	Nunc (Wiesbaden, Germany)
Bottle top filters, 0.22 µm pore size	Millipore (Schwalbach, Germany)
Centricon YM30	Millipore (Schwalbach, Germany)
Coverslips (11 mm diameter)	Nunc (Wiesbaden, Germany)
Dounce homogenizer 2 ml and 40 ml, Pestil B	Kontes Glass, Co (Vineland, USA)
Filter paper	Whatman (Dassel, Germany)
Gene Pulser™	Biorad (München, Germany)
Gene Pulser® cuvette	Biorad (München, Germany)
General glass ware	Schott (Jena, Germany)
General plastic ware	Nunc (Wiesbaden, Germany)
Immobilon™-P Transfer Membrane	Millipore (Schwalbach, Germany)
KODAK BioMax XAR Film	Sigma-Aldrich (Steinheim, Germany)
MoBiCol	MoBiTec (Göttingen, Germany)
Mono Q HR	Pharmacia Biotech (Freiburg, Germany)
Microlance™ sterile needles	Becton Dickinson (Heidelberg, Germany)
Microscope slides	Nunc (Wiesbaden, Germany)
Neubauer chamber	LO-Laboroptik (Friedrichsdorf, Germany)
Plastic cuvettes	Nunc (Wiesbaden, Germany)
Robocycler®	Stratagene (La Jolla, USA)
Scintillation vials	Greiner (Frickenhausen, Germany)
SDS-PAGE Minigel system	Biorad (München, Germany)
Spectra/Por Membrane	Carl Roth (Karlsruhe, Germany)
Superdex 200 HR1	Pharmacia Biotech (Freiburg, Germany)
Syringes	Becton Dickinson (Heidelberg, Germany)
Ultracentrifuge tubes	Beckman (Krefeld, Germany)

5.1.4 Instrumental equipment

5.1.4.1 Centrifuges and rotors

Centrifuges:

Heraeus Megafuge 1.0
Heraeus BiofugeA
Beckman L8-70M
Beckman Coulter Optima TLX
Beckman Coulter Avanti J-20 XP
Du Pont Instruments Sorvall RC-5B

Rotors:

Beckman SW55Ti
Beckman SW40
Beckman JLA-8.1000
Beckman TLA100.4
Sorvall SS34
Sorvall HB6

5.1.4.2 Others

Air liquide ESPACE 331 GAZ (Liquid nitrogen tank)
Amersham Biosciences Ultraspec 2100 pro (Spectrometer)
Avestin EmulsiFlex-C5 (Homogeniser)
B. Braun, Thermomic Bu (Waterbath)
Biorad Power Pac 300 (Power supply)
Biorad gelelectrophoresis system
Biorad Transfer Cell (Western blot wet blot chamber)
Biorad Gene Pulser™
Branson Sonifier B15, Tip: Branson Converter BSB7 (Sonicator)
FPLC LKB (Pharmacia Biotech)
Hera cell 240 (Incubator)
Infors AG HT (Shaking incubators)
Leica DMIRE2, Leica confocal software TCS SP2
Philips CM120 BioTwin (electron microscope)
Pharmacia Biotech Controller LCC-501 Plus (FPLC System)
Radiometer Copenhagen pH M82 Standard pH Meter
Snijders Scientific test tube rotator Model 34528

5.1.5 Nucleotide sequences

5.1.5.1 cDNA sequences

X. laevis Mel28 expressed sequence tags (ESTs):

CA790829
BU913218
BG363745
BU911025
BJ039820
BG486972
BU911216
BU911644
AW642642
BU916589
CA792499
BI477619
BU913754
BI477619

X. laevis Nup155 full length cDNA from RZPD: Clone ID: IMAGp998J1010564Q3

X. laevis Mel28 full length cDNA from RZPD: Clone ID: IMAGE6637561

5.1.5.2 Primers

Primers used to sequence and clone xMel28:

P585: GGAGGATCCATGCAAAACCTTGAAGCTCAGGZC
 P586: GTAAGAGTCACATTATTCCACGTCCAC
 P587: TAACAGGTGTCTTGTCGCTGGCCTGCT
 P588: GCAGTCATGCATTCCAGTGCATTTGGA
 P589: TGCAGAGCTGGCACTCACAGAAATGCA
 P590: CGGAAGTCATCAAAGCCTGCTGAC
 P547: GCTGTCAACGATACGCTACGTAACG
 PS: TGCTCTAGATCATCTCATCTTTTCGCCGCGTGACAGG
 PDS: TGCTCTAGAGTCATTTTTAACTTT
 P1: ATGTTGGACATGTA CTCTTATT
 P2: TCTGGCATTGTGCTTGATAACC
 P3: CACAGGAAAATACCCACCTGC
 P4: CATGGAAAGAGATTTTTGTTTCTT
 P5: CCCCTTTGAATGGTCCAAATGCAC
 P6: CCGGTACCAAGCTTGATGCATAGC
 P7: CACCTTCTGTGGAAGATTTACAAG
 P8: GTTCTTGTAGATGGACCAGAG
 P9: TGAAAATTGTGAACTACTGAG
 P10: CATGATCACTGTCCACAAGAGGGG
 P11: GACCCTTAGTTGGAGTAGAAGGC
 P12: TAACATCAGATGACATCAGAGAG
 GAP1: ATGAAGTCACATCGCCTGATA
 Gap3: ATATACTAGTATCACTCCTCAGTC
 GAP2: AAAATCAGGAGCTGCTATTGGTGC
 P6n: ACTGAGAAAATACCTGCGAATATGT
 P7n: CACCTTCTGGGGAAGATTTACAAG
 Pa: AAGATCTAGCGTGCGCACTAC
 Pb: CAGTTACAGAACTGCGCTGC
 Pc: ATCTTGAAAGCAAGATCCTGG
 Pd: GATCTTGTAATTCTGGTAGGA

Primers to clone xMel28 fragments for protein expression:

MelP1NX: CGGGATCCATGCAAAACCTCAAAGCTCAG
 MelP1NP: GGAATTCCATATGCAAAACCTCAAAGCTCAG
 MelP195CXP: CCGCTCGAGTCAAGCTGGGATTCCACTCATGAC
 MelP189NX: CGGGATCCATGGTCATGAGTGGAAATCCCAGCT
 MelP189NP: CTAGCTAGCATGGTCATGAGTGGAAATCCCAGCT
 MelP1026CX: CATGCCATGGTCATAACGGTTGTGGTCTAGCAAC
 MelP1026CP: CGGGATCCTCATAACGGTTGTGGTCTAGCAAC
 MelP1918NX: CGGGATCCATGAATCAAATAATTAATGCAACT
 MelP1918NP: CTAGCTAGCATGAATCAAATAATTAATGCAACT
 MelPstopXP: CCGCTCGAGTCATATCATCTTTTCGCCGCGAT
 MelP1661NX: CGGGATCCATGAATGCCATGATGTCTTTAGAC
 MelP1661NP: GGAATTCCATATGAATGCCATGATGTCTTTAGAC
 MelP1924CXP: CCGCTCGAGTCAAGTTGCATTAATTATTTGATT
 MelP1388NX: CGGGATCCATGTGCAATGGTCCAAGTGCCTC
 MelP1388NP: GGAATTCCATATGTGCAATGGTCCAAGTGCCTC
 MelP1667CXP: CCGCTCGAGTCAGTCTAAAGACATCATGGCATT

MelP1602NX: CGGGATCCATGGCAAATGTGTCCCCTCTTGTG
 MelP1602NP: CTAGCTAGCATGGCAAATGTGTCCCCTCTTGTG
 MelP2120CXP: CCGCTCGAGTCACCCAACCTTCAGGAACCTCTGT

Primers to clone full length xNup155 for expression:

N155p28N: CTAGCTAGCATGCCCAGTGCAACACCT
 N155p28C: CCAAGCTTGCTAGCTCAACCTCTCCAATT
 N155pM90N: CATGCCATGGGACCCAGTGCAACACCTGGGG
 N155pM90C: TCCCCGCGGTCTAGCTCAACCTCTCCAATT
 N155pM60C: CGGCCGCCCTAGCTCAACCTCTCCAATT

Primers to clone xNup155 fragments for protein expression:

N155N1C: TCCGGCCGCTAGTTTGAGGAAGCAGAAAATCC
 N155N2N: CTAGCTAGCATGGCTTCCTCAAACGTGGAGAAG
 N155N2C: TCCGGCCGCTATGCATGTAGTGCTGACTGTAC
 N155C2N: CTAGCTAGCATGGGGGAGGCTCAGTTGCGTGTA
 N155C2C: TCCGGCCGCTAGACAGGTGGGCCTGGTTTTTT
 N155C1N: CTAGCTAGCATGGCACCACAATCACCCAGTGTT
 N155C1C: TCCGGCCGCTAGCTCAACCTCTCCAATTT

5.1.5.3 siRNAi sequences

Firefly Luciferase: AATCGAAGTATTCCGCGTACG
 Mel28: AATATCTACATAATTGCTCTT
 Nup155: AACAAGGATCATATTCCAATA

5.1.5.4 Plasmids

pET28a-xNup155: The complete ORF of *X. laevis* Nup155 was obtained from RZPD (clone ID: IMAGp998J1010564Q3). Nup155 cDNA in a pCMV-SPORT6 vector was amplified by PCR (chapter 5.2.1.3) using the primers N155p28N/C listed above (chapter 5.1.5.2). pET28a vector (chapter 5.1.5.4) and PCR product were digested (chapter 5.2.1.6) with restriction enzymes NheI and HindIII and Nup155 cDNA was ligated with the vector (chapter 5.2.1.8). The construct was then used for xNup155 expression in bacteria (chapter 5.2.2.1.2).

The following xNup155 fragments were cloned into **pET28a** for expression (for primer sequences see chapter 5.1.5.2):

xNup155-N1(1-395aa) using primers N155p28N and N155N1C; **xNup155-N2**(392-584aa), primers N155N2N/C; **xNup155-N1+N2**(1-584aa) primers N155p28N and N155N2C; **xNup155-C2**(572-1000aa) primers N155C2N/C; **xNup155-C1**(986-1388aa) primers N155C1N/C. All constructs were cloned using NheI (NEB) and EagI restriction sites.

pETM90-xNup155: generated as described for pET28a-xNup155. PCR was performed with the primers N155pM90N/C (chapter 5.1.5.2). Restriction sites NcoI and SacII were used for cloning.

pETM60-xNup155: generated as described for pET28a-xNup155. Primers N155pM90N and N155pM60C (chapter 5.1.5.2) were used for PCR amplification and restriction enzymes NcoI and EagI were employed for cloning.

The following xMel28 fragments were cloned into **pGEX-KG** (chapter 5.1.5.4) for protein expression (for primer sequences see chapter 5.1.5.2):

xMel(1-195aa) primers MelP1X and MelP1195CX; **xMel(189-1026aa)** primers MelP189NX and MelP1026CX; **xMel(1918aa-stop)** primers MelP1918NX and

MelPstopXP; **xMel(1661-1924aa)** primers MelP1661NX and MelP11924CX; **xMel(1388-1667aa)** primers MelP1388NX and MelP1667CX; **xMel(1661aa-stop)** primers MelP1667CX and MelPstopXP; **xMel(1602-2120aa)** primers MelP1602 and MelP2120CX. BamHI and XhoI restriction sites were used to clone all fragments, except **xMel(189-1026aa)** was cut with BamHI and NcoI.

Three xMel28 fragments were cloned into **pET28a** for protein expression: **xMel(189-1026aa)** primers MelP189NP and MelP1026CP; **xMel(1918aa-stop)** primers MelP1918NP and MelPstopXP; **xMel(1602-2120aa)** primers MelP1602NP and MelP2120CXP. For all fragments restriction enzymes NheI and XhoI were used except for xMel(189-1026aa) BamHI was employed instead of XhoI.

5.1.6 Bacteria strains for cloning and protein expression

XL1Blue: genotype: recA1 endA1 gyrA96 thi-1 hsdR17 supE44 relA1 lac (F'proAB lacI^qZDM15 Tn 10 (Tet^r)) (Stratagene).

BL21(DE3): genotype: F⁻ *ompT hsdS_B* (r_B⁻m_B⁻) *gal dcm* (DE3), a lambda prophage carrying the T7 RNA polymerase gene (Novagene).

RosettaTM(DE3): genotype: F⁻ *ompT hsdS_B* (r_B⁻m_B⁻) *gal dcm* (DE3) pRARE² (Cam^R) (Novagene).

5.1.7 Antibodies

5.1.7.1 Primary antibodies

Anti-Nup107 antiserum: polyclonal antibodies were directed against aa76-171 of rat Nup107. The fragment was expressed as a His-tagged fusion protein in the vector pQE30 in BL21 (pRep4). Antibodies were raised in rabbits. ODCT 3rd bleed antiserum used in this study was available in the lab.¹⁸⁹

Anti-Pom121 antibodies: a fragment of *X. laevis* Pom121 (aa381-622) was cloned into the vector pETM60 and expressed in the *E. coli* strain BL21(DE3) and purified on Ni-NTA agarose. The purified fragment was injected into rabbits for polyclonal antibody generation as described in Antonin *et al.*, (2005).¹⁷³ The antiserum was affinity purified and kindly provided by Dr. W. Antonin.

Anti-gp210 antiserum: anti-*X. laevis* gp210 polyclonal antiserum was generated against a C-terminal gp210 fragment as described in Antonin *et al.*, (2005) and kindly provided by the author.¹⁷³

Anti-Schnickschnack antibodies: a fragment of an uncharacterized human INM protein carrying a LEM domain was used for rabbit immunization (Dr. W. Antonin, unpublished data). The antiserum was affinity purified and kindly provided by Dr. W. Antonin.

Anti-importin α antiserum: polyclonal antibodies against full length *X. laevis* importin α were generated in rabbits as described in Hachet *et al.*, (2004) and kindly provided.¹⁸¹

Anti-Nup93 and **anti-Nup205 antisera** were generated against recombinant fragments of the respective *X. laevis* proteins and were raised in rabbits (unpublished). The antisera were kindly provided by Dr. Wolfram Antonin.

Anti-Nup153 antiserum was generated by Dr. Tobias Walther against an N-terminal fragment (aa1-149) of *X. laevis* Nup153 in rabbits.¹²⁹

Anti-Nup35 antiserum: antibodies were raised against full length recombinant *X. laevis* Nup35 as described in Hawryluk-Gara *et al.*, (2005).¹¹⁸ Antiserum was

kindly provided by Richard W. Wozniak.

Anti-Nup155 antiserum: *X. laevis* full length Nup155 was expressed in pET28a in BL21(DE), purified from inclusion bodies (chapter 5.2.2.1.4) and injected for rabbit immunization (this study).

Anti-N-Mel28 antiserum: an N-terminal fragment of *X. laevis* Mel28(1-195aa) was expressed in pGEX-KG in RossettaTM(DE) and purified on glutathione sepharose (chapter 5.2.2.1.1) for injection into rabbits (this study).

Anti-C-Mel28 antiserum: a fragment covering the C-terminal aa1602-2120 of *X. laevis* Mel28 was expressed in pET28a in BL21(DE) and purified on Ni-NTA agarose. Eluates were used for rabbit immunization (chapter 5.2.2.4.1)). Antiserum and affinity purified anti-C-Mel antibodies were used (this study).

Purified mouse **monoclonal Antibody 414 (mAb414)** was purchased from Babco.²²⁴

Anti- α tubulin mouse monoclonal antibody was purchased from Sigma.

5.1.7.2 Secondary antibodies

ECLTM anti-rabbit IgG horseradishperoxidase linked whole antibody from donkey (Amersham Bioscience) was used for antigen detection on Western blots by enhanced chemo luminescence (ECL).

ECLTM anti-mouse IgG horseradishperoxidase linked whole antibody from sheep (Amersham Bioscience) was used to detect mouse monoclonal antibodies on a Western blot by ECL.

Alexa Fluor® 546 goat anti-mouse/rabbit IgG (Invitrogen (Karlsruhe, Germany)) and **Alexa Fluor® 488** goat anti-mouse/rabbit IgG (Invitrogen (Karlsruhe, Germany)) were employed for immunofluorescence.

5.2 Methods

All molecular biology methods were conducted as described in Sambrook *et al.*, (1989), unless otherwise stated.²⁴¹

5.2.1 Molecular biological methods

5.2.1.1 Isolation of DNA and RNA from *X. laevis* oocytes

150 μ l oocytes were incubated with 1.5 ml homomix buffer (50 mM Tris, pH 7.4; 5 mM EDTA; 1.5% (w/v) SDS; 300 mM NaCl; 1.5 mg/ml proteinase K) for 1 h at 50 °C under rotation. SDS in the homomix buffer denatured proteins and proteinase K destroyed nucleases. An equal volume of phenol was added and the reaction was vortexed for 1 min. The oocyte mixture was spun for 4 min at 3000 rpm at 4°C in a Heraeus BiofugeA. Phenol extraction of the supernatant was repeated until it appeared clear after centrifugation. Then, extraction was carried out with half a volume phenol and half a volume chloroform relative to the volume of the extracted oocytes. After vortexing and centrifugation, the final extraction was performed with one volume chloroform (vortexing and centrifugation as described above). The isolated DNA and RNA was precipitated with 2.5 volumes ethanol and frozen at -20°C overnight. Next, the precipitate was pelleted at 7000 rpm for 20 min at 4 °C. The pellet was washed with 70% ethanol, dried and resuspended in 200 μ l TE-buffer (10 mM Tris, pH 7.5; 0.5 mM EDTA).

5.2.1.2 RT-PCR to generate Mel28 cDNA fragments

A cDNA sequence of *X. laevis* Mel28 was not available. Therefore, primers for generation of Mel28 cDNA fragments by reverse transcription and subsequent PCR reactions for subcloning were designed according to *X. laevis* ESTs (chapter 5.1.5.1). These ESTs were selected due to their homology to the human Mel28 cDNA sequence. The 5'-end of *X. laevis* Mel28 cDNA was amplified employing "GeneRacer™ Kit" according to manufacturer's instructions. Truncated mRNA and non-mRNA was eliminated and only capped, full length mRNA remained for the reaction. A GeneRacer™ RNA oligo was fused to the 5'-end from where the amplification by RT-PCR occurred via a GeneRacer™ 5'-primer specific for the added oligo. ESTs covering the 3'-end of the *X. laevis* Mel28 sequence were identified and specific reverse primers employed.

For RT-PCR 5 µg RNA purified from *X. laevis* oocytes was annealed with 0.5 µM (f.c.) of a sequence specific reverse primer and 2 µM (f.c.) of the GeneRacer™ 5'-primer for 5 min at 65 °C. Next, the reaction was cooled on ice and 10x AMV RT buffer, dNTP (0.2 mM each), 1 µl of the reverse transcriptase AMV RT (25 U/µl), 2 µl RNasin and 25 mM DTT were added. The elongation reaction took place at 42 °C for 1 h. The reverse transcriptase was inactivated for 15 min at 85 °C. RNA bound to DNA was digested by RNase H (0.32 U/µl (f.c.)) at 37°C for 20 min.

Isolated fragments were purified and subcloned and sequenced by "Genomics Core Facility" EMBL, Heidelberg.

To obtain the full length *X. laevis* Mel28 sequence, contigs derived from one expressed allele were assembled in "The cap EST assembler" (<http://bio.ifom-firc.it/ASSEMBLY/assemble.html>). New primers were designed to amplify and subclone further regions of the fragments. Annotation of xMel28 cDNA, revealed that one of the obtained IMAGE clones (IMAGE6637561) contained the full length ORF. The clone was entirely sequenced but contained two stop codons. The complete sequence was assembled by ligation of the in frame sequence of the IMAGE clone with one of the cloned fragments derived from the same allele.

5.2.1.3 PCR reactions

PCR reactions to generate DNA fragments for subcloning were routinely set up in a total reaction volume of 50 µl containing: 20 ng of DNA template, dNTPs 250 µM (f.c.) each, forward and reverse primers at 0.4 µM (f.c.), 10x PFU reaction buffer and PFU Polymerase (2.5 U/µl). A typical PCR thermocycle was comprised of 25 cycles. DNA strands were separated for 2 min at 95 °C in the first cycle and 1 min in all subsequent ones. Annealing temperature of the primers was calculated according to the equation $(2(AT) + 4(GC) - 4)$ and set for 30 sec. Product elongation by PFU occurred at 72 °C for 1 min per kilobase template. The final extension step of a PCR cycle was continued for 10 min. All PCR reactions were carried out in a Robocycler®. The amplified PCR product was either purified with a PCR purification kit (chapter 5.2.1.4) after ensuring the correct fragment size on an agarose gel (chapter 5.2.2.5.4), or completely loaded on an agarose gel and purified by gel extraction (chapter 5.2.1.5).

5.2.1.4 Purification of PCR products

A commercial kit (QIAquick® PCR Purification Kit) was used to purify PCR products according to manufacturer's instructions (QIAGEN).

5.2.1.5 DNA purification from agarose gels

A commercial kit from QIAGEN was employed to purify DNA from agarose gels (MiniElute™ Gel Extraction Kit).

5.2.1.6 Restriction digest

1 µg vector DNA or 3 µg of a DNA insert were routinely applied in a 50 µl reaction volume for 1 h at 37 °C for digestion. 10-20 units of restriction enzymes and 1x BSA (NEB) were added if necessary. DNA was purified after digestion by electrophoresis on an agarose gel and gel extraction, or precipitated with sodium acetate and ethanol.²⁴¹

5.2.1.7 DNA extraction from agarose gels

DNA was extracted from agarose gels with a commercial kit (QIAquick Gel Extraction Kit) according to manufacturer's instructions.

5.2.1.8 Ligation of DNA fragments

To diminish self ligation of the cut vector ends, it was treated with shrimp alkaline phosphatase (SAP) (1 U/µl) for 30 min at 37 °C in a 30 µl reaction volume. The reaction was stopped by heat inactivation of SAP at 65 °C.

For ligation, vector and insert were added in a molar ratio of 1:3. A standard reaction contained ~100 ng vector DNA and respective amounts of the DNA insert, T4 DNA ligase and ligase reaction buffer according to manufacturer's instructions. Ligation reactions were incubated for 1 h at room temperature or overnight at 16 °C and transformed into competent *E. coli* bacteria (chapter 5.2.1.9-12).

5.2.1.9 Preparation of chemically competent cells

For uptake of DNA plasmids by heat shock bacteria were prepared according to the following standard procedure. *E. coli* strains stored at -80 °C as glycerol stocks were applied to a LB-agar plate and incubated at 37 °C. The following day, a single colony was picked and grown to saturation in LB-media overnight. 5 ml of the overnight culture was used to inoculate 1 l of LB-media and grown to an optical density of 0.3 at 600 nm wavelength. The culture was chilled on ice for 15 min and the bacteria spun down by centrifugation at 4 °C by 4000 rpm in a Sorvall RC-5B centrifuge. The cell pellet was resuspended in 500 ml ice cold 50 mM CaCl₂. The centrifugation step was repeated and the pellet resuspended in 80 ml 50 mM CaCl₂, 15% (v/v) glycerol. Cells were aliquoted and frozen in liquid nitrogen.

5.2.1.10 Transformation of plasmid DNA into chemically competent cells

10-20 µl of a standard ligation reaction (chapter 5.2.1.8) was transformed into chemically competent *E. coli* cells by heat shock. Cells were thawed quickly and

incubated with plasmid DNA for 30 min on ice. Bacteria were heat shocked for 45 sec at 42 °C and next cooled on ice for 5 min. 1 ml LB-media without antibiotics was added and incubated for 30 min at 37 °C under rotation to allow for the expression of the antibiotic resistance. 200 µl of the bacteria suspension was plated on LB agar plates containing 100 µg/ml Ampicillin and/or 30 µg/ml Kanamycin corresponding to the resistance gene of the vector. After incubation overnight at 37 °C, colonies were picked, diluted in 50 µl water and subjected to PCR to confirm insertion of desired constructs.

5.2.1.11 Preparation of electro-competent cells

Cells were prepared according to standard procedures similarly as described above for chemically competent cells (chapter 5.2.1.9) but resuspension of the cell pellet was done in ice cold water, supplemented with 10% (v/v) glycerol.

5.2.1.12 Transformation of plasmid DNA into electro-competent cells

Electro-competent cells were thawed on ice. Ligation reactions were mixed with the cells and transferred to a chilled Gene Pulser® cuvette. An electric pulse was applied with a Gene Pulser™ according to manufacturer's instructions and cells were immediately recovered with 1 ml of prewarmed LB-media. Cells were grown for 1 h at 37 °C and plated on LB-Agar plates with respective antibiotics.

5.2.1.13 Preparation of DNA from *E. coli*

Bacteria were transformed with the respective DNA plasmid and grown to saturation under standard conditions. Plasmids were purified from bacteria using a commercial kit (QIAprep Miniprep spin Kit®) according to manufacturer's instructions.

5.2.2 Biochemical standard methods

5.2.2.1 Protein expression and purification

5.2.2.1.1 Expression and purification of GST-fusion proteins

pGEX-KG-xMel constructs were transfected into the *E. coli* strain Rosetta™ (DE) (chapter 5.1.6) for expression. Rosetta host strains are BL21 (Novagen) derivatives designed to enhance the expression of eukaryotic proteins that contain codons rarely used in *E. coli*. Therefore, tRNAs for these codons are supplied on an additional plasmid. Transformants were plated on LB-agar plates containing 100 µg/ml Ampicillin, 0.33 µg/ml Chloramphenicol and incubated overnight at 37 °C. A single colony was picked to inoculate LB culture that was grown overnight to saturation. From this culture 1 l LB-medium was inoculated for protein expression and cultures were grown to an OD of 0.6 at 600 nm wavelength. Protein expression was induced by addition of 0.2 mM IPTG (f.c.) for 4-5 h at 21 °C. Cells were harvested by centrifugation at 4000 rpm for 30 min at 4 °C in a Sorvall RC-5B centrifuge. The bacteria pellet corresponding to 1 l culture was resuspended in 10 ml purification buffer (20 mM HEPES, pH 7.5; 300 mM NaCl; 5% (v/v) glycerol; 2 mM MgCl₂; 2 mM β-mercaptoethanol and 1 mM PMSF). Cells were lysed in an Avestin EmulsiFlex-C5 homogenizer and Triton-X100 was added to 0.1% (v/v) final

concentration and incubated at room temperature (RT) for 30 min under rotation. The lysate was cleared by centrifugation at 12000 rpm for 20 min at 4 °C in a Sorvall RC-5B centrifuge using an SS34 rotor. The supernatant was applied to 0.5 ml equilibrated glutathione sepharose per 1 l culture and incubated for 1 h at 4 °C under rotation. The resin was transferred to a plastic affinity chromatography column and was washed twice with 10 bed volumes purification buffer. Further, one wash was performed with purification buffer supplemented with 500 mM NaCl, 2 mM ATP, and 5 mM MgCl₂. The resin was equilibrated with purification buffer before elution of the GST-fusion proteins with 20 mM glutathione. It was tried to remove the GST-tag by cleavage with Thrombin according to manufacturer's instructions, but xMel(1-195aa) was instable without the fusion tag. GST-xMel(1-195aa) was used for polyclonal antibody generation in rabbits (chapter 5.2.2.4.1).

5.2.2.1.2 Expression and purification of His-fusion proteins

Expression of His-fusion proteins in pET28a were performed as described above with the following modifications: vectors were transformed into BL21(DE) for expression. The purification buffer contained: 20 mM HEPES, pH 7.5; 300 mM NaCl; 5% (v/v) glycerol; 2 mM MgCl₂; 2 mM β-mercaptoethanol; 10 mM imidazole and 1x CompleteTM EDTA-free Protease Inhibitor Cocktail. The bacteria suspension was lysed in an Avestin EmulsiFlex-C5 homogenizer and cleared by centrifugation. The supernatant was applied to Ni-NTA agarose equilibrated in purification buffer (0.3 ml resin per 1 l bacteria culture). His-tagged proteins were incubated with affinity resin for 1 h at 4 °C on a rotating wheel. After extensive washes, fusion proteins were eluted with 300 mM imidazole in purification buffer.

For purification of Nup155, eluted fractions containing Nup155 were pooled and concentrated in YM-30 centricons by centrifugation in a Heraeus Megafuge 1.0 at 4000 rpm at 4 °C. At the same time purification buffer was exchanged with S250 buffer.

Removal of the His-tag of xMel(1602-2120aa) was assessed by cleavage with thrombin according to manufacturer's instructions but the protein was degraded by the protease.

5.2.2.1.3 Protein purification under denaturing conditions

E. coli cell pellet was resuspended in 70 ml of the respective purification buffer per 1 l expression culture. Urea was added to a final concentration of 4 M and the solution was homogenized with a hand blender. The lysate was cleared by centrifugation and bound to an affinity resin, washed and eluted as described above. If proteins did not elute in the standard purification buffer supplemented with imidazole, urea elutions with 50 mM NaH₂PO₄, 8 M urea at pH 5.8 and pH 4.5 were performed.

5.2.2.1.4 Purification of inclusion bodies containing expressed protein

After protein expression *E. coli* cells were pelleted and resuspended in 13 ml of 50 mM Tris-Cl, pH 8.0; 25% sucrose, and 10 mM DTT per 1 l culture. Cells were lysed by sonication and 100 μl lysozyme (50 mg/ml in H₂O), 250 μl DNaseI (1 mg/ml in 50% glycerol, 75 mM NaCl), and 50 μl MgCl₂ (1 M) was added. The solution was vortexed, 12.5 ml lysis buffer (50 mM Tris-Cl, pH 8.9; 1% (v/v) Triton X-100; 1% (w/v) sodium deoxycholate; 100 mM NaCl; 10 mM DTT) were added and vortexed. The

suspension was incubated for 1 h at RT, frozen in liquid nitrogen and thawed again at 37 °C for 30 min. 200 µl MgCl₂ (1 M) was added and incubated until the viscosity decreased. 350 ml EDTA (0.5 M in 50 mM Tris-Cl, pH 8.9) was adjusted to chelate Mg²⁺. The *E. coli* lysate was pelleted at 11000 g for 20 min at 4 °C in a Sorvall RC-5B centrifuge and the pellet resuspended in 10 ml washing buffer (50 mM Tris-Cl, pH 8.0; 100 mM NaCl; 1 mM DTT; 1 mM EDTA), sonicated and centrifuged as before. The pellet was then resuspended in washing buffer with Triton X-100 (50 mM Tris-Cl, pH 8.0; 1% Triton X-100; 100 mM NaCl; 1 mM DTT), sonicated and centrifuged. The pellet consisted mainly of purified inclusion bodies that were dissolved in 8 M urea by incubation at RT, aliquoted, frozen in liquid nitrogen, and stored at -80 °C. Inclusion bodies were purified by the “Protein Expression and Purification Core Facility”, EMBL Heidelberg.

5.2.2.2 Purification of proteins by fast protein liquid chromatography

Further purification of xMel(1-195aa) and xMel(1602-2120aa) fusion proteins was tested by ion exchange chromatography on a MonoQ column on a FPLC LKB apparatus. Proteins were dialysed into 20 mM HEPES, pH 7.5; 50 mM NaCl; 5% (v/v) glycerol, 2 mM β-mercaptoethanol, and 1 mM MgCl₂ and loaded onto the column according to manufacturer’s instructions. However, during elution with increasing salt concentrations, both fusion proteins precipitated on the column. Alternatively, xMel(1602-2120aa) was loaded on a Superdex 200 gelfiltration column to separate contaminating proteins by size but it was not possible to remove copurifying proteins efficiently.

His-xNup155 precipitated during every attempt to exchange it into a different buffer required for FPLC purification and therefore, could not be purified any further.

5.2.2.3 Identification of proteins by mass spectrometric analysis

Malgorzata Schelder did mass spectrometric analysis of proteins that co-immunoprecipitated with anti-Nup155 antibodies and such that copurified with full length Nup155 under native conditions.

5.2.2.4 Antibodies

5.2.2.4.1 Polyclonal antibody generation in rabbits

All antigens used for rabbit immunization were recombinant proteins, purified either under native conditions (chapter 5.2.2.1.1/2) or from inclusion bodies (chapter 5.2.2.1.4). Per boost and rabbit, 0.5 mg recombinant protein was diluted with PBS to 300 µl and mixed with 300 µl Titer Max Gold adjuvant. The emulsion was sonicated with a Branson Sonifier B15, tip B5B7 until it became white and viscous. 500 µl of the emulsion were injected per rabbit. After the primary immunization, rabbits were boosted three times in a 14 day rhythm. Subsequent boosts were repeated every four weeks. Rabbit bleeds were heated to 37 °C for 1 h and stored overnight at 4 °C. The following day, the coagulated blood was spun down at 4000 rpm for 30 min in a Heraeus Megafuge 1.0, the serum was collected, frozen in N₂ and stored at -80 °C. Rabbit immunizations were performed by the “Laboratory Animal Resources” EMBL, Heidelberg. Antibodies for this study were generated against His-xNup155 purified with inclusion bodies, GST-xMel(1-195aa) and His-xMel(1602-2120aa).

5.2.2.4.2 Affinity purification of polyclonal antibody serum

His-xMel(1602-2120aa), a C-terminal fragment of Mel28, was expressed and purified as described (chapter 5.2.2.1.2). The protein solution was dialyzed against buffer A (100 mM NaHCO₃, pH 8.3; 500 mM NaCl; 2 mM MgCl₂). CNBr-activated Sepharose™ 4B was swollen in ice cold 1 mM HCl, pH 2-3, and equilibrated in buffer A. 10 ml protein solution at a concentration of 3.5 mg/ml protein was incubated with 1 ml CNBr Sepharose™ 4B for 1 h at RT under rotation. Excess ligand was washed off with 5x bed volume buffer A. Remaining, free binding sites of CNBr Sepharose™ 4B were blocked with 1 M ethanolamine, pH 8 in buffer A for 2 h at RT. The resin was washed in two cycles, twice with buffer A and twice with buffer B (100 mM acetate, pH 4.2; 500 mM NaCl; 2 mM MgCl₂). The sepharose was equilibrated in PBS and pre-eluted with 200 mM glycine, pH 2.2 and 150 mM NaCl. 30 ml rabbit antiserum was incubated with the affinity resin overnight at 4 °C under rotation. The resin was sedimented by low speed centrifugation at 1000 rpm in a Heraeus, Megafuge 1.0. The serum was removed and the beads were washed with PBS, 0.05% (v/v) Tween®-20. Antibodies bound to recombinant His-xMel(aa1602-2120) were eluted by applying 10x 1.5 ml 200 mM glycine, pH 2.7; 150 mM NaCl. Eluates were immediately neutralized by addition of 120 µl 1.5 M Tris, pH 8.8. This procedure was repeated with 200 mM glycine, pH 2.2, neutralized with 200 µl 1.5 M Tris, pH 8.8. Purified antibodies were precipitated with 60% (w/v) ammonium sulfate on ice overnight. The precipitate was sedimented by centrifugation at 4000 rpm for 30 min at 4 °C in a Sorvall RC-5B, HB6 rotor and the pellet was resuspended in PBS, 5% (v/v) glycerol, dialysed against the same buffer and aliquots were frozen in liquid nitrogen.

5.2.2.5 Electrophoretic Methods

5.2.2.5.1 Sodium dodecyl sulfate polyacrylamide gel electrophoresis

The standard method of Laemmli for discontinuous gel electrophoresis under denaturing conditions was used in this study.²⁴²

The glass-plate sandwich of the electrophoresis apparatus was assembled according to manufacturer's instructions. Separation gel was induced to polymerize and poured between the two glass plates. To guarantee a straight surface, the gel solution was overlaid with water-saturated 1-butanol. After gel polymerization 1-butanol was decanted and the gel surface was rinsed with water. The stacking gel solution was added onto the polymerized gel and a comb was inserted, providing gel pockets. The gel polymerized and the comb was removed. The gel sandwich was attached to the upper and lower buffer chambers and buffer was filled into both containers.

Protein samples containing 1x sample buffer at final concentration were denatured at 95 °C or 65 °C for 10 min and pipetted into the gel wells. Molecular weight markers (5 µl on minigels and 12 µl on large gels) were included at all times. Minigels were run at 130 V through the stacking gel and were separated under 200 V in the resolving gel until the dye front had entered the buffer in the lower buffer chamber.

After the separation by SDS-PAGE proteins were either stained in the gel (chapter 5.2.2.5.2/3) or transferred to membranes for immunodetection (chapter 5.2.2.6).

5.2.2.5.2 Staining of proteins with Coomassie Brilliant Blue

After electrophoresis, gels were removed from the glass plate and incubated for 1 h in Coomassie Brilliant Blue staining solution (40% (v/v) methanol, 10% (v/v) acetic acid and 0.2% (w/v) Coomassie Brilliant Blue) on a rocking table at RT. Next, the dye solution was removed and gels were incubated in destain solution (40% (v/v) methanol, 10% (v/v) acetic acid) on a shaker until the background of the gel became clear. The destain solution was renewed several times.

5.2.2.5.3 Silver staining of proteins

For silver staining, proteins in SDS-gels were fixed with 50% (v/v) methanol, 12% (v/v) acetic acid, 0.05% (v/v) formaldehyde for 30 min shaking at RT. The gel was washed twice for 10 min in 50% ethanol on a shaker. The alcohol was removed and the gel incubated for 1 min in 0.02% (w/v) $\text{Na}_2\text{S}_2\text{O}_3$ -solution followed by three washes with water 10 seconds each. The gel was incubated for 15 min with 0.2% (w/v) silver nitrate in water. The gel was washed several times with water and was developed in 6% (w/v) Na_2CO_3 , 0.05% (v/v) formaldehyde, 0.0004% (w/v) $\text{Na}_2\text{S}_2\text{O}_3$ -solution, placed on an illuminator to control the staining. Reaction was stopped with 50 mM EDTA before the background became dark.

5.2.2.5.4 Agarose gel electrophoresis

Agarose was dissolved to the desired concentration (w/v) in 1x TBE and heated to boiling in a microwave. When the agarose was completely dissolved, ethidium bromide was added 1:40000 from the stock solution (10 mg/ml). The gel solution was poured into a horizontal gel carrier and a comb for forming wells was inserted. When the gel was polymerized, the comb was removed and the carrier was placed into the gel container. The gel and both gel chambers were filled with TBE buffer. The DNA samples and DNA molecular weight markers were loaded into gel wells. Agarose gels were run at 100 V until the dye front reached the last quarter of a gel. DNA was visualized by the fluorophor emitting light when placed on an UV illuminator.

5.2.2.5.5 Wet Blotting

The SDS gel was soaked in transfer buffer (25 mM Tris, 200 mM glycine, 10% methanol) for 15 min at RT. A polyvinylidene difluoride (PVDF) membrane was activated in 100% methanol for 1 min and was soaked in water for 5 min afterwards. Before the gel/membrane sandwich was assembled, the membrane was washed briefly in transfer buffer. The gel and membrane were placed between two pieces of Whatman paper and covered by two sponges. These layers were held by a lattice cassette and placed into a Biorad Transfer Cell according to manufacturer's instructions. The sandwich was placed upright into the container filled with transfer buffer. The transfer of proteins took place at 300 mA for 4 h at 4 °C and was controlled by monitoring the transfer of prestained molecular weight standards present in the gel.

5.2.2.6 ECL detection

Following transfer PVDF membranes were incubated in 5% milk powder, PBS, 0.05% Tween®-20 (PBS-T) shaking at RT for 1 h or at 4°C overnight to saturate non-specific protein background on the membrane. The blocking reagent was removed and the immobilized proteins were incubated in primary antibody at RT for 1 h while shaking or at 4°C overnight.

The antibody solution was retained for repeated use and the membrane was washed three times in PBS-T for 5 min on a shaker to remove remaining primary antibody that was not tightly bound. The secondary antibodies, ECL™ anti-rabbit or anti-mouse IgG linked to horseradishperoxidase, were applied and incubated at RT for 1 h on a shaker. The blot was washed ten times in PBS-T. To localize the bound antibody, the membrane was covered with Western Lightning™ Chemiluminescence reagent according to manufacturer's instructions. After 1 min incubation on the membrane, the reagent was removed and the membrane was covered with Saran Wrap. The membrane was exposed to an X-ray film for 1-5 min in a dark room and the film was developed mechanically.

5.2.2.7 Determination of protein concentration

The protein concentration of a solution was determined using BCA™ Protein Assay Kit (Pierce) following manufacturer's instructions. Briefly, bovine serum albumin (BSA) protein standard dilutions were made in duplicates ranging from 2 µg-50 µg protein and several dilutions of the protein solution in 100 µl H₂O. 900 µl BCA working solution (49 units buffer A and 1 unit buffer B supplied with the kit) were added and samples incubated for 30 min at 37 °C. Optical density was determined at a wavelength of 562 nm and the protein concentration was calculated via a standard curve.

5.2.3 Biochemical methods related to the *X. laevis* egg extract system

5.2.3.1 Preparation of *X. laevis* egg extract

The protocol was modified from Newmeyer and Wilson, (1991) and Hartl *et al.*, (1994).^{208, 243}

Female *X. laevis* frogs were primed by injection with pregnant mare serum gonadotropin (PMSG) (1000 U in 0.5 ml per frog) that triggered eggs to complete meiosis I and arrest in metaphase of meiosis II. Ovulation of mature eggs was stimulated with human chorionic gonadotropin (hCG, 1000 U/frog). Ten days later, frogs were transferred into plastic boxes, covered with ~0.5 l 1x MMR buffer (50 mM HEPES, pH 7.9; 100 mM NaCl; 10 mM MgCl₂; 20 mM CaCl₂; 1 mM EDTA) and incubated at 16 °C for 16 h in the dark. The following day, eggs laid in MMR buffer were collected and frogs were returned to normal tanks. Damaged eggs (white) were selected and discarded. Dirt and debris was washed away with MMR buffer. The jelly coat of the eggs was removed by incubation in a freshly prepared 0.25x MMR supplemented with 2% cystein. As soon as eggs started to become closely packed (~10 min), dejellying solution was discarded and eggs were extensively washed with MMR. Following dejellying, exposure to air was avoided since the eggs were very fragile and lysed easily after removal of the jelly coat. Eggs were released from cell cycle arrest at metaphase of meiosis II by addition of the calcium ionophore A23187

(8 μ l, (2 mg/ml in ethanol) per 100 ml MMR) that mimicks fertilization. Animal cap contraction was visible after 3 min, as judged by an upturn of the vegetal, black pool. Activation was stopped after 7-10 min by thorough washing with MMR buffer which removed the ionophore. Eggs were incubated at RT for 15 min and subsequently washed 3x with S250 buffer (20 mM HEPES, pH 7.5; 250 mM sucrose; 50 mM KCl; 2.5 mM MgCl₂). Necrotic eggs were removed with a pasteur pipette. Remaining eggs were transferred with an edgeless plastic Pasteur pipette to SW55 plastic centrifuge tubes and supplemented with 1 mM DTT, 44 μ g/ml cycloheximide, 5 μ g/ml cytochalasin B, and 1x Complete™ EDTA-free Proteinase Inhibitor Cocktail. Cycloheximide, a protein synthesis inhibitor, was included to prevent further progression of the extracts into mitosis. Cytochalasin B inhibited actin polymerization and prevented the extract from coagulation. Low speed centrifugation for 30 sec at 800 rpm followed by a 30 sec spin at 1600 rpm (Heraeus, Megafuge 1.0 R), was used to pack eggs and remove additional buffer. Centrifuge tubes were filled to the top with additional eggs and subjected to a “low speed” centrifugation for 20 min at 25000g (4 °C) in a Beckman L8-70M ultracentrifuge employing a SW55Ti rotor. Tubes were broached with a syringe and nuclear material, organelles and glycogen were removed, leaving lipids, yolk and pigment behind. DTT, cycloheximide, cytochalasin B and Complete™ EDTA-free Proteinase Inhibitor Cocktail were added to this low speed extract as described above and subjected to a high speed centrifugation at 225000g for 40 min using the same centrifuge and rotor as in the previous step. Repeatedly, cytosol, membranes and mitochondria were removed with a syringe, diluted with 0.3 fold AB-buffer (20 mM HEPES, pH 7.4; 100 mM KOAc; 3 mM KCl; 50 mM EGTA; 150 mM sucrose) and spun again at the same centrifugation settings. Cytosol was removed with a Gilson P1000 pipette, glycerol was added to 3% (v/v) and aliquots of 50 μ l were snap frozen in liquid nitrogen and stored at -160 °C. Cytosol for immunodepletion was immediately processed as described in chapter 5.2.3.4. Membranes were further purified as described (chapter 5.2.3.3).

5.2.3.2 Preparation of sperm chromatin

This protocol was modified from Gurdon *et al.*, (1976).²⁴⁴ Testis were removed from male *X. laevis* frogs and separated into smaller pieces with forceps in HPS buffer (15 mM HEPES, pH 7.4; 250 mM sucrose; 0.5 mM spermidine tetrachloride; 0.2 mM spermine). Resuspended organ fragments were further dispersed by pressing the solution through a 1 ml syringe onto a glass plate. To remove debris, the solution was filtered through cheese cloth. Material was pelleted by 2000 rpm for 10 min at 4 °C in a Heraeus Megafuge 1.0R. The cell pellet was resuspended in 1 ml HSP supplemented with 0.3 mM PMSF and 50 μ l 10 mg/ml lysolecithin. Plasma membranes were permeabilized for 5 min at RT and the reaction was stopped by addition of 10 ml chilled HSP buffer containing 0.3 mM PMSF and 3% BSA. Cells were pelleted repeatedly as described above and washed with 3 ml HSP, 0.3 mM PMSF, 0.3% (w/v) BSA and sedimented again. Sperm heads were resuspended in 2.5 ml HSP buffer, 0.3% (w/v) BSA, and 30% (v/v) glycerol, diluted and counted on a Neubauer chamber according to manufacturer's instructions. Staining with trypan blue showed whether cells had been properly permeabilized. The preparation was diluted to 3000 sperm heads/ μ l, aliquoted, snap frozen, and stored at -80 °C.

5.2.3.3 Preparation of the total membrane fraction from *X. laevis* egg extracts

For preparation of total membranes, the membrane fraction was diluted in 20 volumes S250+ buffer (1mM DTT and Complete™ EDTA-free Proteinase Inhibitor Cocktail), homogenized in a 40 ml dounce homogenizer (pestil B) and laid on top of a 800 µl S500+ buffer cushion. Membranes were sedimented through the cushion at 28000g for 15 min (4° C) in a Beckman L8-70M ultracentrifuge employing a SW40 rotor. Membranes were resuspended and homogenized in 1/10th of the corresponding cytosol volume in S250+ buffer in a 2 ml dounce homogenizer (pestil B), snap frozen and stored at -160 °C.¹⁷⁸

5.2.3.4 Preparation of floated membranes

To generate a discontinuous sucrose step gradient, the following sucrose solutions were prepared in S250 buffer and supplemented with 1mM DTT and 0.1x Complete™ EDTA-free Proteinase Inhibitor Cocktail: 2.1 M, 1.4 M, 1.3 M, 1.1 M, 0.9 M and 0.7 M. Membranes were homogenized with 2 ml 2.1 M sucrose solution per ml membranes in a chilled 40 ml dounce homogenizer. 2 ml of the membrane solution were added into a Beckman centrifuge tube suitable for SW40Ti rotor and overlaid with 1.6 ml of each sucrose solution with decreasing density. On top of the gradient S250 buffer was added to fill the tube. Membranes were floated for 4 h at 250000g at 4 °C with slowed deceleration. The membrane fraction with lowest density was collected, diluted 1:2.5 in S250 buffer containing 1 mM DTT and Complete™ EDTA-free Proteinase Inhibitor Cocktail and pelleted in a Beckman Coulter Optima TLX, TLA100.4 rotor at 420000g for 30 min at 4 °C. The pellet was resuspended in 1/30th of the cytosol volume in S250 buffer, homogenized in a 2 ml dounce homogenizer (pestil B) and frozen in liquid nitrogen. Membranes were stored at -160 °C.²⁴⁵

5.2.3.5 Immunodepletion of proteins form *X. laevis* egg cytosol

For immunodepletion of proteins from *X. laevis* egg cytosol respective antibodies were crosslinked to protein A sepharose to generate antibody columns. 1 ml protein A sepharose resin was equilibrated in PBS and incubated with 3 ml of antiserum over night at 4 °C. The resin was pelleted by centrifugation at low speed, and the serum was removed. Beads were washed twice in coupling buffer (200 mM NaHCO₃, pH 9.3; 100 mM NaCl). Antibodies were crosslinked to protein A sepharose with 10 mM dimethylpimelimidate (DMP) in coupling buffer for 10 min at RT on a rotating wheel. The resin was pelleted, washed with coupling buffer, and the crosslinking step was repeated. Subsequently, antibody-resin was washed twice alternating in buffer A (100 mM NaOAc, pH 4.2; 500 mM NaCl) and buffer B (100 mM NaHCO₃, pH 8.3; 500 mM NaCl). The antibody column was then washed in S250 buffer and blocked for 1 h at 4 °C on a rotator in S250 buffer supplemented with 3% BSA and Complete™ EDTA free Protienase Inhibitor Cocktail. Beads were stored in this blocking solution containing 0.02% NaN₃.

Before use, beads were washed in blocking solution and transferred to Mobicols columns. For depletion of Nup155 from cytosol, beads were preblocked with inactive Nup155-depleted cytosol for 30 min at 4 °C to reduce loss of unspecific proteins from the cytosol. Freshly prepared cytosol was mixed in a 1.3:1 ratio with the

antibody column, and incubated for 30 min at 4 °C under rotation. The flow through was collected and the depletion step repeated on fresh, preblocked antibody resin. Depleted cytosol was recovered and immediately used for *in vitro* nuclear reconstitution reactions (chapter 5.2.3.6).

5.2.3.6 *In vitro* nuclear envelope assembly

For a typical NE assembly reaction, 0.5 µl sperm chromatin (3000 sperm heads/µl) was incubated for 10 min at 20 °C in 10 µl cytosol. To start the NE assembly reaction, 0.5 µl floated membranes, 1 µl 10x energy mix (chapter 5.1.2) and 0.2 µl glycogen (20 mg/ml) were added. Nuclear reconstitution took place for 2 h in a waterbath, cooled to 20 °C.

At the initial decondensation step, cytosolic nucleoplasmin was used to exchange protamines with histones (Figure 5.1 upper left picture).²⁴⁶ After the reaction was started, membrane vesicles associated with the chromatin template and started to fuse. This led to an intermediate membrane network that covered the peripheral chromatin. Once the NE was sealed, nucleocytoplasmic transport took place, the chromatin decondensed further and the nucleus rounded (Figure 5.1, lower left picture).

Reconstituted nuclei were either processed for immunofluorescence (chapter 5.2.3.6), membranes were stained with the lipophilic dye DiI₁₈ (chapter 5.2.3.7), or reactions were prepared for transmission electron microscopy (chapter 5.2.4.2).

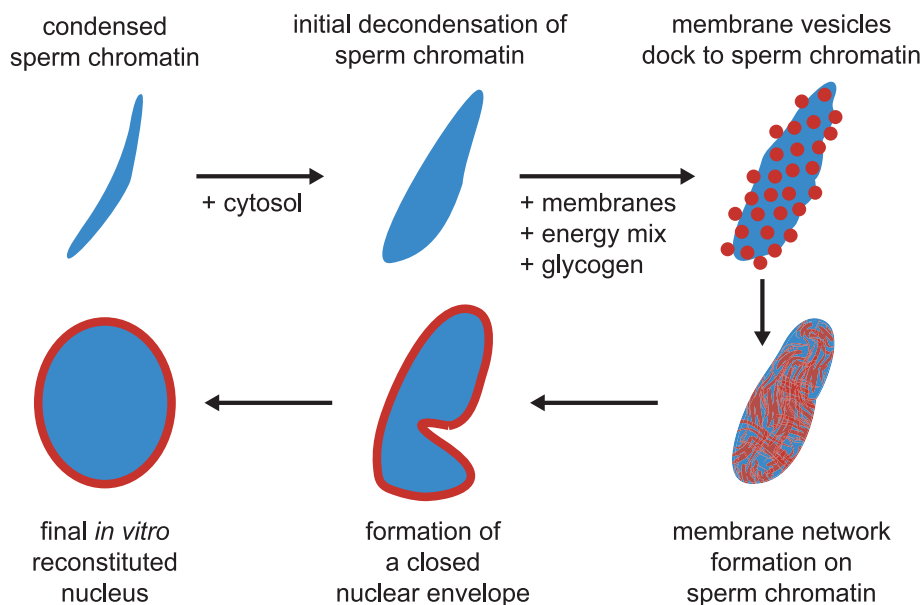


Figure 5.1: *Schematic illustration of basic steps during nuclear envelope formation in vitro.* Sperm chromatin was decondensed before NE assembly reaction was started by addition of membranes, energy mix and glycogen. Membranes docked to the chromatin template and formed a membrane network, nuclear envelope membranes sealed, transport occurred and chromatin reached its final stage of decondensation. Chromatin is depicted in blue and membranes in red.

5.2.3.7 Immunofluorescence of *in vitro* reconstituted nuclei

An NE assembly reaction was fixed in 0.5 ml 4% PFA in PBS and incubated for 30 min on ice. Cover slips (round, 11 mm in diameter) were coated with poly-L-lysine solution for 5 min at RT. Poly-L-lysine solution was removed and cover slips dried and transferred to scintillation vials. Fixed NE assembly reactions were applied to 0.7 ml 30% sucrose in S250 buffer. The reaction was spun through the cushion onto cover slips at 4000 rpm for 15 min (4 °C) in a Heraeus Megafuge 1.0R. Cover slips were lifted by puncturing the vials from the bottom with a syringe needle and then removed with forceps. Immunofluorescence staining was performed in a 24-well plate. The fixative was quenched with 50 mM NH₄Cl in PBS for 5 min at RT. Blocking solution contained 3% BSA in 0.1% Triton-X100 in PBS and was applied to the cover slips for 30 min at RT. Antibodies were diluted in blocking solution. Primary antibodies were incubated with the nuclei on the cover slips for 1.5 h, followed by 5 washes with 0.1% Triton-X100 in PBS. Secondary antibodies coupled to fluorophors (Alexa Fluor® 488/546 goat anti-mouse/rabbit IgG were diluted 1:2000 in blocking solution and applied for 45 min. After labeling with secondary antibodies, cover slips were washed 10 times with 0.1% Triton-X100 in PBS and 1x with PBS. To stain the chromatin, DAPI (1 mg/ml) was diluted 1:10000 in PBS and reactions on cover slips were stained for 5 min at RT. After two additional washes with PBS and H₂O, cover slips were removed from solutions and remaining liquid was removed. Samples were mounted on a drop of Vectarshield® mounting media on glass slides. Liquid was removed from the rim of the cover slips with a tissue and the preparation was sealed with nail polish at the perimeter. Reactions were evaluated by confocal microscopy.²⁴⁷

A modified protocol was used when membranes were investigated. Viki-fix (80 mM Pipes, pH 6.8; 1 mM MgCl₂; 150 mM sucrose; 0.5% glutaraldehyde; 2% paraformaldehyde) yielded better conservation of nuclear membranes due to the presence of glutaraldehyde. The fixation step was quenched with 1mg/ml NaBH₄ in PBS for 10 min at RT. The cross linking potential for glutaraldehyde was higher than for formaldehyde. Aldehyde groups that remained free could unspecifically bind proteinaceous reagents, for example, antibodies. However, mAb414 was employed on reactions fixed in the presence of glutaraldehyde, leading to well preserved nuclear membranes in which a subset of nucleoporins were stained by mAb414.

5.2.3.8 DiIC₁₈ labeling of membranes

Membranes in an NE assembly reaction were stained before fixation with 0.2 µl of the lipophilic dye DiIC₁₈ (0.1 mg/ml in DMSO) for 5 min at RT. For better preservation of the membranes Viki-fix was used (80 mM Pipes pH 6.8; 1 mM MgCl₂; 150 mM sucrose; 0.5% glutaraldehyde; 2% paraformaldehyde; 0.1 µg/ml DAPI). Samples were spun as described (chapter 5.2.3.7), mounted and processed for confocal microscopy.¹⁷³

5.2.3.9 Immunoprecipitation of proteins from *X. laevis* egg cytosol

Egg cytosol was diluted 1:1 with PBS supplemented with Complete™ EDTA-free Proteinase Inhibitor Cocktail and spun for 20 min at 55000g in a TLA100.4 rotor. 50 µl antiserum were added to 800 µl cytosol after centrifugation and incubated for 2 h at 4 °C. 100 µl Protein A sepharose was added as 50% slurry and incubation

continued for 1 h. Beads were sedimented, supernatant removed, and the resin was washed 10x with PBS. Bound proteins were eluted in 40 μ l 1x SDS-sample buffer supplemented with 100 mM DTT. 10 μ l of the eluates were separated on 8% polyacrylamide gels and analyzed by immunostaining on Western blots (chapter 5.2.2.5.5).

5.2.4 Microscopy

5.2.4.1 Light microscopy

A Leica AOBs Sirius DMIRE2 confocal microscope was used for immunofluorescence. Laser lines at 405 nm, 488 nm and 532 nm were employed to excite respective fluorophores, which were predominantly DAPI, Alexa 488 and Alexa 546. Settings were adjusted to exclude cross-talk between different channels. For image processing “ImageJ, Version 1.34k” and “Adobe Photoshop 7.0” were used.

5.2.4.2 Transmission electron microscopy

NE assembly reactions (chapter 5.2.3.5) were scaled up to 60 μ l and fixed in 1 ml Viki-fix (chapter 5.1.2) for 30 min on ice. Reactions were spun through a cushion of 0.8 ml 30% sucrose in S250 at 3500 rpm for 15 min at 4 °C in a Heraeus Megafuge 1.0 onto poly-L-lysine coated coverslips. Coverslips were washed in 1x PBS and fixed for 1 h on ice in 1% (v/v) glutaraldehyde in fix-buffer (25 mM HEPES, pH 7.5; 25 mM Pipes; 1 mM EGTA; 50 mM KCl; 2 mM MgAc; 5% sucrose). Reactions on coverslips were subsequently subjected to a second fixation for 2 h in 2.5% glutaraldehyde and 10 mg/ml tannic acid in fix-buffer. Samples were handed over for OsO₄ treatment and epon embedding to the Electron Microscopy core facility, EMBL Heidelberg.

5.2.5 Cell culture

HeLa “Kyoto” (received from Shuh Narumiya Department of Pharmacology, Kyoto University Graduate School of Medicine) and HeLa CCL2 cell strains were maintained in Dulbecco’s modified Eagle medium (DMEM), high glucose, provided by EMBL’s media kitchen, supplemented with 10% fetal calf serum, 2 mM glutamine, 100 μ g/ml penicillin and 100 U/ml streptomycin. Cells were grown in a Hera cell 240 incubator at 37 °C under 5% CO₂.

XI177 were maintained by Dr. Wolfram Antonin and propagated according to published procedures.²⁴⁸

5.2.6 siRNA knock down of gene expression in HeLa cells

6x10⁵ cells were seeded on round coverslips (11 mm in diameter) per 6-well 19 h prior transfection. siRNA oligos were designed and purchased from MWG-Biotech. siRNA duplexes were transfected using oligofectamine according to manufacturer’s instructions, yielding 200 nM siRNA oligos. Cells were overlaid with the transfection reaction in DMEM, high glucose, supplemented with 2 mM glutamine and incubated for 4 h at 37 °C, 5% CO₂ in a Hera cell 240 incubator. Transfection was stopped by addition of DMEM high glucose containing 2 mM glutamine, 30% fetal calf serum, 100 μ g/ml penicillin and 100 U/ml streptomycin. Samples were taken

after 24 h, 48 h, and 72 h by removing cover slips and subjecting them to fixation in 4% PFA and immunofluorescence as described (chapter 5.2.3.6) with the only exception that for detection of Nup155 cells were preextracted before fixation in PBS, 0.1% TritonX-100 for 2 min at RT. To assess the knock down efficiency of proteins by Western blot, cells were harvested and lysed by resuspension in 1% NP-40, 0.5% sodium deoxycholate, 0.1% Complete™ EDTA free Protease Inhibitor Cocktail in PBS. Protein concentration was determined by BCA (chapter 5.2.2.7) and equal amounts of total protein loaded per lane on a SDS-PAGE (chapter 5.2.2.5.1).

6 References

- ¹ Alberts, B., Johnson, A., Lewis, J., Raff, M., Roberts, K., and Walther, P. (2002). Molecular biology of the cell, 4th edition.
- ² Rabut, G., Lénárt, P., and Ellenberg, J. (2004). Dynamics of NPC organization through the cell cycle. *Curr. Opin. Cell Biol.* 16, 314-321.
- ³ De Souza, C. P. C., Osmani, A. H., Hashmi, S. B., and Osmani, S. A. (2004). Partial NPC disassembly during closed mitosis in *Aspergillus nidulans*. *Curr. Biol.* 14, 1973-1984.
- ⁴ Straube, A., Weber, I., and Steinberg, G. (2005). A novel mechanism of NE break-down in a fungus: nuclear migration strips off the envelope. *EMBO J.* 24, 1674-1685
- ⁵ Margalit, A., Vlcek, S., Gruenbaum, Y., and Foisner, R. (2005). Breaking and making of the NE. *J. Cell Biochem.* 95, 454-465.
- ⁶ Burke, B., and Ellenberg, J. (2002). Remodelling the walls of the nucleus. *Nat. Rev. Mol. Cell Biol.* 3, 487-497.
- ⁷ Malone, C. J., Fixsen, W. D., Horvitz, H. R., and Han, M. (1999). UNC-84 localizes to the NE and is required for nuclear migration and anchoring during *C. elegans* development. *Development* 126, 3171-3181.
- ⁸ Lee, K. K., Starr, D., Cohen, M., Liu, J., Han, M., Wilson, K. L., and Gruenbaum, Y. (2002). Lamin-dependent localization of UNC-84, a protein required for nuclear migration in *C. elegans*. *Mol. Biol. Cell* 13, 892-901.
- ⁹ Starr, D. A., Hermann, G. J., Marlone, C. J., Fixsen, W., Priess, J. R., Horvitz, H. R., and Han, M. (2001). Unc-83 encodes a novel component of the NE and is essential for proper nuclear migration. *Development* 128, 5039-5050.
- ¹⁰ Zhen, Y. Y., Libotte, R., Munck, M., Noegel, A. A. and Korenbaum, E. (2002). NUANCE, a giant protein connecting the nucleus and actin cytoskeleton. *J. Cell Sci.* 115, 3207-3222.
- ¹¹ Padmakumar, V. C., Abraham, S., Braune, S., Noegel, A. A., Tunggal, B., Karakesisoglou, J., and Korenbaum, E. (2004) Enaptin, a giant actin-binding protein, is an element of the nuclear membrane and the actin cytoskeleton. *Exp. Cell Res.* 295, 330-339.
- ¹² Starr, D. A., and Han, M. (2002). Role of ANC-1 in tethering nuclei to the actin cytoskeleton. *Science* 11, 406-409.
- ¹³ Dreger, M., Bengtsson, L., Schöneberg, T., Otto, H., and Hucho, F. (2001). NE proteomics: Novel integral membrane proteins of the inner nuclear membrane. *Proc Natl Acad Sci USA*, 98, (21), 11943-11948.
- ¹⁴ Schirmer, E. C., Florenx, L., Guan, T., Yates III, J. R., and Gerace, L. (2003). Nuclear Membrane Proteins with potential disease links found by subtractive proteomics. *Science* 301, 1380-1382.
- ¹⁵ Lee, K. K., and Wilson K. L. (2004). All in the family: evidence for four new LEM-domain proteins Lem2 (NET-25), Lem3, Lem4 and Lem5 in the human genome. *Symp Soc Exp Biol.* 56, 329-339.
- ¹⁶ Worman, H. J., and Courvalin, J. C. (2000). The inner nuclear membrane. *J. Membr. Biol.* 177, 1-11.
- ¹⁷ Hetzer, M., Walther, T. C., and Mattaj, I. W. (2005). Pushing the Envelope: Structure, function and dynamics of the nuclear periphery. *Annu. Rev. Cell Dev. Biol.* in press.
- ¹⁸ Laguri, C., Gilquin, B., Wolff, N., Romi-Lebrun, R., Louchay, K., Callebaut, I., Worman, H. J., and Zinn-Justin, S. (2001). Structural characterization of the LEM motif common to three human inner nuclear membrane proteins. *Structure* 9, 503-511.
- ¹⁹ Cai, M., Huang, Y., Ghirlando, R., Wilson, K. L., Craigie, R., and Clore, G. M. (2001). Solution structure of the constant region of NE protein LAP2 reveals two LEM-domain structures: one binds BAF and the other binds DNA. *EMBO J.* 20, 4399-4407.
- ²⁰ Foisner, R., and Gerace, L. (1993). Integral membrane proteins of the NE interact with lamins and chromosomes, and binding is modulated by mitotic phosphorylation. *Cell* 73, 1267-1279.
- ²¹ Lee, M. S., and Craigie, R. (1994). Protection of retroviral DNA from autointegration: involvement of a cellular factor. *Proc. Natl. Acad. Sci. USA* 91, 9823-9827.
- ²² Furukawa, K. (1999). LAP2 binding protein (L2BP1/BAF) is a candidate mediator of LAP2-chromatin interaction. *J. Cell Sci.* 112, 2485-2492.
- ²³ Segura-Totten, M., and Wilson, K. L. (2004). BAF: roles in chromatin, nuclear structure and retrovirus integration. *Trends Cell Biol.* 14, 261-266.
- ²⁴ Martins, S., Eikvar, S., Furukawa, K., and Collas, P. (2003). HA95 and LAP2 β mediate a novel chromatin-NE interaction implicated in initiation of DNA replication. *J. Cell Biol.* 160, 177-188.
- ²⁵ Vlcek, S., Dechat, T., and Foisner, R. (2001). NE and nuclear matrix: interactions and dynamics. *Cell. Mol. Life. Sci.* 58, 1758-1765.

- ²⁶ Nili, E., Cojocaru, G. S., Kalma, Y., Ginsberg, D., Copeland, N. G., Gilbert, D. J., Jenkins, W. A., Berger, R., Shaklai, S., Amariglio, N., Brok-Simoni, F., Simon, A. J., and Rechavi, G. (2001). Nuclear membrane protein, LAP2 β , mediates transcriptional repression alone and together with its binding partner GCL (germ cell-less). (2001). *J. Cell Sci.* 114, 4575-4585.
- ²⁷ Jongens, T. A., Ackerman, L. D., Swedlow, J. R., Jan, L. Y., and Jan, Y. N. (1994). Germ cell-less encodes a cell type-specific nuclear pore-associated protein and functions early in the germ-cell specification pathway of *Drosophila*. *Genes Dev.* 8, 2123-2136.
- ²⁸ Holaska, J. M., Lee, K. K., Kowalski, A. K., and Wilson, K. L. (2003). Transcriptional repressor germ cell-less (GCL) and barrier-to-autointegration factor (BAF) compete for binding to emerin *in vitro*. (2003). *J. Biol. Chem.* 278, 6969-6975.
- ²⁹ Lee, K. K., Haraguchi, T., Lee R. S., Koujin, T., Hiraoka, Y., and Wilson, K. L. (2001). Distinct functional domains in emerin bind lamin A and DNA-bridging protein BAF. *J. Cell Sci.* 114, 4567-4573.
- ³⁰ Morris, G. E. (2001). The role of the NE in Emery-Dreifuss muscular dystrophy. *Trends. Mol. Med.* 7, 572-577.
- ³¹ Haraguchi, T., Holaska, J. M., Yamane, M., Koujin, T., Hashiguchi, N., Mori, C., Wilson, K. L., and Hiraoka, Y. (2004). Emerin binding to Btf, a death-promoting transcriptional repressor, is disrupted by a missense mutation that causes Emery-Dreifuss muscular dystrophy. *Eur. J. Biochem.* 271, 1035-1045.
- ³² Lin, F., Morrison, J. M., Wu, W., and Worman, H. J. (2000). MAN1, an inner nuclear membrane protein that shares the LEM domain with lamina-associated polypeptide2 and emerin. *J. Biol. Chem.* 275, 4840-4847.
- ³³ Osada, S., Ohmori, S. Y., and Taira, M. (2003). XMAN1, an inner nuclear membrane protein, antagonizes BMP signaling by interacting with Smad1 in *Xenopus* embryos. *Development* 130, 1783-1794.
- ³⁴ Ten Dijke, P. and Hill, C. S. New insights into TGF- β -Smad signaling. (2004). *Trends Biochem. Sci.* 29, 265-273.
- ³⁵ Worman, H. J., Yuan, J., Blobel, G., and Georgatos, S. D. (1988). A lamin B receptor in the NE. *Proc Natl Acad Sci USA* 85, 8531-4.
- ³⁶ Ye, Q., and Worman, H. J. (1996). Interaction between an integral protein of the NE inner membrane and human chromodomain proteins homologous to *Drosophila* HP1. *J. Biol. Chem.* 271, 14653-14656.
- ³⁷ Holmer, L., and Worman, H. J. (2001). Inner nuclear membrane proteins: functions and targeting. *Cell. Mol. Life Sci.* 58, 1741-1747.
- ³⁸ Gruenbaum, Y., Margalit, A., Goldman, R. D., Shumaker, D. K., and Wilson, K. L. (2005). The nuclear lamina comes of age. *Nat. Rev. Mol. Cell Biol.* 6, 21-31.
- ³⁹ Hutchison, C. J. (2002). Lamins: Building blocks or regulators of gene expression? *Nature Rev. Mol Cell Biol.* 3, 848-858.
- ⁴⁰ Herrmann, H. and Aebi, U., (2000). Intermediate filaments and their associates: multi-talented structural elements specifying cytoarchitecture and cytodynamics. *Curr. Opin, Cell Biol.*, 12, 79-90.
- ⁴¹ Döring, V., and Stick, R., (1990). Gene structure of nuclear lamin LII of *Xenopus laevis*; a model for the evolution of IF proteins from lamin-like ancestor. *EMBO J.* 9, 4073-4081.
- ⁴² Dodemont, H., Reimer, D., and Weber, K. (1990). Structure of an invertebrate gene encoding cytoplasmic intermediate filament proteins: implications for the origin and the diversification of IF proteins. *EMBO J.*, 9, 4083-4094.
- ⁴³ Fragioni, J., and Neel, B. (1993). Use of a general purpose mammalian expression vector for studying intracellular protein targeting: identification of critical residues in the nuclear lamin A/C nuclear localization sequence. *J. Cell Sci.* 105, 481-488.
- ⁴⁴ Krohne, G., Waisenegger, I., and Hoger, T. (1989). The conserved carboxy-terminal cysteine of nuclear lamins is essential for lamin association with the NE. *J. Cell Biol.* 109, 2003-2011.
- ⁴⁵ Vorburger, K., Kitten, G. T. and Nigg, E. A. (1989). Modification of nuclear lamin proteins by a mevalonic acid derivative occurs in reticulocyte lysates and requires the cysteine residue of the C-terminal CxxM motif. *EMBO J.* 8, 4007-4013.
- ⁴⁶ Machiels, B. M., Zorenc, A. H., Endert, J. M., Kuijpers, H. J., van Eys, G. J., Raemakers, F. C., and Broers, I. L. (1996). An alternative splicing product of the lamin A/C gene lacks exon 10. *J. Biol. Chem.* 271, 9249-9253.
- ⁴⁷ Weber, K., Plessmann, U., and Traub, P. (1989). Maturation of nuclear lamin A involves a specific carboxy-terminal trimming, which removes the polyisoprenylation site from the precursor: implications for the structure of the nuclear lamina. *FEBS Lett.* 257, 411-414.

-
- ⁴⁸ Lodish, H., Berk, A., Zipursky, S. L., Matsudaira, P., Baltimore, D., and Darnell, J. E. (1999). *Molecular Cell Biology*. Fourth Edition, Freeman Publishing.
- ⁴⁹ Aebi, U., Cohn, J., Buhle, L., and Gerace, L. (1986). The nuclear lamina is a meshwork of intermediate filament type filaments. *Nature* 323, 560-564.
- ⁵⁰ Belmont, A. S., Zhai, Y., and Helenius, A. Lamin B distribution and association with peripheral chromatin revealed by optical sectioning and electron tomography. *J. Cell Biol.* 51, 383-392.
- ⁵¹ Zhang, Q., Skepper, J. N., Yang, F., Davies, J. D., Hegyi, L., Roberts, R. G., Weissberg, P. L., Ellis, J. A., and Shanahan, C. M. (2001). Nesprins: a novel family of spectrin-repeat-containing proteins that localize to the nuclear membrane in multiple tissues. *J. Cell Sci.* 114, 4485-4498.
- ⁵² Mislow, J. M., Holaska, J. M., Kim, M. S., Lee, K. K., Segura-Totten, M., Wilson, K. L., and McNally, E. M. (2002). Nesprin-1 α self-associated and binds directly to emerin and lamin A *in vitro*. *FEBS Lett.* 525, 135-140.
- ⁵³ Lenz-Böhme, B., Wismar, J., Fuchs, S., Reifegerste, R., Buchner, E., Betz, H., and Schmitt, B. (1997). Insertional mutation of the *Drosophila* nuclear lamin Dm0 gene results in defective NEs, clustering of NPCs, and accumulation of annulate lamellae. *J. Cell Biol.* 137, 1001-1016.
- ⁵⁴ Lui, J., Rolef Ben-Shahar, T., Riemer, D., Treinin, M., Spann, P., Weber, K., Fire, A., and Gruenbaum, Y. (2000). Essential roles of *Caenorhabditis elegans* lamin gene in nuclear organization, cell cycle progression, and spatial organization of NPCs. *Mol. Biol. Cell* 11, 3937-3947.
- ⁵⁵ Harborth, J., Elbashir, S. M., Bechert, K., Tuschl, T., and Weber, K. (2001). Identification of essential genes in cultured mammalian cells using small interfering RNAs. *J. Cell Sci.* 114, 4557-4565.
- ⁵⁶ Röber, R. A., Weber, K., and Osborn, M. (1989). Differential timing of nuclear lamin A/C expression in the various organs of the mouse embryo and the young animal: a developmental study. *Development* 105, 365-378.
- ⁵⁷ Stick, R., and Hausen, P. (1985). Changes in the nuclear lamina composition during early development of *Xenopus laevis*. *Cell* 41, 191-200.
- ⁵⁸ Hinshaw, J. C., Carragher, B. O., and Milligan, R. A. (1992). Architecture and design of the NPC. *Cell* 69, 1133-1141.
- ⁵⁹ Yang, Q., Allis, C. D., Tempst, P., and Svejstrup, J. Q. (1998). Three-dimensional architecture of the isolated yeast NPC: functional and evolutionary implications. *Mol. Cell* 1, 223-234.
- ⁶⁰ Akey, C. W., and Radermacher, M. (1993). Architecture of the *Xenopus* NPC revealed by three-dimensional cryoelectron microscopy. *J. Cell Biol.* 122, 1-19.
- ⁶¹ Stoffler, D., Feja, B., Fahrenkrog, B., Walz, J., Typke, D., and Aebi, U. (2003). Cryoelectron tomography provides novel insights into nuclear pore architecture: implications for nucleocytoplasmic transport. *J. Mol. Biol.* 328, 119-130.
- ⁶² Beck, M., Förster, F., Ecke, M., Plitzko, M., Melchior, F., Gerisch, G., Baumeister, W., and Medalia, O. (2004). NPC structure and dynamics revealed by cryoelectron tomography. *Science* 306, 1387-1390.
- ⁶³ Maul, G. G. (1971). On the octagonality of the NPC. *J. Cell Biol.* 51, 558-63.
- ⁶⁴ Suntharalingam, M., and Wenthe, S. R. (2003). Peering through the pore: NPC structure, assembly, and function. *Dev. Cell* 4, 775-789.
- ⁶⁵ Fahrenkrog, B., Köser, J., and Aebi, U. (2004). The NPC: a jack of all trades? *Trends Biochem. Sci.* 29, 175-182.
- ⁶⁶ Rout, M. P., Aitchison, J. D., Suprato, A., Hjertaas, K., Zhao, Y., and Chait, B. T. (2000). The yeast NPC: composition, architecture, and transport mechanism. *J. Cell Biol.* 148, 635-651.
- ⁶⁷ Cronshaw, J. M., Krutchinsky, A. N., Zhang, W., Chait, B. T., and Matunis, M. J. (2002). Proteomic analysis of the mammalian NPC. *J. Cell Biol.* 158, 915-927.
- ⁶⁸ Rout, M. P., and Blobel, G. (1993). Isolation of the yeast nuclear pore complex. *J. Cell Biol.* 123, 771-783.
- ⁶⁹ Yang, Q., Rout, M. P., and Akey, C. W. (1998). Three-dimensional architecture of the isolated yeast nuclear pore complex: functional and evolutionary implications. *Mol. Cell* 1, 223-234.
- ⁷⁰ Reichelt, R., Holzenburg, A., Buhle, E. L. Jr., Jarnik, M., Engel, A., and Aebi, U. (1990). Correlation between structure and mass distribution of the nuclear pore complex and of distinct pore complex components. *J. Cell Biol.* 110, 883-894.
- ⁷¹ Pante, N. and Kann, M. (2002). NPC is able to transport macromolecules with diameters of about 39nm. *Mol. Biol. Cell* 13, 425-434.
-

- ⁷² Paulillo, S. M., Phillips, E. M., Köser, J., Sauder, U., Ullman, K. S., Powers, M. A., and Fahrenkrog, B. (2005). Nucleoporin domain topology is linked to the transport status of the nuclear pore complex. *J. Mol. Biol.* 351, 784-798.
- ⁷³ Fahrenkrog, B., Aris, J. P., Hurt, E. C., Pante, N., and Aebi, U. (2000). Comparative spatial localization of protein-A-tagged and authentic yeast NPC proteins by immunogold electron microscopy. *J. Struct. Biol.* 129, 295-305.
- ⁷⁴ Rout, M. P., Aitchison, J. D., Magnasco, M. O., and Chait, B. T. (2003). Virtual gating and nuclear transport: the hole picture. *Trends Cell Biol.* 13, 622-628.
- ⁷⁵ Krull, S., Thyberg, J., Björkroth, B., Rackwitz, H. R., and Cordes, V. C. (2004). Nucleoporins as components of the NPC core structure and Tpr as the architectural element of the nuclear basket. *Mol. Biol. Cell* 15, 4261-4277.
- ⁷⁶ Gerace, L., Ottaviano, Y., and Kondor-Koch, C. (1982). Identification of a major polypeptide of the NPC. *J. Cell Biol.* 95, 826-837.
- ⁷⁷ Wozniak, R. W., Bartnik, E., and Blobel, G. (1989). Primary structure analysis of an integral membrane glycoprotein of the nuclear pore. *J. Cell Biol.* 108, 2083-2092.
- ⁷⁸ Hallberg, E., Wozniak, R. W., and Blobel, G. (1993). An integral membrane protein of the pore membrane domain of the NE contains a nucleoporin-like region. *J. Cell Biol.* 122, 513-521.
- ⁷⁹ Wozniak, R. W., Blobel, G., and Rout, M. P. (1994). Pom152 is an integral protein of the pore membrane domain of the yeast NE. *J. Cell Biol.* 125, 31-42.
- ⁸⁰ Chial, H. J., Rout, M. P., Giddings, T. H., and Winey, M. (1998). *Saccharomyces cerevisiae* Ndc1p is a shared component of NPCs and spindle pole bodies. *J. Cell Biol.* 143, 1789-1800.
- ⁸¹ Mans, B. J., Anantharaman, V., Aravind, L., and Koonin, E. V. (2004). Comparative genomics, evolution and origins of the nuclear envelope and nuclear pore complex. *Cell Cycle* 3, 1612-1637.
- ⁸² Rout, M. P., and Wentz, S. R. (1994). Pores for thought: NPC proteins. *Trends Cell Biol.* 4, 357-365.
- ⁸³ Strawn, L. A., Shen, T., Shulga, N., Goldfarb, D. S., and Wentz, S. R. (2004). Minimal NPCs define FG repeat domains essential for transport. *Nat. Cell Biol.* 6, 197-206.
- ⁸⁴ Denning, D. P., Patel, S. S., Uversky, V., Fink, A. L., and Rexach, M. (2003). Disorder in the NPC: The FG repeat regions of nucleoporins are natively unfolded. *Natl. Acad. Sci. USA* 100, 2450-2455.
- ⁸⁵ Schwartz, T. U. (2005). Modularity within the architecture of the NPC. *Curr. Opin. Struct. Biol.* 15, 221-226.
- ⁸⁶ Berke, I. C., Boehmer, T., Blobel, G., and Schwartz, T. U. (2004). Structural and functional analysis of Nup133 domains reveals modular building blocks of the NPC. *J. Cell Biol.* 167, 591-597.
- ⁸⁷ Weirich, C. S., Erzberger, J. P., Berger, J. M., and Weis, K. (2004). The N-terminal domain of Nup159 forms a beta-propeller that functions in mRNA export by tethering the helicase Dbp5 to the nuclear pore. *Mol Cell* 16, 749-760.
- ⁸⁸ Loidice, I., Alves, A., Rabut, G., van Overbeek, M., Ellenberg, J., Sibarita, J. B., and Doye, V. (2004). The entire Nup107-160 complex, including three new members is targeted as one entity to kinetochores in mitosis. *Mol. Biol. Cell* 15, 3333-3344.
- ⁸⁹ Devos, D., Dokudovskaya, S., Alber, R., Williams, R., Chait, B. T., Sali, A., and Rout, M. P. (2004). Components of coated vesicles and NPCs share a common molecular architecture. *PLoS Biol.* 2, 1-9.
- ⁹⁰ Allen, N. P. C., Patel, S. S., Huang, L., Chalkley, R. J., Burlingame, A., Lutzmann, M., Hurt, E. C., and Rexach, M. (2002). Deciphering networks of protein interactions at the NPC. *Mol. Cell. Proteomics* 1, 930-946.
- ⁹¹ Huang, L., Baldwin, M. A., Maltby, D. A., Medzihradzky, K. F., Baker, P. R., Allen, N., Rexach, M., Edmondson, R. D., Campbell, J., Juhasz, P., Martin, S. A., Vestal, M. L., and Burlingame, A. L. (2002). The identification of protein-protein interactions of the NPC of *Saccharomyces cerevisiae* using high throughput matrix-associated laser desorption ionization time-of-flight tandem mass spectrometry. *Mol. Cell. Proteomics.* 1-434-450.
- ⁹² Panté, N., Bastos, R., McMorro, I., Burke, B., and Aebi, U. (1994). Interactions and three-dimensional localization of a group of NPC proteins. *J. Cell Biol.* 126, 603-617.
- ⁹³ Allen, N. P. C., Huang, L., Burlingame, A., and Rexach, M. (2001). Proteomic analysis of nucleoporin interacting proteins. *J. Biol. Chem.* 276, 29268-29274.

- ⁹⁴ Yokoyama, N., Hayashi, N., Seki, T., Pante, N., Ohba, T., Nishii, K., Kuma, K., Hayashida, T., Miyata, T., Aebi, U. *et al.* (1995). A giant nucleopore protein that binds Ran/TC4. *Nature* 376, 184-188.
- ⁹⁵ Delphin, C., Guan, T., Melchior, F., and Gerace, L. (1997). RanGTP targets p97 to RanBP2, a filamentous protein localized at the cytoplasmic periphery of the NPC. *Mol. Biol. Cell* 8, 2379-2390.
- ⁹⁶ Pichler, A., Gast, A., Seeler, J. S., Dejean, A., and Melchior, F. (2002). The nucleoporin RanBP2 has SUMO1 E3 ligase activity. *Cell* 108, 109-120.
- ⁹⁷ Saitoh, H., Pu, R., Cabenagh, M., and Dasso, M. (1997). RanBP2 associates with Ubc9p and a modified form of RanGAP1. *Proc. Natl. Acad. Sci. USA* 94, 3736-3741.
- ⁹⁸ Mahajan, R., Delphin, D., Guan, T., Gerace, L., and Melchior, F. (1997). A small ubiquitin-related polypeptide involved in targeting RanGAP1 to NPC protein RanBP2. *Cell* 88, 97-107.
- ⁹⁹ Matunis, M. J., Wu, J., and Blobel, G. (1998). SUMO-1 modification and its role in targeting the Ran GTPase-activating protein, RanGAP1, to the NPC. *J. Cell Biol.* 140, 499-509.
- ¹⁰⁰ Yaseen, N. R., and Blobel, G. (1999). Two distinct classes of Ran-binding sites on the nucleoporin Nup358. *Proc. Natl. Acad. Sci. USA* 96, 5516-5521.
- ¹⁰¹ Bernad, R., van der Velde, H., Fornerod, M., and Pickersgill, H. (2004). Nup358/RanBP2 attaches to the nuclear pore complex via association with Nup88 and Nup214/CAN and plays a supporting role in CRM1-mediated nuclear protein export. *Mol. Cell Biol.* 2373-2384.
- ¹⁰² Kehlenbach, R. H., Dickmanns, A., Kehlenbach, A., Guan, T., and Gerace, L. (1999). A role for RanBP1 in the release of CRM1 from the nuclear pore complex in a terminal step of nuclear export. *J. Cell Biol.* 145, 644-657.
- ¹⁰³ Walther, T. C., Pickersgill, H. S., Cordes, V. C., Goldberg, M. W., Allen, T. D., Mattaj, I. W., and Fornerod, M. (2002). The cytoplasmic filaments of the NPC are dispensable for selective nuclear protein import. *J. Cell Biol.* 158, 63-77.
- ¹⁰⁴ Salina, D., Enarson, P., Rattner, J. B., and Burke, B. (2003). Nup358 integrates NE breakdown with kinetochore assembly. *J. Cell Biol.* 162, 991-1001.
- ¹⁰⁵ Joseph, J., Tan, S. H., Karpova, T. S., McNally, J. G., and Dasso, M. (2002). SUMO-1 targets RanGAP1 to kinetochores and mitotic spindles. *J. Cell Biol.* 156, 595-602.
- ¹⁰⁶ Campbell, M. S., Chan, G. K., and Yen, T. J. (2001). Mitotic checkpoint proteins HsMAD1 and HsMAD2 are associated with NPCs in interphase. *J. Cell Sci.* 114, 953-963.
- ¹⁰⁷ Fornerod, M., van Deursen, J., van Baal, S., Reynolds, A., Davis, D., Murti, K. G., Fransen, J., and Grosveld, G. (1997). The human homologue of yeast CRM1 is in a dynamic subcomplex with CAN/Nup214 and a novel nuclear pore component Nup88. *EMBO J.* 16, 807-816.
- ¹⁰⁸ Bastos, R., Ribas de Pouplana, L., Bodoor, K., and Burke, B. (1997). Nup84, a novel nucleoporin that is associated with CAN/Nup214 on the cytoplasmic face of the NPC. *J. Cell Biol.* 137, 989-1000.
- ¹⁰⁹ Lutzmann, M., Kunze, R., Buerer, A., Aebi, U., and Hurt, E. (2002). Modular self-assembly of a Y-shaped multiprotein complex from seven nucleoporins. *EMBO J.* 21, 387-397.
- ¹¹⁰ Goldberg, M. W., Wiese, C., Allen, T. D., and Wilson, K. L. (1997). Dimples, pores, star-rings, and thin rings on growing NEs: evidence for structural intermediates in NPC assembly. *J. Cell Sci.* 110, 409-420.
- ¹¹¹ Belgareh, N., Rabut, G., Bai, S. W., van Overbeek, M., Beaudouin, J., Daigle, N., Zatssepina, O. V., Pasteau, F., Labas, V., Fromont-Racine, M., Ellenberg, J., and Doye, V. (2001). An evolutionarily conserved NPC subcomplex, which redistributes in part to kinetochores in mammalian cells. *J. Cell Biol.* 154, 1147-1160.
- ¹¹² Siniosoglou, S., Lutzmann, M., Santos-Rosa, H., Leonard, K., Mueller, S., Aebi, U., and Hurt, E. (2000). Structure and assembly of the Nup84p complex. *J. Cell Biol.* 149, 41-54.
- ¹¹³ Siniosoglou, S., Wimmer, C., Rieger, M., Doye, V., Tekotte, H., Weise, C., Emig, S., Segref, A., and Hurt, E. C. (1996). A novel complex of nucleoporins, which includes Sec13p and a Sec13p homolog, is essential for normal nuclear pores. *Cell* 84, 265-275.
- ¹¹⁴ Bai, S. W., Rouquette, J., Umeda, M., Faigle, W., Loew, D., Sazer, S., and Doye, V. (2004). The fission yeast Nup107-120 complex functionally interacts with the small GTPase Ran/Spi1 and is required for mRNA export, nuclear pore distribution, and proper cell division. *Mol. Cell Biol.* 24, 6379-6392.
- ¹¹⁵ Vasu, S., Sha, S., Orjalo, A., Park, M., Fischer, W. H., and Forbes, D. J. (2001). Novel vertebrate nucleoporins Nup133 and Nup160 play a role in mRNA export. *J. Cell Biol.* 155, 339-353.
- ¹¹⁶ Grandi, P., Dang, R., Pané, N., Shevchenko, A., Mann, M., Forbes, D., and Hurt, E. (1997). Nup93, a vertebrate homologue of yeast Nic96p, forms a complex with a novel 205-kDa protein and is required for correct nuclear pore assembly. *Mol. Biol. Cell* 8, 2017-2038.

- 117 Miller, B. R., Powers, M., Park, M., Fischer, W., and Forbes, D. J. (2000). Identification of a new vertebrate nucleoporin, Nup188, with the use of a novel organelle trap assay. *Mol. Biol. Cell* 11, 3381-3396.
- 118 Hawryluk-Gara, L., Shibuya, E. K., and Wozniak, R. W. (2005). Vertebrate Nup53 interacts with the nuclear lamina and is required for the assembly of a Nup93-containing complex. *Mol. Cell Biol.* 16, 2382-2394.
- 119 Galy, V., Mattaj, I. W., and Askjaer, P. (2003). *Caenorhabditis elegans* nucleoporins Nup93 and Nup205 determine the limit of NPC size exclusion *in vivo*. *Mol. Biol. Cell* 14, 5104-5115.
- 120 Kita, K., Omata, S., and Horigome, T. (1993). Purification and characterization of a nuclear pore glycoprotein complex containing p62. *J. Biochem. (Tokyo)* 113, 377-382.
- 121 Hu, T., Guan, T., and Gerace, L. (1996). Molecular and functional characterization of the p62 complex, an assembly of NPC glycoproteins. *J. Cell Biol.* 134, 589-601.
- 122 Finlay, D. R., Meier, E., Bradley, P., Horecka, J., and Forbes, D. J. (1991). A complex of nuclear pore proteins required for pore function. *J. Cell Biol.* 114, 169-183.
- 123 Radu, A., Blobel, G., and Wozniak, R. W. (1993). Nup155 is a novel NPC protein that contains neither repetitive sequence motifs nor reacts with WGA. *J. Cell Biol.* 121, 1-9.
- 124 Rayala, H. J., Kendirgi, R., Barry, D. M., Majerus, P. W., and Wentte, S. R. (2004). The mRNA export factor human Gle1 interacts with the NPC protein Nup155. *Mol. Cell Proteomics* 3,145-155.
- 125 Kendirgi, F., Barry, D. M., Griffis, E. R., Powers, M. A., and Wentte, S. R. (2003). An essential role for hGle1 nucleocytoplasmic shuttling in mRNA export. *J. Cell Biol.* 160, 1029-1040.
- 126 Kendirgi, F., Rexer, D. J., Alcázar-Román, A. R., Onishko, H. M., and Wentte, S. R. (2005). Interaction between the shuttling mRNA export factor Gle1 and the nucleoporin hCG1: a conserved mechanism in the export of Hsp70 mRNA. *Mol. Biol. Cell* 16, 4304-4315.
- 127 Cordes, V. C., Reidenbach, S., Rackwitz, H. R., and Franke, W. W. (1997). Identification of protein p270/Tpr as a constitutive component of the NPC-attached intranuclear filaments. *J. Cell Biol.* 136, 515-529.
- 128 Hase, M. E., Kuznetsov, N., and Cordes, V. C. (2001). Amino acid substitutions of coiled-coil protein Tpr abrogate anchorage to the NPC but not parallel, in-register homodimerization. *Mol. Biol. Cell* 12, 2433-2452.
- 129 Walther, T. C., Fornerod, M., Pickersgill, H., Goldberg, M., Allen, T. D., and Mattaj, I. W. (2001). The nucleoporin Nup153 is required for nuclear pore basket formation, nuclear pore complex anchoring and import of a subset of nuclear proteins. *EMBO J.* 15, 5703-5714.
- 130 Hase, M. E., and Cordes, V. C. (2003). Direct interaction with Nup153 mediates binding of Tpr to the periphery of the NPC. *Mol. Biol. Cell* 14, 1923-1940.
- 131 Smythe, C., Jenkins, H. E., and Hutchison, C. J. (2000). Incorporation of the nuclear pore basket protein Nup153 into nuclear pore structures is dependent upon lamina assembly: evidence from cell-free extracts of *Xenopus* eggs. *EMBO J.* 19, 3918-3931.
- 132 Hallberg, E., Wozniak, R. W., and Blobel, G. (1993). An integral membrane protein of the pore membrane domain of the NE contains a nucleoporin-like region. *J. Cell Biol.* 122, 513-521.
- 133 Wozniak, R. W., Bartnik, E., and Blobel, G. (1989). Primary structure analysis of an integral membrane glycoprotein of the nuclear pore. *J. Cell Biol.* 108, 2083-2092.
- 134 Gerace, L., Ottaviano, Y., and Kondor-Koch, C. (1982). Identification of a major polypeptide of the NPC. *J. Cell Biol.* 95, 826-837.
- 135 Greber, U. F., Senior, A., and Gerace, L. (1990). A major glycoprotein of the NPC is a membrane-spanning polypeptide with a large luminal domain and a small cytoplasmic tail. *EMBO J.* 9, 1495-1502.
- 136 Cohen, M., Feinstein, N., Wilson, K. L., and Gruenbaum, Y. (2003). Nuclear pore protein gp210 is essential for viability in HeLa cells and *Caenorhabditis elegans*. *Mol. Biol. Cell* 14, 4230-4237.
- 137 Olsson, M., Schéele, S., and Ekblom, P. (2004). Limited expression of nuclear pore membrane glycoprotein 210 in cell lines and tissues suggests cell-type specific nuclear pores in metazoans. *Exp. Cell Res.* 292, 359-370.
- 138 Macaulay, C., Meier, E., and Forbes, D. J. (1995). Differential mitotic phosphorylation of proteins of the NPC. *J. Biol. Chem.* 270, 254-262.
- 139 Finlay, D. R., and Forbes, D. J. (1990). Reconstitution of biochemically altered nuclear pores: transport can be eliminated and restored. *Cell* 60, 17-29.
- 140 Miller, M. W., Caracciolo, M. R., Berlin, W. K., and Hanover, J. A. (1999). Phosphorylation and glycosylation of nucleoporins. *Arch. Biochem. Biophys.* 367, 51-60.

- ¹⁴¹ Daigle, N., Beaudoin, J., Hartnell, L., Imreh, G., Hallberg, E., Lippincott-Schwartz, J., and Ellenberg, J. (2001). NPCs form immobile networks and have a very low turnover in live mammalian cells. *J. Cell Biol.* 154, 71-84.
- ¹⁴² Cronshaw, J. M. and Matunis, M. J. (2003). The NPC protein ALADIN is mislocalized in triple A syndrome. *Proc. Natl. Acad. Sci. USA* 100, 5823-5827.
- ¹⁴³ Rabut, G., Doye, V., and Ellenberg, J. (2004). Mapping the dynamic organization of the NPC inside single living cells. *Nat. Cell Biol.* 6, 1114-1121.
- ¹⁴⁴ Kuersten, S., Ohno, M., and Mattaj, I. W. (2001). Nucleocytoplasmic transport: Ran, beta and beyond. *Trends Cell Biol.* 11, 497-503.
- ¹⁴⁵ Weis, K. (2003). Regulating access to the genome: nucleocytoplasmic transport throughout the cell cycle. *Cell* 112, 441-451.
- ¹⁴⁶ Matunis, M. J., Coutavas, E., and Blobel, G. (1996). A novel ubiquitin-like modification modulates the partitioning of the Ran-GTPase-activating protein RanGAP1 between the cytosol and the NPC. *J. Cell Biol.* 135, 1457-1470.
- ¹⁴⁷ Kalderon, D., Roberts, B. L., Richardson, W. D., and Smith, A. E. (1984). A short amino acid sequence able to specify nuclear location. *Cell* 39, 499-509.
- ¹⁴⁸ Lanford, R. E., and Butel, J. S. (1984). Construction and characterization of an SV40 mutant defective in nuclear transport of T antigen. *Cell* 37, 801-813.
- ¹⁴⁹ Fischer, U., Huber, J., Boelens, W. C., Mattaj, I. W., and Lührmann, R. (1995). The HIV-1 Rev activation domain is a nuclear export signal that accesses an export pathway used by specific cellular RNAs. *Cell* 82, 475-483.
- ¹⁵⁰ Wen, W., Meinkoth, J. L., Tsien, R. Y., and Taylor, S. S. (1995). Identification of a signal for rapid export of proteins from the nucleus. *Cell* 82, 463-473.
- ¹⁵¹ Ribbeck, K., Lipowsky, G., Kent, H. M., Stewart, M., and Görlich, D. (1998). NTF2 mediates nuclear import of Ran. *EMBO J.* 17, 6587-6598.
- ¹⁵² Conti, E., and Izaurralde, E. (2001). Nucleocytoplasmic transport enters the atomic age. *Curr. Opin. Cell Biol.* 13, 310-319.
- ¹⁵³ Clouse, K. N., Luo, M. J., Zhou, Z., and Reed R. (2001). A Ran-independent pathway for export of spliced mRNA. *Nat. Cell Biol.* 3, 97-99.
- ¹⁵⁴ Izaurralde, E., Kutay, U., von Kobbe, C., Mattaj, I. W., and Görlich, D. (1997). The asymmetric distribution of the constituents of the Ran system is essential for transport into and out of the nucleus. *EMBO J.* 16, 6535-6547.
- ¹⁵⁵ Kalab, P., Weis, K., and Heald, R. (2002). Visualization of a Ran-GTP gradient in interphase and mitotic *Xenopus* egg extracts. *Science* 295, 2452-2456.
- ¹⁵⁶ Carazo-Salas, R. E., Guarguaglini, G., Gruss, O. J., Segref, A., Karsenti, E., and Mattaj, I. W. (1999). Generation of GTP-bound Ran by RCC1 is required for chromatin-induced mitotic spindle formation. *Nature* 400, 178-181.
- ¹⁵⁷ Ohba, T., Nakamura, M., Nishitani, H., and Nishimoto, T. (1999). Self-organization of microtubule asters induced in *Xenopus* egg extracts by GTP-bound Ran. *Science* 284, 1356-1358.
- ¹⁵⁸ Wilde, A., and Zheng, Y. (1999). Stimulation of microtubule aster formation and spindle assembly by the small GTPase Ran. *Science* 284, 1359-1362.
- ¹⁵⁹ Gruss, O. J., Carazo-Salas, R. E., Schatz, C. A., Guarguaglini, G., Kast, J., Wilm, M., Le Bot, N., Vernos, I., Karsenti, E., and Mattaj, I. W. (2001). Ran induces spindle assembly by reversing the inhibitory effect of importin alpha on TPX2 activity. *Cell* 104, 83-93.
- ¹⁶⁰ Nachury, M. V., Maresca, T. J., Salmon, W. C., Waterman-Storer, C. M., Heald, R., and Weis, K. (2001). Importin beta is a mitotic target of the small GTPase Ran in spindle assembly. *Cell* 104, 95-106.
- ¹⁶¹ Wiese, C., Wilde, A., Moore, M. S., Adam, S. A., Merdes, A., and Zheng, Y. (2001). Role of importin-beta in coupling Ran to downstream targets in microtubule assembly. *Science* 291, 653-656.
- ¹⁶² Chaudhary, N., and Courvalin, J. C. (1993). Stepwise reassembly of the nuclear envelope at the end of mitosis. *J. Cell Biol.* 122, 295-306.
- ¹⁶³ Newport, J. W., Wilson, K. L., and Dunphy, W. G. (1990). A lamin-independent pathway for nuclear envelope assembly. *J. Cell Biol.* 111, 2247-2259.
- ¹⁶⁴ Ellenberg, J., Siggia, E. D., Moreira, J. C., Smith, C. L., Presley, J. F., Worman, H. J., and Lippincott-Schwartz, J. (1997). Nuclear membrane dynamics and reassembly in living cells: targeting of an inner nuclear membrane protein in interphase and mitosis. *J. Cell Biol.* 138, 1193-1206.
- ¹⁶⁵ Yang, L., Guan, T., and Gerace, L. (1997). Integral membrane proteins of the NE are dispersed throughout the endoplasmic reticulum during mitosis. *J. Cell Biol.* 137, 1199-1210.

- 166 Mattaj, I. W. (2004). Sorting out the NE from the endoplasmic reticulum. *Nat. Rev. Mol. Cell Biol.* 5, 1-5.
- 167 Collas, P., and Courvalin, J. C. (2000). Sorting nuclear membrane proteins at mitosis. *Trends Cell Biol.* 10, 5-8.
- 168 Vigers, G. P. A., and Lohka, M. J. (1991). A distinct vesicle population targets membranes and pore complexes to the NE in *Xenopus* eggs. *J. Cell Biol.* 112, 545-556.
- 169 Collas, P., and Poccia, D. (1996). Distinct egg membrane vesicles differing in binding and fusion properties contribute to sea urchin male proNEs formed *in vitro*. *J. Cell Sci.* 109, 1275-1283.
- 170 Drummond, S., Ferrigno, P., Lyon, C., Murphy, J., Goldberg, M., Allen, T., Smythe, C., and Hutchison, C. J. (1999). Temporal differences in the appearance of NEP-B78 and an LBR-like protein during *Xenopus* NE reassembly reflect the ordered recruitment of functionally discrete vesicle types. *J. Cell Biol.* 144, 225-240.
- 171 Wiese, C., Goldberg, M. W., Allen, T. D., and Wilson, K. L. (1997). NE assembly in *Xenopus* extracts visualized by scanning EM reveals a transport-dependent „envelope smoothing“ event. *J. Cell Sci.* 110, 1489-1502.
- 172 Wilson, K. L., and Newport, J. (1988). A trypsin-sensitive receptor on membrane vesicles is required for NE formation *in vitro*. *J. Cell Biol.* 107, 57-68.
- 173 Antonin, W., Franz, C., Haselmann, U., Antony, C., and Mattaj, I. W. (2005). The integral membrane nucleoporin pom121 functionally links NPC assembly and NE reformation. *Mol. Cell* 17, 83-92.
- 174 Hetzer, M., Meyer, H. H., Walther, T. C., Bilbao-Cortés, D., Warren, G., and Mattaj, I. W. (2001). Distinct AAA-ATPase p97 complexes function in discrete steps of nuclear assembly. *Nature Cell Biol.* 3, 1086-1091.
- 175 Pyrpasopoulou, A., Meier, J., Maison, C., Simos, G., and Georgatos, S. D. (1996). The lamin B receptor (LBR) provides essential chromatin docking sites at the NE. *EMBO J.* 15, 7108-7119.
- 176 Boman, A. L., Dennialoy, M. R., and Wilson, K. L. (1992). GTP hydrolysis is required for vesicle fusion during NE assembly *in vitro*. *J. Cell Biol.* 116, 281-294.
- 177 Macaulay, C. and Forbes, D. J. (1996). Assembly of the nuclear pore: biochemically distinct steps revealed with NEM, GTP γ S, and BAPTA. *J. Cell Biol.* 132, 5-20.
- 178 Hetzer, M., Bilbao-Cortés, D., Walther, T. C., Gruss, O. J., and Mattaj, I. W. (2000). GTP hydrolysis by Ran is required for NE assembly. *Mol. Cell* 5, 1013-1024.
- 179 Zhang, C., and Clarke, P. R. (2000). Chromatin-independent NE assembly induced by Ran GTPase in *Xenopus* egg extracts. *Science* 288, 1429-1432.
- 180 Harel, A., Chan, R. C., Lachish-Zalait, A., Zimmermann, E., Elbaum, M., and Forbes, D. J. (2003). Importin β negatively regulates nuclear membrane fusion and NPC assembly. *Mol. Biol. Cell* 14, 4387-4396.
- 181 Hachet, V., Köcher, T., Wilm, M., and Mattaj, I. W. (2004). Importin α associates with membranes and participates in NE assembly *in vitro*. *EMBO J.* 23, 1526-1535.
- 182 Askjaer, P., Galy, V., Hannak, E., and Mattaj, I. W. (2002). Ran GTPase cycle and importin α and β are essential for spindle formation and NE assembly in living *Caenorhabditis elegans* embryos. *Mol. Cell Biol.* 13, 4355-4370.
- 183 Bamba, C., Bobinnec, Y., Fukuda, M., and Nishida, E. (2002). The GTPase Ran regulates chromosome positioning and NE assembly *in vivo*. *Curr. Biol.* 12, 503-507.
- 184 Walther, T. C., Askjaer, P., Gentzel, M., Habermann, A., Griffith, G., Wilm, M., Mattaj, I. W., and Hetzer, M. (2003). RanGTP mediates NPC assembly. *Nature* 424, 689-694.
- 185 Kessel, R. B. (1992). Annulate lamellae: a last frontier in cellular organelles. *Int. Rev. Cytol.* 133, 43-120.
- 186 Bischoff, F. R., Klebe, C., Kretschmer, J., Wittinghofer, A., and Ponstingl, H. (1994). RanGAP1 induces GTPase activity of nuclear Ras-related Ran. *Proc. Natl. Acad. Sci. USA* 91, 2587-2591.
- 187 Ryan, K. J., McCaffery, J. M., and Wenthe, S. R. (2003). The RanGTPase cycle is required for yeast NPC assembly. *J. Cell Biol.* 160, 1041-1053.
- 188 Sheehan, M. A., Mills, A. D., Sleeman, A. M., Laskey, R. A., and Blow, J. J. (1988). Steps in the assembly of replication-competent nuclei in a cell-free system from *Xenopus* eggs. *J. Cell Biol.* 106, 1-12.
- 189 Walther, T. C., Alves, A., Pickersgill, H., Loidice, I., Hetzer, M., Galy, V., Hulsmann, B. B., Köcher, T., Wilm, M., Allen, T., Mattaj, I. W., and Doye, V. (2003). The conserved Nup107-160 complex is critical for NPC assembly. *Cell* 113, 195-206.

- ¹⁹⁰ Boodor, K., Shaikh, S., Salina, D., Raharjo, W. H., Bastos, R., Lohka, M., and Burke, B. (1999). Sequential recruitment of NPC proteins to the nuclear periphery at the end of mitosis. *J. Cell Sci.* 112, 2253-2264.
- ¹⁹¹ Harel, A., Orjalo, A. V., Vincent, T., Lachish-Zalait, A., Vysu, S., Sha, S., Zimmerman, E., Elbaum, M., and Forbes, D. J. (2003). Removal of a single pore subcomplex results in vertebrate nuclei devoid of nuclear pores. *Mol. Cell* 11, 853-864.
- ¹⁹² Powers, M. A., Macaulay, C., Masiarz, F. R., and Forbes, D. J. (1995). Reconstituted nuclei depleted of a vertebrate GLFG nuclear pore protein, p97, import but are defective in nuclear growth and replication. *J. Cell Biol.* 128, 721-736.
- ¹⁹³ Zipperlen, P., Fraser, G. F., Kamath, R. S., Martinez-Campos, M., and Ahringer, J. (2001). Roles for 147 embryonic lethal genes on *C. elegans* chromosome I identified by RNA interference and video microscopy. *EMBO J.* 20, 3984-3992.
- ¹⁹⁴ Sönnichsen, B., Koski, L. B., Walsh, A., Marschall, P., Neumann, B., Brehm, M., Alleaume, A. M., Artelt, J., Bettencourt, P., Cassin, E., Hewitson, M., Holz, C., Khan, M., Lazik, S., Martin, C., Nitzsche, B., Ruer, M., Stamford, J., Winzi, M., Heinkel, R., Roder, M., Finell, J., Hantsch, H., Jones, S. J., Jones, M., Piano, F., Gunsalus, K. C., Oegema, K., Gonczy, P., Coulson, A., Hyman, A. A., and Echeverri, C. J. (2005). Full-genome RNAi profiling of early embryogenesis in *C. elegans*. *Nature* 434, (7032), 462-469.
- ¹⁹⁵ Colaiácovo, M. P., Stanfield, G. M., Reddy, K. C., Reinke, V., Kim, K. S., and Villeneuve, A. M. (2002). A targeted RNAi screen for genes involved in chromosome morphogenesis and nuclear organization in the *Caenorhabditis elegans* germline. *Genetics* 162, 113-128.
- ¹⁹⁶ Bodoor, K., Shaikh, S., Salina, D., Raharjo, W. H., Bastos, R., Lohka, M., Burke, B. (1999). Sequential recruitment of NPC proteins to the nuclear periphery at the end of mitosis. *J. Cell Sci.* 112, 2253-2264.
- ¹⁹⁷ Haraguchi, T., Koujin, T., Hayakawa, T., Kaneda, T., Tsutsumi, C., Imamoto, N., Akazawa, C., Sukegawa, J., Yoneda, Y., and Hiroaka, Y. (2000). Live fluorescence imaging reveals early recruitment of emerin, LBR, RanBP2, and Nup153 to reforming functional nuclear envelopes. *J. Cell Sci.* 113, 779-794.
- ¹⁹⁸ Burke, B., and Gerace, L. (1986). A cell-free system to study reassembly of the NE at the end of mitosis. *Cell* 44, 639-652.
- ¹⁹⁹ Nakagawa, J., Kitten, G. T., and Nigg, E. A. (1989). A somatic cell-derived system for studying both early and late mitotic events *in vitro*. *J. Cell Sci.* 94, 449-462.
- ²⁰⁰ Lohka, M. J. (1998). Analysis of NE assembly using extracts of *Xenopus* eggs. *Methods Cell Biol.* 53, 367-395.
- ²⁰¹ Lohka, M. J., and Masui, Y. (1983). Formation *in vitro* of sperm pronuclei and mitotic chromosomes induced by amphibian ooplasmic components. *Science* 220, 719-721.
- ²⁰² Laskey, R. A., Gurdon, J. B. and Trendelenberg, M. (1979). Accumulation of materials involved in rapid chromosome replication. In "Maternal Effects in Development" (D. R. Newth, and M. Ball, eds.), pp. 65-80. Cambridge University Press, Cambridge, UK.
- ²⁰³ Lohka, M. J., and Maller, J. L. (1985). Induction of NE breakdown, chromosome condensation and spindle formation in cell-free extracts. *J. Cell Biol.* 101, 518-523.
- ²⁰⁴ Murray, M. W. (1991). Cell cycle extracts. *Methods Cell Biol.* 36, 581-605.
- ²⁰⁵ Newmeyer, D. D., Lucoq, J. M., Buerklin, T. R. and De Robertis, E. M. (1986). Assembly *in vitro* of nuclei active in nuclear protein transport : ATP is required for nucleoplasmin accumulation. *EMBO J.* 5, 501-510.
- ²⁰⁶ Blow, J. J., and Laskey, R. A. (1986). Initiation of DNA replication in nuclei and purified DNA by a cell-free extract of *Xenopus* eggs. *Cell* 47, 577-587.
- ²⁰⁷ Hutchison, C. J., Cox, R., Drepaal, R. S., Gomperts, M., and Ford, C. C. (1987). Periodic DNA synthesis in cell-free extracts of *Xenopus* eggs. *EMBO J.* 6, 2003-2010.
- ²⁰⁸ Newmeyer, D. D. and Wilson, K. L. (1991). Egg extracts for nuclear import and nuclear assembly reactions. *Methods Cell Biol.* 36, 607-634.
- ²⁰⁹ Finlay, D. R., and Forbes, D. J. (1990). Reconstitution of biochemically altered nuclear pores: Transport can be eliminated and restored. *Cell.* 60, 17-29.
- ²¹⁰ Kendirgi, F., Rexer, D. J., Alcázar-Román, A., Onishko, H. M., and Wenthe, S. R. (2005). Interaction between the shuttling mRNA export factor Gle1 and the nucleoporin hCG1: a conserved mechanism in the export of Hsp70 mRNA. *Mol. Biol. Cell* 16, 4304-4315.
- ²¹¹ Aitchison, J. D., Rout, M. P., Marelli, M., Blobel, G., and Wozniak, R. W. (1995). Two novel related yeast nucleoporins Nup170p and Nup157p: complementation with the vertebrate homologue Nup155p and functional interactions with the yeast nuclear pore-membrane protein Pom152p. *J. Cell Biol.* 131, 1133-1148.

- ²¹² Marelli, M., Lusk, C. P., Chan, H., Aitchison, J. D., and Wozniak, R. W. (2001). A link between the synthesis of nucleoporins and the biogenesis of the NE. *J. Cell Biol.* 153, 709-723.
- ²¹³ Kenna, M. A., Petranka, J. G., Reilly, J. L., and Davis, L. I. (1996). Yeast Nle3p/Nup170p is required for normal stoichiometry of FG nucleoporins within the NPC. *Mol. Cell. Biol.* 16, 2025-2036.
- ²¹⁴ Marelli, M., Aitchison, J. D., and Wozniak, R. W. (1998). Specific binding of the karyopherin Kap121p to a subunit of the NPC containing Nup53p, Nup59p, and Nup170p. *J. Cell Biol.* 143, 1813-1830.
- ²¹⁵ Kerscher, O., Hieter, P., Winey, M., and Basrai, M. A. (2001). Novel role for a *Saccharomyces cerevisiae* nucleoporin, Nup170p, in chromosome segregation. *Genetics* 157, 1543-1553.
- ²¹⁶ Gigliotti, S., Callaini, G., Andone, S., Riparbelli, M. G., Pernas-Alonso, R., Hoffmann, G., Graziani, F., and Malva, C. (1998). Nup154, a new *Drosophila* gene essential for male and female gametogenesis is related to the Nup155 vertebrate nucleoporin gene. *J. Cell Biol.* 142, 1195-1207.
- ²¹⁷ Kiger, A. A., Gigliotti, S., and Fuller, M. T. (1999). Developmental genetics of the essential *Drosophila* nucleoporin nup154: allelic differences due to an outward-directed promoter in the P-element 3'end. *Genetics* 153, 799-812.
- ²¹⁸ Zhang, X., Yang, H., Corydon, M. J., Zhang, X., Pedersen, S., Korenberg, J. R., Chen, X. N., Laporte, J., Gregersen, N., Niebuhr, E., Liu, G., and Bolund, L. (1999). Localization of a human nucleoporin Nup155 gene (NUP155) to the 5p13 region and cloning of its cDNA. *Genomics* 57, 144-151.
- ²¹⁹ Zhang, Y., Yang, H., Yu, J., Chen, C., Zhang, G., Bao, J., Du, Y., Kibukawa, M., Li, Z., Wang, J., Hu, S., Dong, W., Wang, J., Gregersen, N., Niebuhr, E., and Bolund, L. (2002). Genomic organization, transcript variants and comparative analysis of the human nucleoporin 155 (NUP155) gene. *Gene* 288, 9-18.
- ²²⁰ Gönczy, P., Schnabel, H., Kaletta, T., Amores, A. D., Hyman, T., and Schnabel, R. (1999). Dissection of cell division processes in the one cell stage *Caenorhabditis elegans* embryo by mutational analysis. *J. Cell Biol.* 144, 927-946.
- ²²¹ Gönczy, P., Echeverri, C., Oegema, K., Coulson, A., Jones, S. J., Copley, R. R., Duperon, J., Oegema, J., Brehm, M., Cassin, E., Hannak, E., Kirkham, M., Pichler, S., Flohrs, K., Goessen, A., Leidel, S., Alleaume, A. M., Martin, C., Ozlu, N., Bork, P., Hyman, A. A. (2000). Functional genomic analysis of cell division in *C. elegans* using RNAi of genes on chromosome III. *Nature* 408, 331-336.
- ²²² Colaiácovo, M. P., Stanfield, G. M., Reddy, K. C., Reinke, V., Kim, S. K., and Villeneuve, A. M. (2002). A targeted RNAi screen for genes involved in chromosome morphogenesis and nuclear organization in the *Caenorhabditis elegans* germline. *Genetics* 162, 113-128.
- ²²³ Piano, F., Schetter, A. J., Morton, D. G., Gunsalus, K. C., Reinke, V., Kim, S. K., and Kempthues, K. J. (2002). Gene clustering based on RNAi phenotypes of ovary-enriched genes in *C. elegans*. *Curr. Biol.* 12, 1959-1964.
- ²²⁴ Davis, L. I., and Blobel, G. (1987). Nuclear pore complex contains a family of glycoproteins that includes p62: glycosylation through a previously unidentified cellular pathway. *Proc. Natl. Acad. Sci. USA* 84, 7552-7556.
- ²²⁵ Franz, C., Askjaer, P., Antonin, W., López Iglesias, C., Haselmann, U., Schelder, M., de Marco, A., Wilm, M., Antony, C., and Mattaj, I. W. (2005). Nup155 is essential for nuclear envelope and nuclear pore complex formation in nematodes and vertebrates. *EMBO J. in press*.
- ²²⁶ Kimura, H., Takizawa, M., Okita, K., Natori, O., Igarashi, K., Ueno, M., Nakashima, K., Nobuhisa, I., and Taga, T., (2002). Identification of a novel transcription factor, ELYS, expressed predominantly in mouse foetal haematopoietic tissues. *Genes to Cell* 7, 435-446.
- ²²⁷ Okita, K., Nobuhisa, I., Takizawa, M., Ueno, M., Kimura, N., and Taga, T. (2003). Genomic organization and characterization of the mouse ELYS gene. *Biochem. Biophys. Res. Commun.* 305, 327-332.
- ²²⁸ Okita, K., Kiyonari, H., Nobuhisa, I., Kimura, N., Aizawa, S., and Taga, T. (2004). Targeted disruption of the mouse ELYS gene results in embryonic death at peri-implantation development. *Genes to Cell* 9, 1083-1091.
- ²²⁹ Andrade, M. A., and Bork, P. (1995). HEAT repeats in the Huntington's disease protein. *Nat. Genet.* 11, 115-116.
- ²³⁰ Perry, J., and Kleckner, N. (2003). The ATRs, ATMs, and TORs are giant HEAT repeat proteins. *Cell* 112, 151-155
- ²³¹ Linding, R., Russel, R. B., Neduva, V., and Gibson, T. J. (2003). *Nucl. Acids Res.* 31, 3701-3708.

-
- ²³² Aravind, L., and Landsman, D. (1998). AT-hook motifs identified in a wide variety of DNA-binding proteins. *Nucl. Acids Res.* 26, 4413-4421.
- ²³³ Edgar, R. C. (2004). MUSCLE: multiple sequence alignment with a high accuracy and high throughput. *Nucl. Acids Res.* 32, 1792-97.
- ²³⁴ Rost, B. (1996). PHD: predicting one-dimensional protein structure by profile-based neural networks. *Methods Enzymol.* 266, 525-39.
- ²³⁵ Rost, B., Sander, C. (1993) Prediction of protein secondary structure at better than 70% accuracy. *J. Mol. Biol.* 20; 584-99.
- ²³⁶ Altschul, S. F., Madden, T. L., Schäffer, A. A., Zhang, J., Zhang, Z., Miller, W., and Lipman, D. J. (1997). Gapped BLAST and PSI-BLAST: a new generation of protein database search programs. *Nucleic Acids Res.* 25, 3389-3402.
- ²³⁷ Hart, G. W., Haltiwanger, R. S., Holt, G. D., and Kelly, W. G. (1989). Glycosylation in the nucleus and the cytoplasm. *Annu. Rev. Biochem.* 58, 841-874.
- ²³⁸ Vasu, S. K., and Forbes, D. J. (2001). Nuclear pore complexes and nuclear assembly. *Curr. Opin. Cell Biol.* 13, 363-375.
- ²³⁹ Haraguchi, T., Koujin, T., Hayakawa, T., Kaneda, T., Tsutsumi, C., Imamoto, N., Akazawa, C., Sukegawa, J., Yoneda, Y., and Hiraoka, Y. (2000). Live fluorescence imaging reveals early recruitment of emerin, LBR, RanBP2, and Nup153 to reforming functional nuclear envelopes. *J. Cell Sci.* 113, 779-794.
- ²⁴⁰ Klein, S., and Gerhard, D. S. (2004). National Institutes of Health, Xenopus Gene Collection (XGC), National Institute of Child Health and Human Development, 6100 Executive Boulevard, Room 4B01, Rockville, MD 20892-7510, USA.
- ²⁴¹ Sambrook, J., Fritsch, E. F., and Maniatis, T. (1989). Molecular cloning: a laboratory manual. *Cold Spring Harbour Laboratory Press, New York.*
- ²⁴² Laemmli, U. (1970). Cleavage of structural proteins during assembly of the head of bacteriophage 14. *Nature* 227, 680-685.
- ²⁴³ Hartl, P., Olson, E., Dang, T., and Forbes, D. J. (1994). Nuclear assembly with λ DNA in fractionated *Xenopus* egg extracts: and unexpected role for glycogen in formation of a higher order chromatin intermediate. *J. Cell Biol.* 124, 235-248.
- ²⁴⁴ Wilson, K. L., and Newport, J. (1988). A trypsin-sensitive receptor on membrane vesicles is required for nuclear envelope formation in vitro. *J. Cell Biol.* 107, 57-68.
- ²⁴⁵ Philpott, A., Leno, G. H., and Laskey, R. A. (1991). Sperm decondensation in *Xenopus* egg cytoplasm is mediated by nucleoplasmin. *Cell* 108, 569-578.
- ²⁴⁶ Arts, G. J., Englmeier, L., and Mattaj, I. W. (1997). Energy- and temperature-dependent in vitro export of RNA from synthetic nuclei. *Biol. Chem.* 378, 641-649.
- ²⁴⁷ Gurdon, J. B. (1976). Injected nuclei in frog oocytes: fate, enlargement, and chromatin dispersal. *J. Embryol. Exp. Morphol.* 36, 523-540.
- ²⁴⁸ Miller, L., and Daniel, J. C. (1977). Comparison of *in vivo* and *in vitro* ribosomal RNA synthesis in nucleolar mutants of *Xenopus laevis*. *In Vitro* 13, 557-567.

7 Appendix

7.1 *Curriculum vitae*

Name: Cerstin Franz, Diplom-Humanbiologin
 Date and place of birth: 07.10.1976, Gießen
 Nationality: german Gender: female
 Current address: Permanent address:
 Römerstraße 253 Verstalstraße 2
 D-69126 Heidelberg D-35102 Lohra

Education:

10/2001 – present: PhD at the European Molecular Biology Laboratory in Dr. Iain Mattaj's lab.

 10/1996 – 09/2001 Study of theoretical medicine (Humanbiologie) at the Philipps-University of Marburg.
 09/2001 Diploma.
 03/2000 – 10/2000 Diploma thesis at the University of California at Berkeley in Prof. Dr. Randy Schekman's lab.
 10/1998 Prediploma.

 06/1996 Abitur at the "Freiherr vom Stein Schule", Gladenbach.

Competitive scholarships:

04/2002 – 04/2004 PhD fellowship of the German National Academic Foundation (Studienstiftung des deutschen Volkes).

 03/2000 – 07/2000 Fellowship of the "Prof. Dr. Adolf Schmidtman Stiftung", Philipps-University Marburg for diploma thesis work at the University of California at Berkeley.

 02/1997 – 09/2001 Scholar of the German National Academic Foundation.

Heidelberg, Cerstin Franz

7.2 Declaration

Hiermit bestätige ich, dass ich die Arbeit selbständig verfasst und keine anderen als die angegebenen Quellen und Hilfsmittel benutzt habe. Die in den benutzten Werken wörtlich oder inhaltlich entnommenen Stellen wurden als solche kenntlich gemacht.

Heidelberg, im Oktober 2005

Cerstin Franz

7.3 Publications

7.3.1 Publications

W. Antonin, C. Franz, U. Haselmann, C. Antony and I.W. Mattaj (2005). The Integral Membrane Nucleoporin Pom121 Functionally links Nuclear Pore Complex Assembly and Nuclear Envelope Formation. *Mol Cell* 17(1), 83-92.

C. Franz, P. Askjaer, W. Antonin, C. López Iglesias, U. Haselmann, M. Schelder, A. de Marco, M. Wilm, C. Antony and I.W. Mattaj (2005). Nup155 Regulates Nuclear Envelope and Nuclear Pore Complex Formation in Nematodes and Vertebrates. *EMBO J*, in press.^{*)}

7.3.2 Poster Presentation

C. Franz, W. Antonin, A. Askjaer, V. Galy and I. Mattaj (2004). Characterization of Nup155 in Nuclear Envelope and Nuclear Pore Complex Formation. *Mol. Biol. Cell* 15, 327a-327a. (41th ASCB Meeting, Washington, DC.)

7.3.3 Future publication

C. Franz *et al.*, (2005/6). Function of Mel28, a Novel Protein Required for Nuclear Envelope Formation.

^{*)} Parts of this study were published in this article.

Acknowledgements

I am very grateful that I could perform my PhD-work in Iain Mattaj's lab and I would like to thank him for his support. His amazing time management and reliability made any kind of professional interactions very efficient and pleasant and is exemplary. Ailsa and Iain hosted very nice Christmas parties and BBQs which I will love to remember.

I thank the members of my thesis advisory committee, Iain Mattaj, Jan Ellenberg, Damian Brunner, and Dirk Ostareck for their time, suggestions and support. Special thanks go to Dirk Ostareck who made it possible for me to submit my thesis to the Martin-Luther University Halle.

Ich bedanke mich bei dem Fachbereich Biochemie/Biotechnologie der Martin-Luther Universität Halle, daß man mich als externe Doktorandin angenommen hat und bei allen Angestellten der Universität, die Ihre Zeit zu diesem Zweck aufwenden werden.

I thank Carsten Schultz for his support, especially at the beginning of my PhD.

Wolfram Antonin is a fantastic scientist and supported me during good and bad times of my PhD with his professional and personal advice for which I am very grateful.

I thank the National German Merit Foundation and EMBL for financial support during my PhD.

I would like to thank all past and present members of the Mattaj lab for nice times, in particular Christoph Schatz for runs through the forest, Virginie Hachet and Margy Koffa for discussions about women's issues, Kevin Czaplinski for his sense of humor, the Glühwein-sessions and his support, Uli Bauer for organizing the lab and having an eye on me and Vincent Galy and Peter Askjaer for their nice work that generated my projects.

I wish all the best to the present PhD-students in the lab, Claudia, Sevil, and Rudolf. In the end, everything will be fine.

EMBL is a fantastic place to work as there are many people that contribute to making all kinds of experiments efficient and help with advice. I had very fruitful and pleasant cooperations with Uta Haselmann, Dr. Ario de Marco, Dr. Tobias Doerks, and Malgorzata Schelder. Dr. Timo Zimmermann, Dr. Jens Rietdorf, and Dr. Stefan Terjung were always helpful with questions concerning confocal microscopy.

I thank Oliver Wichmann and Sirius Zarbakhsh for very entertaining lunches.

Udo Ringeisen, Martina Menke and Andeas Schleifenbaum helped me with

issues concerning the layout of my thesis. Justin Brumbaugh, Kevin Czaplinski, Russ Hodge, Wolfram Antonin and Andreas Schleifenbaum read my thesis and made critical suggestions.

Josef Stegemann and Robert Venzki spread their adventurous and passionate attitudes about science which inspired me.

Christina Kjaer always had a nice word and a smile for me, thanks a lot!

Klaus and his team provided delicious and healthy food throughout the past years. A nice lunch could often cheer me up again. Thank you!!

Meine Eltern haben das Fundament für meinen Werdegang gelegt, und ohne ihre Unterstützung hätte ich meine Ziele nicht verwirklichen können. Vielen Dank.

Ich danke meinen Großeltern für Ihr Interesse an meinem Leben.

Lieber Andreas, ich danke Dir für unsere glückliche, gemeinsame Zeit in Heidelberg und freue mich auf neue Abenteuer mit Dir.